THEORY OF ARBITRARILY POLARIZED QUANTUM HALL STATES, AND INTEGER QUANTUM HALL EFFECT AT FINITE TEMPERATURES

by

SUDHANSU SEKHAR MANDAL

DEPARTMENT OF PHYSICS

INDIAN INSTITUTE OF TECHNOLOGY KANPUR

JULY, 1996

THEORY OF ARBITRARILY POLARIZED QUANTUM HALL STATES, AND INTEGER QUANTUM HALL EFFECT AT FINITE TEMPERATURES

A Thesis Submitted

in Partial Fulfillment of the Requirements

for the Degree of

Doctor of Philosophy

by

SUDHANSU SEKHAR MANDAL

to the

DEPARTMENT OF PHYSICS

INDIAN INSTITUTE OF TECHNOLOGY, KANPUR

July, 1996

Dedicated to the mem
of my brother
Brishaketu

CERTIFICATE

It is certified that the work contained in this thesis entitled *Theory of arbitrarily polarized quantum Hall states, and integer quantum Hall effect at finite temperatures* by *Sudhansu Sekhar Mandal* has been carried out under my supervision and that this work has not been submitted elsewhere for a degree.

V. Ravishankar
Department of Physics
Indian Institute of Technology
Kanpur

3 July, 1996

SYNOPSIS

Ever since the surprising discoveries of integer quantum Hall effect (IQHE) [1] and fractional quantum Hall effect (FQHE) [2] in two dimensional electron gas were made, they have drawn considerable interest. In IQHE, the Hall conductivity gets quantized at integer filling factors with a high accuracy and the diagonal conductivity vanishes at the same time. A similar phenomenon also occurs at fractional filling factors in relatively high mobility samples, and is known as FQHE. While the single particle excitation gap is the 'charge gap' in IQHE, it is the electron electron interaction that produces the charge gap in FQHE.

In an attempt to describe IQHE and FQHE on the same footing, Jain [3] has proposed the composite fermion model (CFM) where an even number of flux quantum are attached to each particle. This model has proved to be highly successful in describing fully polarized quantum Hall states (QHS). However, as Halperin [4] pointed out, systems with low Zeeman energy need not be fully polarized; they may be partially polarized or unpolarized. Such systems have been observed experimentally [5].

In this thesis, we propose a model and develop a theory for these arbitrarily polarized QHS, by employing a doublet of Chern Simons (CS) gauge fields. Recall that a field theoretic version of the CFM for fully polarized systems has been developed by Lopez and Fradkin [6] by introducing a CS gauge field. We follow the same approach here. We then suggest experiments which can directly determine a composite fermion parameter, *viz.*, the effective number (p) of Landau levels (LL) filled by the composite fermions (CF). We further study spin-wave and spin-flip excitations of these QHS.

As we have mentioned earlier, the Hall conductivity σ_{xy} gets quantized in IQHE with a high accuracy at the value ie^2/h (i an integer). It is also experimentally observed [7] that the value of quantization changes with temperature and approaches the value ie^2/h only as temperature $T \to 0$. In this thesis, we study the effect of temperature on the accuracy quantization for QHS in the presence of weak disorder.

In short, in this thesis, we are considering two important issues in quantum Hall effect: (i) the role of spin and (ii) the combined effect of temperature and impurity on the accuracy of quantization. I now give a brief chapter wise summary of the thesis.

Chapter 1 is devoted to a brief introduction.

In chapter 2, we propose and discuss the doublet model. The model is characterized by a doublet of abelian CS gauge fields with the strength of the CS term in the action given by a coupling matrix. It is shown that the model describes almost all known QHS with arbitrary spin polarization. The model is employed within the CF picture and is based on mean field (MF) analysis.

In chapter 3, we consider the gauge field fluctuations about the MF considered in the model. We confirm by an explicit one-loop computation that σ_{xy} does indeed get quantized at these filling factors. We shall show that the quantum fluctuations restore the Kohn mode. We further determine the modulus square of the ground state many body wave functions for the arbitrarily polarized QHS that follow from the model. We remarkably recover the well known Laughlin wave function and Halperin wave function for unpolarized $\nu = 2/5$ state which are microscopically determined from general principles. Finally, the wave functions are shown to be non-analytic, *i.e.*, multivalued in general. We have given here a physical picture for this multivaluedness in terms of the vortices that are induced by quantum fluctuations.

In chapter 4, we improve upon the random phase approximation, which is considered in chapter 3, by time dependent Hartree Fock approximation (TDHFA) for studying the charge density and spin density correlations. This analysis holds for states away from even denominator filling factors. We identify the effective number of LL, filled by CF of up (or down) spin to be the order parameter in spin transitions. Therefore, the value of static spin density correlation function undergoes a discontinuous jump in the spin transitions. We show that neutron scattering experiments can unambiguously determine a CF parameter, *viz.*, p. We also show that depolarized Raman scattering experiments can directly measure the effective cyclotron energy which is the energy scale of CF; p will also be determined thereby if the effective mass of CF is given.

We observe that for this purpose, one needs partially polarized or more preferably unpolarized QHS.

In chapter 5, we consider the spin-wave and spin-flip excitations of the arbitrarily polarized QHS in the TDHFA. Interestingly, we find that the gauge field fluctuations do not change these excitations. In other words, all the QHS with the same numerator but different odd denominator have similar excitations, since they correspond to the same MF. We show that all odd numerator states may have spin-wave excitations in their ferromagnetic ground states. All states possess spin-flip type of excitations.

In chapter 6, we study the IQHE at finite temperatures in a fully polarized system with weak disorder. Due to the impurity in the system, LL will be broadened into a band. We treat the scale of broadening perturbatively in the self consistent Born approximation. We find the finite temperature contribution to σ_{xy} in the zero-th order of broadening. The diagonal conductivity σ_{xx} survives only when both temperature and disorder are non-zero. At low temperatures, σ_{xx} activates with a temperature dependent prefactor. Inverting the conductivity matrix, we determine the resistivities. The deviation of the off-diagonal resistivity ρ_{xy} from its zero temperature value and the diagonal resistivity activate with a temperature dependent prefactor at low temperatures, in agreement with experiments. Further, we find two physical regimes both of which are at low temperatures and weak broadening, which in agreement with experiments, show a linear relationship between the deviation of ρ_{xy} and ρ_{xx} with different signs. We estimate also the effective mass of electron from the experimental data and find them to be reasonable. Finally, our result on compressibility as a function of temperature shows that there is no phase transition involved in the system as far as the temperature is concerned.

An introduction is provided in each of the chapters from 2–6. In addition we make a brief survey of the literature in chapter 7, which by no means exhausts all the aspects of QHE, but provides a setting for the topics discussed in this thesis.

References

[1] K. von Klitzing, G. Dorda, and M. Pepper, Phys. Rev. Lett. **45**, 494 (1980).

[2] D. C. Tsui, H. L. Stormer, and A. C. Gossard, Phys. Rev. Lett. **48**, 1559 (1982).

[3] J. K. Jain, Phys. Rev. Lett. **63**, 199 (1989).

[4] A. Lopez and E. Fradkin, Phys. Rev. **B 44**, 5246 (1991).

[5] B. I. Halperin, Helv. Phys. Acta. **56**, 75 (1983).

[6] R. G. Clark, S. R. Haynes, A. M. Suckling, J. R. Mallett, P. W. Wright, J. J. Harris, and C. T. Foxon, Phys. Rev. Lett. **62**, 1536 (1989).

[7] M. E. Cage, B. F. Field, R. F. Dziuba, S. M. Girvin, A. C. Gossard, and D. C. Tsui, Phys. Rev. **B 30**, 2286 (1984).

Acknowledgments

I am grateful to Dr. V. Ravishankar for his guidance and supervision in the course of this work. He was always ready to discuss with me, no matter what the place is—be it in the office, on the tea table or at his home. He was very enthusiastic to rectify my doubts whenever required. I admired him for his simple way of teaching. I acknowledge his inspiration throughout the period of my work, especially during my bad days.

I thank Dr. S. Ramaswamy with whom I had an opportunity to collaborate in the early part of my research career. I am grateful to him along with Dr. V. Ravishankar for introducing me in the field of two dimensional condensed matter systems which is the subject of study in this thesis.

I highly thank Dr. A. K. Majumdar, Dr. J. K. Bhattacharjee, and Dr. A. Singh for many discussions and for their patience and interest when I used to present my work in front of them.

I thank all of my friends who created a congenial atmosphere for research in IIT Kanpur and shared joy and sorrows with me. I thank also the office staff of our department, in particular Pandaji and Rathaurji, for their kind help whenever needed.

I am indebted to my neighbours and relatives who have shown enough commitment to me. I acknowledge my parents' patience and affection which have constantly been a source of inspiration. I thank my brother, who is not now with us, and my sister for their encouragement.

Finally, I thank Minstry of Human Resource and Development, Government of India for financial assistance.

Sudhansu Sekhar Mandal

Contents

Chapter 1

Introduction

In recent years, the quantum Hall effect (QHE) has drawn much interest. This phenomenon occurs at very low temperatures (≤ 4 K) in a high mobility two dimensional electron gas (2DEG) in the presence of strong perpendicular magnetic field ($B \sim 1$–30 T). The 2DEG can be achieved in the interface between a semiconductor and an insulator (Si-SiO_2 in Si- MOSFET), or two semiconductors (GaAs-$Al_xGa_{1-x}As$). Under suitable experimental conditions, all the conduction electrons occupy the lowest subband and hence they are trapped along a direction perpendicular to the interface. Further, the electrons can move freely in the plane of the interface with a very long mean free path. In 1980, Klitzing *et al* [1] first observed that the Hall conductance of such a system gets quantized, with a high accuracy (one part in 10^5), at *integer* multiple of quantum of conductance e^2/h not only at integer filling factor, but in its neighbourhood as well. The diagonal conductance vanishes at the same time. This phenomenon is known as integer QHE (IQHE). The Hall conductance shows an almost discontinuous jump and the diagonal conductance shows a sharp maximum when a transition from one IQHE state to another occurs (see Fig. 1.1 where the corresponding resistivities are shown). Two years later, Tsui *et al* [2] discovered that at lower temperatures and in higher mobility samples, a similar phenomenon occurs at *fractional* filling factors as well. This latter unexpected phenomenon is known as fractional QHE (FQHE). (See Fig. 1.2 for a series of experimentally observed FQHE states). The early developments of QHE are excellently reviewed in two books [5, 6].

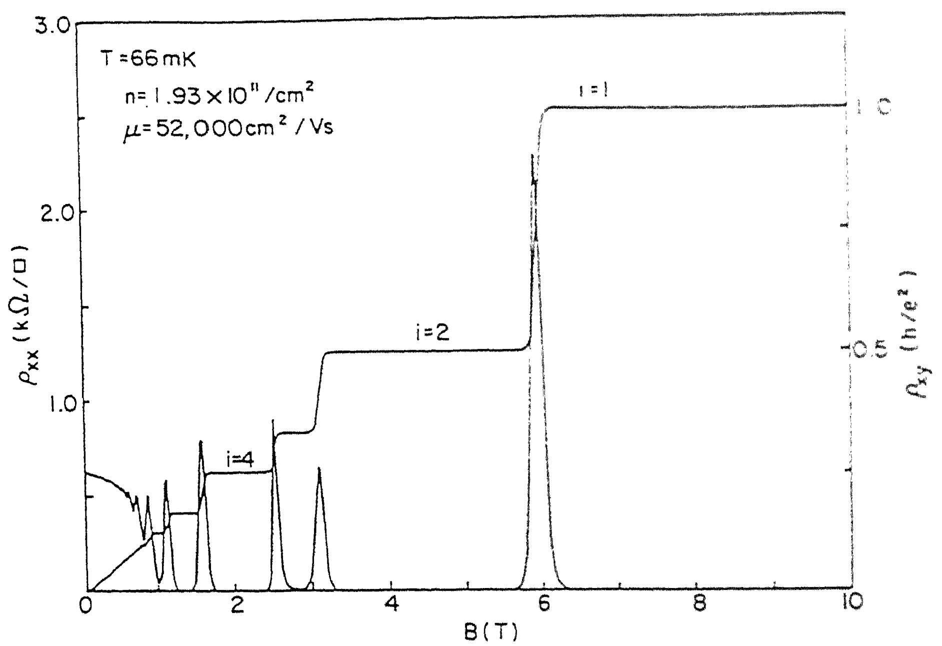

Figure 1.1: The resistivities ρ_{xx} and ρ_{xy} are plotted against magnetic field B for relatively low mobility GaAs-AlGaAs sample showing the IQHE (from Ref. [3]).

The IQHE occurs due to the presence of 'charge gap' in the single particle excitation. The electron electron interaction has no major role (only perturbative [7]) for producing the gap. As long as the Fermi energy lies in the region of localized states, the Hall conductivity σ_{xy} gets quantized and the diagonal conductivity σ_{xx} vanishes [8–10]. A transition from one IQHE state to another occurs when the Fermi energy hits the extended states. The quantization in σ_{xy}, which is universal, is exhibited due to the gauge invariance and the existence of the mobility gap [9, 10]. σ_{xy} is also topological in nature [11]. Strictly speaking, the value of quantization, changes with temperature and it approaches the value ie^2/h only asymptotically as $T \to 0$ [12, 13].

Although electron electron interaction is not important for producing the charge gap in the IQHE, it is, in fact, the most responsible for producing the charge gap in the FQHE. The electrons are strongly correlated, and therefore the simple single particle spectrum no longer explains the effect. In his pioneering work, Laughlin [14] has made a variational guess to obtain a good approximate ground state wave function

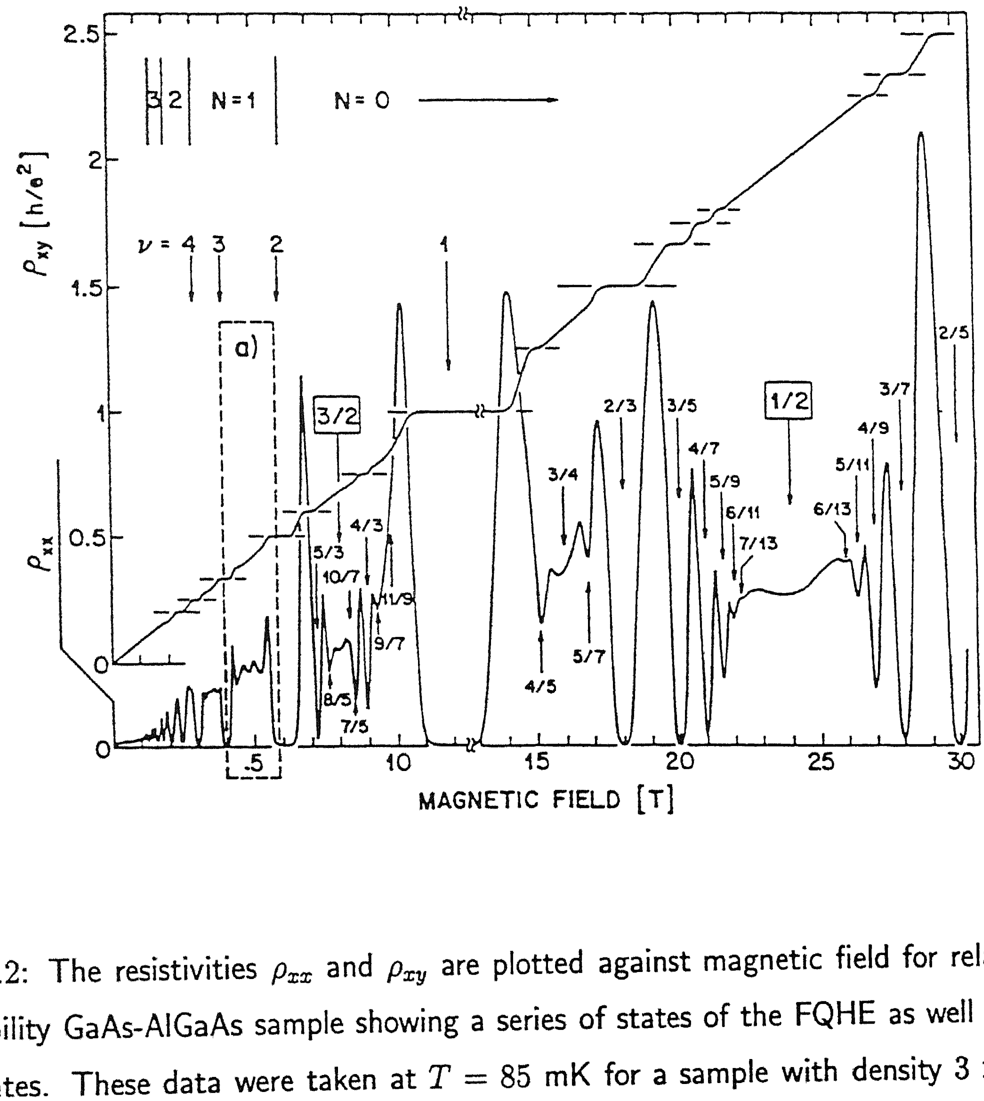

Figure 1.2: The resistivities ρ_{xx} and ρ_{xy} are plotted against magnetic field for relatively high mobility GaAs-AlGaAs sample showing a series of states of the FQHE as well as the IQHE states. These data were taken at $T = 85$ mK for a sample with density 3×10^{11} cm^{-2} and mobility 1.3×10^6 cm^2/Vs (from Ref. [4]).

for $\nu = 1/m$ (m odd) states. In his picture, the charge [14] and statistics [15, 16] of the quasiparticle or qasihole excitations of these ground states are fractional. These quasiparticles (quasiholes) at their magic densities condense into a Laughlin like state to form a hierarchy of the FQHE states [15, 17].

By now, however, the composite fermion model (CFM), which was proposed by Jain [18], has emerged to be a successful model as an alternative to the above hierarchy. Employing a Chern-Simons (CS) gauge field, a field theoretic description of the model has been developed by Lopez and Fradkin [19] for spinless electrons, *i.e.*, all the electrons are polarized in the direction of magnetic field. In the CFM, the charge gap is due to the single particle spectrum of the composite fermions (CF) defined to be composite objects of electron with an even number of flux quantum hc/e. In the mean field approximation, these fluxes produce a uniform CS magnetic field in the opposite direction to the applied magnetic field. The CF move in an effective magnetic field which is sum of the applied and CS magnetic fields. The excitation gap is determined by this effective magnetic field. In particular, the gap *vanishes* at the half filling factor and therefore the quantum liquid at half filling behaves like a Fermi liquid, as predicted by Halperin, Lee, and Read [20]. A good number of experiments [21–33] have been subsequently performed to test the existence of CF.

Recall that the above development of the CFM is with the assumption that the electrons are spinless. This assumption is justified when the Zeeman energy is large enough so that all the electrons become polarized in the direction of the magnetic field. However, as Halperin [34] argued, there is the possibility that all the QHE states are not necessarily fully polarized. Such a case arises when the Zeeman energy is smaller than both Coulomb energy as well as cyclotron energy in GaAs. Indeed both experiments [35–38] and exact diagonalization studies [39–41] have confirmed the above prediction. Experiments [35–38] further reveal that the unpolarized or partially polarized quantum Hall states (QHS) make transitions to their fully polarized phase with the increase of Zeeman energy. These phenomena lie beyond the scope of the standard CFM (which does not incorporate spin degree of freedom dynamically).

To fill the above gap, we propose, in this thesis, a model which can describe almost all the observed QHS both with respect to the filling factors and their polarizations. In this 'doublet model' [42], with explicit CF requirement, new states are also predicted. An explicit one-loop analysis does indeed show the quantization of σ_{xy} at the appropriate values. We further derive the modulus square of the ground state wave function for these arbitrarily polarized QHS. Finally, we show that the model can, in fact, suggest [43] experiments which can determine the crucial composite fermion parameter, *viz.*, the effective number (p) of Landau levels (LL) filled by the CF. The parameter p is otherwise hidden in the fully polarized phase. However, in the unpolarized or partially polarized phase, this parameter appears explicitly in the observables and is measurable. With a view to suggesting appropriate experiments, we study charge density and spin density ($\delta S_z = 0$) correlations. We show that neutron scattering experiments can unambiguously determine p. We also show that Raman scattering experiments can directly measure effective cyclotron frequency $\bar{\omega}_c$ of CF, and p will also be determined thereby if the effective mass of CF is given. We also study [44] the spin-wave and spin-flip excitations ($\delta S_z = \pm 1$) of the arbitrarily polarized QHS.

As we have mentioned earlier, it is observed experimentally [12, 13] that the value of quantization in σ_{xy} changes with temperature. To understand this temperature dependence, we consider [45] a weak disordered spinless system exactly at integer fillings in this thesis. The broadening of the LL is treated as perturbation in the self consistent Born approximation (SCBA). We find that σ_{xy} gets a temperature dependent contribution in the zero-th order of broadening; the diagonal conductivity σ_{xx} is non-zero only when both temperature and impurity are non-zero. We find a linear relationship between the deviation of the Hall resistivity from its zero temperature value and the diagonal resistivity, in agreement with experiments [12, 13].

In short, in this thesis, we are considering two important issues in QHE: (i) the role of spin and (ii) the combined effect of temperature and impurity on the accuracy of quantization. A chapter wise summary is given in the synopsis (see pages v and vi).

Chapter 2

Model for arbitrarily polarized quantum Hall states

2.1 Introduction

A two dimensional electron gas can exhibit QHE at low temperatures and in the presence of high magnetic field B. If the magnetic field is large enough, the spin degree of freedom of the electron gets frozen in the direction of the magnetic field (which is perpendicular to the plane of the system) and has no dynamical role. These electrons are called spinless. Thus one assumes that the electrons are spinless for these fully polarized QHS. The CFM, which describes these states well, was proposed by Jain [18]. In the CFM, spinless electrons are attached with even number ($2s$) of flux quantum $2\pi/e$. (Hereafter we set the units $\hbar = c = 1$.) The statistics of the charge-flux composites remains fermionic, and hence they are called CF. The strong correlation between electrons in original electronic systems are replaced by the CF with a weak interaction between them in this model. In the MF approximation, the fluxes are chosen to produce a uniform magnetic field in the opposite direction to the applied magnetic field. Therefore, the CF feel a reduced effective magnetic field $\bar{B} = B - (2\pi/e)\rho(2s)$, where ρ is the mean particle density. Now if p be the number of filled Landau levels (LL) by CF, the actual filling factor in the electronic system becomes $\nu = p/(2sp+1)$. Note that p can be negative as well in which case $\bar{B}$ is antiparallel to B. The IQHE of CF leads to the FQHE in the original electronic system. In the CFM, the charge excitation

gap is the effective cyclotron energy of CF, $\bar{\omega}_c = e\bar{B}/m^*$, where m^* is the effective mass of CF. Using a single CS parameter $\theta = (e^2/2\pi)(1/2s)$, Lopez and Fradkin (LF) [19] have constructed a CS action which incorporates the essentials of the CFM in a field theory of spinless fermions.

The above analysis, which ignores spin, fails, however, for relatively low density GaAs samples. As Halperin [34] has argued, such a sample possesses very low Zeeman energy ($g \sim 0.45$) compared to cyclotron energy ($m^* = 0.07$ m_e), and is less than even the Coulomb energy which is responsible for producing charge gap in the FQHE states. This led him to conclude that all the QHS may not be fully polarized; some of them could be even unpolarized. Indeed, experiments reveal that at relatively small values of B, the QHS at filling factors $\nu = \frac{4}{3}, \frac{8}{5}, \frac{10}{7}$ (Refs.[35, 36]) and $\frac{2}{3}$ (Refs.[36, 38]) are unpolarized (spin singlet) while the states at $\nu = \frac{3}{5}$ (Ref.[38]) and $\frac{7}{5}$ (Ref.[35]) are partially polarized. Further, it is also known experimentally that the states which are in the partially polarized or unpolarized phase to start with pass over to their fully polarized phase as the Zeeman energy is increased sufficiently — either by increasing the tilting angle of the magnetic field keeping the perpendicular component of it fixed [35–38], or by increasing the electron density [37], since g factor becomes enhanced with the densities [46]. In the vanishing Zeeman splitting (VZS) limit, it has been found from numerical computations [39–41] that the states with $\nu = 2/(2n+1)$ (n is an integer) are unpolarized and those of the Laughlin sequence [14] with $\nu = 1/(2n+1)$ are fully polarized, in the thermodynamic limit. Also the state at $\nu = \frac{3}{5}$ has been found to be partially polarized by an exact diagonalization study [47], in agreement with experiments. Wu, Dev and Jain [48] have constructed trial wave functions for these states by employing the CFM and found good overlap with the numerically diagonalized states. They report that, in the VZS limit, all the even numerator QHS are unpolarized and all those states which have both the numerator and denominator (of ν) odd are partially/fully polarized.

While there seem to be no theory for these arbitrarily polarized QHS, Frohlich *et al* [49] and Balatsky and Fradkin [50] have attempted to study the unpolarized QHS,

by employing a non-abelian CS model. In this picture, electrons are composites of holons and spinons. While charged spinless holons interact with a $U(1)$ CS gauge field, neutral spin-1/2 spinons interact with a $SU(2)$ CS gauge field. Both the holons and spinons obey semionic statistics, and ensure the statistics of the electron to be fermionic. Note that apart from the complicated interaction involving $SU(2)$ CS gauge field, the limitation of this model is that it can not describe all the arbitrarily polarized QHS. In contrast, we develop here a model, by employing an *abelian* doublet[1] of CS gauge fields within the CFM. This model, which we shall call the doublet model, is shown to describe arbitrarily polarized QHS. We shall show that the polarization of the QHS emerges naturally from the model. In general, the model incorporates the idea that each particle has two kinds of vortices — one of which is seen by like spin particles and the other by the particles of unlike spin. A similar interpretation[2] has been given by Belkhir and Jain [51] from the wave function that they have constructed for the unpolarized states of sequence $\nu = 2n/(3n+2)$ (n is an integer).

Before we conclude this section, we may mention that technological developments have made it possible to create double layer 2DEG systems. Such a spin polarized bilayer system can be mapped into a single layer spin-1/2 system, when the separation between the layers is not very large. In this mapping, the layer degree of freedom acts as a 'pseudo-spin', in analogy with spin-1/2 system in a single layer. LF [52] have recently described the double layered QHS using an abelian doublet of CS gauge fields, analogous to that of ours in a single layer spin-1/2 system. However, the two models, which describe two different physical situations, have distinct differences. We shall make a comparison between them in the next chapter. Nevertheless, there exists certain similarities and we shall show that the doublet model can describe the double layer system as well.

---

[1]Models with matrix valued coupling have been considered earlier, in a different context by X. G. Wen and A. Zee, Phys. Rev. B 46, 2290 (1992).

[2]According to Belkhir and Jain, each composite fermion carries two different types of vortices — one of which seen by all electrons while the other is visible only to an electron of like spin. However, we shall show that their interpretation does not lead to the unpolarized sequence $\nu = 2n/(3n+2)$.

2.2 The doublet model

Consider a two-dimensional system of non-relativistic spin-1/2 electrons in the presence of a magnetic field perpendicular to the plane. We assume that the (effective) Zeeman energy may be small but non-zero, *i.e.*, *SU(2)* spin symmetry is broken but *U(1)*$\otimes$*U(1)* charge symmetry is intact. The complicated interaction among electrons is represented by the interaction of electrons with CS gauge fields and (weak) fermion fermion interaction, (although we neglect the latter interaction for describing the model for the sake of simplicity). The dynamics of the system is then represented by the Lagrangian density

$$\mathcal{L} = \psi_\uparrow^* \mathcal{D}(a_\mu^\uparrow)\psi_\uparrow + \psi_\downarrow^* \mathcal{D}(a_\mu^\downarrow)\psi_\downarrow + \frac{1}{2}\tilde{a}_\mu \epsilon^{\mu\nu\lambda}\Theta\partial_\nu a_\lambda \ . \tag{2.1}$$

Here ψ is the fermionic field and $\uparrow$ and $\downarrow$ represent the spin up and down respectively. The operator

$$\mathcal{D}(a_\mu^r) = iD_0^r + (1/2m^*)D_k^{r\,2} + \mu + (g/2)\mu_B(B + b^r)\sigma \tag{2.2}$$

with $D_\mu^r = \partial_\mu - ie(A_\mu + a_\mu^r)$ where A_μ is the external electromagnetic field and a_μ^r is the CS field which interacts with the particles having spin indices $r =\uparrow, \downarrow$. The fixed density of particles in the system is implemented by the introduction of chemical potential μ which acts as a Lagrange multiplier. e and m^* are the charge and effective mass of the fermions respectively. We have introduced a doublet of CS gauge fields in (2.1) as

$$a_\mu = \begin{pmatrix} a_\mu^\uparrow \\ a_\mu^\downarrow \end{pmatrix} , \tag{2.3}$$

and the strength of the CS term is taken to be matrix valued:

$$\Theta = \begin{pmatrix} \theta_1 & \theta_2 \\ \theta_2 & \theta_1 \end{pmatrix} . \tag{2.4}$$

$\tilde{a}_\mu$ is the transpose of the doublet field a_μ. Note that the choice of the matrix (2.4) is the most general one that one can consider for a spin-1/2 single layer system,[3]

[3]For a double layered spinless system, such a symmetry is not necessary: the diagonal elements are not same in general, however the off-diagonal elements have to be same, as in this case, because of interlayer symmetry.

following from the requirement that the parity operation transform the up spin to down spin fermions and vice versa. The CS interactions provide flux tube attachment with the particles. In the MF approximation, these fluxes smear out to produce mean CS magnetic fields. Note that the Zeeman term in Eq. (2.1) comprises of both the external magnetic field B and the CS field b^r. μ_B is the Bohr magneton, $\sigma = +1(-1)$ for spin-up(down) electrons. The action given by Eq. (2.1) is invariant under the $U(1)$ gauge transformations

$$a_\mu^{\uparrow,\downarrow} \to a_\mu^{\uparrow,\downarrow} + \partial_\mu \lambda^{\uparrow,\downarrow}(x)\,,\ \psi_{\uparrow,\downarrow}(x) \to \exp[ie\lambda^{\uparrow,\downarrow}(x)]\psi_{\uparrow,\downarrow}(x)\,. \tag{2.5}$$

In other words, the doublet model is abelian.

In tilted field experiments, the B field is not perpendicular to the plane. In those cases, the spin labels $\uparrow, \downarrow$ associated with fermionic fields refer to the quantization axis defined by $\mathbf{B} + \mathbf{b}^r$. The CS field $\mathbf{b}^r$ is of course always perpendicular to the plane. We note further that the g factor acquires the effective value $g_{\text{eff}} = g|\mathbf{B} + \mathbf{b}^r|/(B_\perp + b^r)$. Note that g_{eff} is a tunable parameter.

The above Lagrangian density has several interesting features. Let us diagonalize the matrix Θ, with eigen values $\theta_\pm = \theta_1 \pm \theta_2$, and denote a_μ in the eigen basis by

$$a_\mu = \begin{pmatrix} a_\mu^+ \\ a_\mu^- \end{pmatrix}\,. \tag{2.6}$$

By simple rescalings Eq. (2.1) may be written as

$$\mathcal{L} = \psi_\uparrow^* \mathcal{D}(a_\mu^+ + a_\mu^-)\psi_\uparrow + \psi_\downarrow^* \mathcal{D}(a_\mu^+ - a_\mu^-)\psi_\downarrow + \frac{\theta_+}{2}\epsilon^{\mu\nu\lambda} a_\mu^+ \partial_\nu a_\lambda^+ + \frac{\theta_-}{2}\epsilon^{\mu\nu\lambda} a_\mu^- \partial_\nu a_\lambda^-\,. \tag{2.7}$$

This incorporates the idea that each electron, in general, has two kinds of vortices associated with it — while they interact in phase with spin up particles, spin down particles get their subtracted contribution. The relevant equations of motion now read

$$\mathcal{D}(a_\mu^+ + a_\mu^- \equiv a_\mu^\uparrow)\psi_\uparrow(x) = 0\ ;\quad \mathcal{D}(a_\mu^+ - a_\mu^- \equiv a_\mu^\downarrow)\psi_\downarrow(x) = 0\,; \tag{2.8}$$

$$\theta_+ b^+(x) = -e(\rho_\uparrow(x) + \rho_\downarrow(x)) \equiv -e\rho(x)\,; \tag{2.9}$$

$$\theta_- b^-(x) = -e(\rho_\uparrow(x) - \rho_\downarrow(x)) \equiv -e\Delta\rho(x)\,, \tag{2.10}$$

where $\rho_\uparrow(\rho_\downarrow)$ is the density of spin up (down) particles.

2.2.1 Case–I: Unpolarized states

We first study the case $\theta_1 = \theta_2 = \theta \Rightarrow \theta_+ = \theta$ and $\theta_- \equiv 0$. Thus the CS gauge field a_μ^- decouples dynamically and merely plays the role of a Lagrange multiplier: $\frac{\partial \mathcal{L}}{\partial a_0^-} = \Delta\rho(x) \equiv 0$. Thus the unpolarized case is accomplished by the choice $\theta_1 = \theta_2$. We parametrize $\theta = \frac{e^2}{2\pi}(\frac{1}{2s})$ (s is an integer) in order to impose composite fermion picture on the model. Note that the ensuing CFM is different from the one envisaged by Belkhir and Jain who distinguish between the relative phase between like spin particles and unlike spin particles for singlet states. In this model, there is no such phase distinction.

The determination of the filling fractions is now straight forward. Since there is only one CS gauge field a_μ^+, a standard MF ansatz leads to an average CS magnetic field $\langle b^+\rangle = -\frac{e\rho}{\theta}$ which is seen by *all* the electrons. Demanding that the effective LL formed by the effective magnetic field $\bar{B} = B + \langle b^+\rangle$ accommodate all the particles at an integer filling factor $2p$, (p for up spin and p for down), the true filling fraction ν is obtained as

$$\nu = \frac{2p}{4sp+1} . \tag{2.11}$$

The energy corresponding to each level is obtained as $\varepsilon_{n\sigma} = (n + 1/2)\bar{\omega}_c - \frac{g}{2}\mu_B\bar{B}\sigma$ ($n = 0, 1, \ldots$), where the effective cyclotron frequency $\bar{\omega}_c = \frac{e}{m^*}\bar{B}$, which provides the energy scale for CF. All the states obeying Eq. (2.11) are spin unpolarized. Recall that p can be a negative integer as well in which case $\bar{B}$ is antiparallel to B. Note that the sequence (2.11) is exactly the same as that was obtained by Wu *et al* [48], and does indeed accommodate all the known experimentally observed states with $\nu < 1$ and also maintain consistency with the numerical result that all even numerator states are unpolarized. In the limit $p \to \infty$, $\nu \to 1/(2s) \Rightarrow$ that all even denominator states may also be unpolarized. Further by particle-hole symmetry, the states $2-\nu$, and the states $2+\nu$ which are obtained by the addition of LL [48], are also unpolarized. It is indeed true that the even-numerator levels such as $\nu = \frac{4}{3}, \frac{8}{5}$ and $\frac{10}{7}$ [35] and even-denominator state like $\nu = \frac{5}{2}$ have been experimentally observed to be unpolarized [53].

It is worthwhile to note here that the choice $\theta_1 = -\theta_2 = \theta$, *i.e.*, $\theta_+ = 0$ and $\theta_- = \theta$

leads to decouple a_μ^+ field dynamically. This choice provides non-zero spin density but *zero* particle density which is unphysical. Therefore this particular choice is ruled out.

2.2.2 Case-II: Partially Polarized states

We now consider the case $\theta_1 \neq \theta_2$ in order to obtain partially polarized states. In the diagonal basis $\theta_\pm = \theta_1 \pm \theta_2 \neq 0$. The study of the Lagrangian now offers several novel features. In general, the phase picked up by a spin around a like-spin is different from what it would pick up around an unlike-spin. Moreover, the MF ansatz now involves smearing two fields $\langle b^\pm \rangle$ which are not necessarily equal. We find that

$$\bar{B}^\uparrow = B + \langle b^+ \rangle + \langle b^- \rangle \ ; \quad \bar{B}^\downarrow = B + \langle b^+ \rangle - \langle b^- \rangle \tag{2.12}$$

are respectively the fields seen by spin up and spin down particles. Consequently there are two energy scales corresponding to the two gaps at the MF level. It turns out that for known partially polarized QHS, $\bar{B}^\uparrow = \bar{B}^\downarrow$

We again implement the composite fermion requirement. This leads to the condition

$$-e\left(\frac{1}{\theta_+} + \frac{1}{\theta_-}\right) = -\frac{2\pi}{e}(2s) \ . \tag{2.13}$$

However allowing the unlike spins to pick up arbitrary phases we write

$$-e\left(\frac{1}{\theta_+} - \frac{1}{\theta_-}\right) = -\frac{2\pi}{e}k \ , \tag{2.14}$$

where k is arbitrary.

Let us parametrize $\theta_\pm = (e^2/2\pi)(1/s_\pm)$. Demanding that exactly $p_\uparrow(p_\downarrow)$ numbers of effective LL be filled by spin up (down) electrons, we obtain

$$\frac{\rho_\uparrow}{p_\uparrow} = \frac{\rho}{\nu} - [\rho s_+ + (\Delta\rho)s_-] \ , \tag{2.15}$$

$$\frac{\rho_\downarrow}{p_\downarrow} = \frac{\rho}{\nu} - [\rho s_+ - (\Delta\rho)s_-] \ , \tag{2.16}$$

where ρ's are the corresponding mean densities and $\Delta\rho$ is the mean spin density. Note that if $\Delta\rho = 0$, s_- is irrelevant. In other words, the requirement of unpolarized spin

states causes a collapse to Case-I. Solving for $\Delta\rho$ and ν we obtain

$$\frac{\Delta\rho}{\rho} = \frac{p_\uparrow - p_\downarrow}{p_\uparrow + p_\downarrow + 4s_- p_\uparrow p_\downarrow}, \tag{2.17}$$

$$\nu = \frac{p_\uparrow + p_\downarrow + 4s_- p_\uparrow p_\downarrow}{1 + (s_+ + s_-)(p_\uparrow + p_\downarrow) + 4s_+ s_- p_\uparrow p_\downarrow}. \tag{2.18}$$

Observe that $\Delta\rho \neq 0$ if and only if $p_\uparrow \neq p_\downarrow$. Note that for $\Delta\rho = 0$, s_- (being an irrelevant parameter) needs to be dropped. We now discuss different physical situations below.

(i) We study the extreme case $s_- = 0$, *i.e.*, mean CS magnetic field $\langle b^- \rangle = 0$ first. The CS field a_μ^- is decoupled at the tree level (in contrast to the unpolarized states where a_μ^- is completely *non-dynamical*). Notice that this choice corresponds to $\theta_- = \infty$ but finite θ_+. This infinite limit is in the same spirit of IQHE limit of FQHE for fully polarized QHS (see the line below Eq. 2.20). Further partially polarized integer QHS would be obtained in the limit $\theta_+ \to \infty$, *i.e.*, $s_+ = 0$.

We have $s_+ = 2s$ by virtue of composite fermion requirement. Since $\langle b^- \rangle = 0$, the effective magnetic field for both spin up and down particles is same. This leads to the actual filling fraction and the spin density to be

$$\nu = \frac{p_\uparrow + p_\downarrow}{2s(p_\uparrow + p_\downarrow) + 1}\ ; \ \Delta\rho = \rho\left(\frac{p_\uparrow - p_\downarrow}{p_\uparrow + p_\downarrow}\right). \tag{2.19}$$

The relation $p_\uparrow \neq p_\downarrow$ naturally leads to partial polarization. The effective cyclotron frequency $\bar{\omega}_c$ is related to $\omega_c = eB/m^*$ by $\omega_c = \bar{\omega}_c[2s(p_\uparrow + p_\downarrow) + 1]$.

In the limit of high Zeeman energy, only the up spin states will be populated. In other words, $p_\downarrow = 0$. In that limit, we obtain the Jain sequence [18]

$$\nu = \frac{p_\uparrow}{2sp_\uparrow + 1} \tag{2.20}$$

for fully polarized (spinless) QHS. The limit $s = 0$ gives the fully polarized integer QHS. The choice $p_\uparrow = 1$ provides fully polarized Laughlin sequence [14], $\nu = 1/(2s+1)$. Finally the limit $p_\uparrow = \infty$ gives rise to fully polarized even denominator states with $\nu = 1/2s$ with a vanishing gap of excitations ($\bar{\omega}_c = 0$).

For small Zeeman energies, we may take $p_\uparrow = p_\downarrow + 1 = p$ (say). Then

$$\frac{\Delta\rho}{\rho} = \frac{1}{2p-1} \; ; \quad \nu = \frac{2p-1}{2s(2p-1)+1} \, . \tag{2.21}$$

These states are indeed partially polarized, becoming fully polarized when $p = 1$. Then $\nu_{p=1} = 1/(2s+1)$ is again the Laughlin sequence known to be completely polarized [39]. It is interesting that in either of the limits (small or large) of Zeeman energy, the Laughlin sequence is fully polarized. The case $s = 1$ yields the sequence obtained by Wu *et al* [48]. Particle-hole symmetry and the addition of LL imply again that $2 - \nu$ and $2 + \nu$ are also spin-polarized. It turns out that the sequences given by Eqs. (2.11 and 2.19–2.21) exhaust almost all known integer and fractional states — with full, partial or no polarization.

(ii) Consider the case $s_+ = 0$, *i.e.*, $\langle b^+ \rangle = 0$. The CS field a_μ^+ will be decoupled from the tree level. This choice provides $\bar{\omega}_c^\uparrow \neq \bar{\omega}_c^\downarrow$ and $s_- = 2s$ for the composite fermion requirement. The sequence of states with polarizations is given by

$$\frac{\Delta\rho}{\rho} = \frac{p_\uparrow - p_\downarrow}{p_\uparrow + p_\downarrow + 2sp_\uparrow p_\downarrow} \; ; \; \nu = \frac{p_\uparrow + p_\downarrow + 2sp_\uparrow p_\downarrow}{2s(p_\uparrow + p_\downarrow) + 1} \, . \tag{2.22}$$

This sequence of states is not experimentally observed.

(iii) The model can accommodate many more states corresponding to $\bar{B}^\uparrow \neq \bar{B}^\downarrow$. As an interesting exercise, let us construct the sequence of states that would follow from Belkhir and Jain proposal [51]. This corresponds to the choice $k = 1$ in (2.14), whence, $s_+ = 3/2$ and $s_- = 1/2$. We obtain

$$\frac{\Delta\rho}{\rho} = \frac{p_\uparrow - p_\downarrow}{p_\uparrow + p_\downarrow + 2p_\uparrow p_\downarrow} \; ; \tag{2.23}$$

$$\nu = \frac{p_\uparrow + p_\downarrow + 2p_\uparrow p_\downarrow}{1 + 2(p_\uparrow + p_\downarrow) + 3p_\uparrow p_\downarrow} \, , \tag{2.24}$$

which clearly is a new sequence. Therefore, Belkhir and Jain proposal [51] does not correspond to the unpolarized sequence $\nu = 2n/(3n+2)$ that they have studied.

(iv) In general, the family of sequences is given in terms of four independent parameters $(p_\uparrow\,, p_\downarrow\,, s_+, s_-)$, subject to the composite fermion constraint: $s_+ + s_- = 2s$ (an even integer). It raises the interesting question of the uniqueness of the ν values

obtained. We note that the sequences are indeed different, and any accidental degeneracy (*i.e.*, same ν value from different sequences) does not make the model ambiguous. For, it would correspond to different gap energies, which can be determined, say, by the activation of diagonal resistivity. In short, the QHS are labeled by ν as well as $\bar{\omega}_c^{\uparrow,\downarrow}$. These states correspond to $\bar{\omega}_c^{\uparrow} \neq \bar{\omega}_c^{\downarrow}$, in general. One expects that the charge gap is same for both the spins in a single layered system. Therefore, these general states may not occur in such a system. However in a bilayered system, it is certainly possible that the charge gap in two layers are different and hence such a general sequence of states may be possible in bilayered systems.

Chapter 3

Wave functions for arbitrarily polarized quantum Hall states

3.1 Introduction

In the previous chapter, we have described the doublet model for arbitrarily polarized QHS, employing a doublet of CS gauge fields. We have seen that with appropriate choice of parameters, MF ansatz reproduces correctly the experimentally observed sequences of QHS with correct spin polarizations (see Eqs. 2.11 and 2.19–2.21). Recall that these sequences correspond to identical gap of excitations for both the spins, *i.e.*, $\bar{\omega}_c^{\uparrow} = \bar{\omega}_c^{\downarrow}$. In this chapter, we develop fermionic CS theory employing the doublet model and make several theoretical checks for viability of the model. We determine the absolute square of the many body wave functions for these sequences using the same methods as developed by LF [54] for fully polarized QHS. We show that the asymptotic properties of the wave function, in the small Zeeman as well as thermodynamic limits, are completely determined by the long distance behaviour of the equal-time density-density correlation functions of different spin species of electrons. Gratifyingly, we recover the well-known Halperin wave function [34] for spin unpolarized $\nu = 2/5$ state, and Laughlin wave functions. Secondly, as an important exercise, we show that the Hall conductivity gets quantized at the magic filling factors given by the sequences of states that we obtain from the MF ansatz. Finally, we show that quantum fluctuation in CS gauge fields restore the Kohn's theorem [55].

In the context of determination of wave functions, we may mention that Fradkin [56] has proposed a method for determining the absolute square of the many particle wave function for the ground state of a system from a knowledge of correlation functions which are generally computed in field theory. This beautiful method which employs the generating functions for equal-time correlation functions is applicable to any field theoretic problem. If one further knows before hand, or assumes, that the many particle system is non-degenerate, the many particle wave function is also determined thereby, apart from the gauge dependent phase which is essential in determining expectation values of observables such as velocity. Using this formalism, LF [54] have extracted the wave functions for fully polarized QHS within the CFM. Remarkably, they recover the Jastrow part of the Laughlin wave functions unambiguously for filling fractions $\nu = 1/(2n+1)$ which have been known to be exact by the work of Haldane [57], and Kivelson and Trugman [58]. Note that this result vindicates the MF ansatz which one normally employs for the CS field. More generally, LF [54] show that the Jastrow form is indeed generic to all states with filling fractions $\nu = p/(2sp+1)$ (p, s are integer) which occur in the CFM. Further, the long distance properties of the many body wave function are universal, being independent of the microscopic charge-charge interaction. Yet another interesting aspect is that the wave functions are in general non-analytic. That is, the exponents that occur in the Jastrow form are arbitrary rational numbers. We discuss the origin of the non-analyticity below.

There are several other determinations of the wave functions for QHS apart from the one mentioned above. Zhang [59] has derived the Laughlin wave functions from a Chern-Simons-Landau-Ginzburg (CSLG) theory, which is developed by Zhang, Hansson, and Kivelson [60] for $\nu = 1/m$ (m odd) states. In this approach, a Gaussian approximation to the CSLG Lagrangian yields a set of harmonic oscillators, whose ground state is of Jastrow form, with the same long distance behaviour as that of Laughlin wave functions. Recently Rajaraman and Sondhi [61] have set up a bosonic field theory for the FQHE using an operator algebra based on Read's operator [62].

In their analysis, the Laughlin states are obtained at the MF level itself.[1] Ezawa and Iwazaki [63] and Moon *et al* [64] have derived Halperin (m.m.n) states for double layered system using CSLG theory by employing a procedure similar to that of Zhang [59]. As mentioned earlier, we follow the procedure of LF [54]. To that end we derive below the generating functional.

3.2 The generating functional

We now reinstate (weak) short-ranged interactions, which we neglected in the previous section while describing the model, between CF. Then the new Lagrangian density reads [see Eq. (2.7)]

$$\begin{aligned}\mathcal{L} &= \psi_\uparrow^* \mathcal{D}(A_\mu^\uparrow + a_\mu^+ + a_\mu^-)\psi_\uparrow + \psi_\downarrow^* \mathcal{D}(A_\mu^\downarrow + a_\mu^+ - a_\mu^-)\psi_\downarrow + \frac{\theta_+}{2}\epsilon^{\mu\nu\lambda} a_\mu^+ \partial_\nu a_\lambda^+ \\ &+ \frac{\theta_-}{2}\epsilon^{\mu\nu\lambda} a_\mu^- \partial_\nu a_\lambda^- - eA_0^{\text{in}}(x)\rho + \frac{1}{2}\int d^3x' A_0^{\text{in}}(x) V^{-1}(x-x') A_0^{\text{in}}(x') \,. \end{aligned} \tag{3.1}$$

with the new covariant derivative $D_\mu^r = \partial_\mu - ie(A_\mu + A_\mu^r + a_\mu^r + A_0^{\text{in}}\delta_{\mu 0})$, where we have introduced two external probes [2] A_μ^r ($r = \uparrow, \downarrow$), interacting with *only* the particles having spin index r. The field A_0^{in} is identified as an internal scalar potential. The fifth term in Eq. (3.1) describes the charge neutrality of the system. Finally, $V^{-1}(x - x')$ is the inverse of the electron interaction potential (in the operator sense). The quartic form of the interaction of CF would be achieved by an integration over A_0^{in} field.

We employ the path integral formalism to evaluate the partition function

$$\mathcal{Z}\left[A_\mu^\uparrow, A_\mu^\downarrow\right] = \int [da^r][dA_0^{\text{in}}][d\psi^r][d\psi^{r*}]\, e^{i\int d^3x \mathcal{L}(x)} \tag{3.2}$$

from the Lagrangian density in Eq. (3.1). We proceed with the evaluation of $\mathcal{Z}$ by performing the integration over the fermionic fields first. The resulting partition function can then be written in terms of the effective action

$$S = -i\sum_r \text{Tr}\ln\left[iD_0^r + \mu + \frac{1}{2m^*}D_k^{r2} + \frac{g}{2}\mu_B(B + b^r)\sigma\right]$$

[1] They have not considered the fluctuations.

[2] These probes are introduced merely for the calculation purposes, *viz.*, the mixed spin density-density correlations. However, any electromagnetic response of the system has to be determined with the real electromagnetic probe, as we shall do below.

$$+\int d^3x\frac{\theta_+}{2}\epsilon^{\mu\nu\lambda}a_\mu^+\partial_\nu a_\lambda^+ + \int d^3x\frac{\theta_-}{2}\epsilon^{\mu\nu\lambda}a_\mu^-\partial_\nu a_\lambda^- - e\int d^3x A_0^{\rm in}(x)\rho$$
$$+\frac{1}{2}\int d^3x\int d^3x' A_0^{\rm in}(x)V^{-1}(x-x')A_0^{\rm in}(x') \tag{3.3}$$

for the gauge fields, incorporating the bulk effect of fermions of the system.

3.2.1 Fixing of saddle point

The partition function $\mathcal{Z}$ will be approximated now by the expansion of the fields around a saddle point configuration of the action S (3.3) in powers of the fluctuations. Let the saddle point configuration of the gauge fields be

$$a_\mu^\pm(x) = \langle a_\mu^\pm(x)\rangle + \tilde{a}_\mu^\pm(x)\ ,\ A_0^{\rm in}(x) = \langle A_0^{\rm in}(x)\rangle + \tilde{A}_0^{\rm in}(x)\ , \tag{3.4}$$

where $\langle\cdots\rangle$ represents classical value and $\tilde{a}_\mu^\pm(x)$ and $\tilde{A}_0^{\rm in}(x)$ are the corresponding fluctuating parts. The saddle point configuration is of course fixed by demanding that S be stationary under small fluctuations. This requirement yields the classical equations of motion

$$\left.\frac{\delta S}{\delta a_\mu^\pm(x)}\right|_{\langle a_\mu^\pm\rangle,\langle A_0^{\rm in}\rangle} = 0 \Rightarrow \langle j^{\mu\pm}(x)\rangle + \frac{\theta_\pm}{2}\epsilon^{\mu\nu\lambda}\langle f_{\nu\lambda}(x)\rangle = 0\ , \tag{3.5}$$
$$\left.\frac{\delta S}{\delta \lambda(x)}\right|_{\langle a_\mu^\pm\rangle,\langle A_0^{\rm in}\rangle} = 0 \Rightarrow \langle j^0(x)\rangle - \rho + \int d^3x' V^{-1}(x-x')\langle A_0^{\rm in}(x')\rangle = 0\ , \tag{3.6}$$

where $\langle j^\mu(x)\rangle$ represents mean value of the fermionic charge and current. Uniform particle density implies

$$\langle j^{0+}(x)\rangle \equiv \langle j^0(x)\rangle = \rho\ ,\ \langle j^{0-}(x)\rangle = \rho_\uparrow - \rho_\downarrow \equiv \Delta\rho\ . \tag{3.7}$$

As LF [19] have pointed out, these classical equations possess more than one possible solution, *viz.*, the uniform (liquid) state and Wigner crystals. The solution with uniform particle density, which represents a liquid phase, is consistent provided

$$\langle A_0^{\rm in}(x)\rangle = 0\ . \tag{3.8}$$

We discuss only the liquid phase of QHE here.

3.2.2 Mean field ansatz

Since there is a vanishing mean current and non-zero mean particle density, the MF approximation provides (see Eq. 3.5) vanishing average of CS electric field, *i.e.*, $\langle \mathbf{e}^{\pm} \rangle = 0$ and a uniform CS magnetic field $\langle b^{\pm} \rangle$. As we have discussed in the previous chapter, b^- field is absent for unpolarized states while $\langle b^- \rangle = 0$ for partially polarized states. In any case, the net magnetic field $\bar{B}$ is a sum of $\langle b^+ \rangle$ and applied magnetic field B. Therefore the QHS at hand correspond to same gap of excitation for both the spins, *i.e.*, $\bar{\omega}_c^{\uparrow} = \bar{\omega}_c^{\downarrow} = \bar{\omega}_c = \frac{e}{m^*}\bar{B}$.

Let $p_{\uparrow}(p_{\downarrow})$ be the number of LL, which are formed by effective field $\bar{B}$, filled by spin up (down) particles. This leads to the actual filling fraction and spin density [see Eqs. (2.11), (2.19)–(2.21)] to be

$$\nu = \frac{p_{\uparrow} + p_{\downarrow}}{2s(p_{\uparrow} + p_{\downarrow}) + 1}, \quad \Delta\rho = \rho \left(\frac{p_{\uparrow} - p_{\downarrow}}{p_{\uparrow} + p_{\downarrow}} \right) . \tag{3.9}$$

Note that $p_{\uparrow}$ and $p_{\downarrow}$ can be negative integers as well in which case $\bar{B}$ is antiparallel to B. The effective cyclotron frequency $\bar{\omega}_c$ is related to the actual cyclotron frequency $\omega_c = \frac{e}{m^*}B$ by $\omega_c = \bar{\omega}_c[2s(p_{\uparrow} + p_{\downarrow}) + 1]$. For unpolarized QHS, $p_{\uparrow} = p_{\downarrow} = p$ (say) and therefore the states with filling fraction $v = 2p/(4sp + 1)$ are spin unpolarized in the limit of small Zeeman energy. In this limit, $p_{\uparrow} = p_{\downarrow} + 1$ for partially polarized states with $\Delta\rho/\rho = 1/(p_{\uparrow} + p_{\downarrow})$. Fully polarized Laughlin states are obtained for $p_{\uparrow} = 1$, $p_{\downarrow} = 0$. The IQHE states correspond to the choice $s = 0$ (*i.e.*, $\theta_+ = \infty$), in which case mean CS magnetic field is zero.

3.2.3 Gauge field fluctuations

Employing the above MF ansatz, we expand the action S given by Eq. (3.3) in powers of fluctuations of gauge fields. The quadratic term in powers of fluctuations is identified as one-loop effective action and is given by (dropping $\tilde{}$ for the fluctuations)

$$\begin{aligned} S^{(1)} &= -\frac{1}{2}\int d^3x \int d^3x' (A_\mu^{\uparrow} + a_\mu^+ + a_\mu^- + A_0^{\text{in}}\delta_{\mu 0}) \Pi_{\uparrow}^{\mu\nu}(x,x') (A_\nu^{\uparrow} + a_\nu^+ + a_\nu^- + A_0^{\text{in}}\delta_{\nu 0}) \\ &\quad -\frac{1}{2}\int d^3x \int d^3x' (A_\mu^{\downarrow} + a_\mu^+ - a_\mu^- + A_0^{\text{in}}\delta_{\mu 0}) \Pi_{\downarrow}^{\mu\nu}(x,x') (A_\nu^{\downarrow} + a_\nu^+ - a_\nu^- + A_0^{\text{in}}\delta_{\nu 0}) \end{aligned}$$

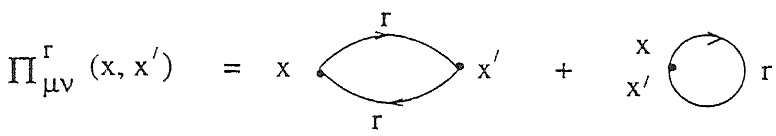

Figure 3.1: The polarization tensor $\Pi^r_{\mu\nu}(x,x')$ is diagrammatically shown. Here x and x' are two space-time points. In the second diagram, x and x' correspond to same space-time point. The lines with arrows represent the single particle Green's functions.

$$
\begin{aligned}
&+\int d^3x \left[\frac{\theta_+}{2}\epsilon^{\mu\nu\lambda}a^+_\mu\partial_\nu a^+_\lambda + \frac{\theta_-}{2}\epsilon^{\mu\nu\lambda}a^-_\mu\partial_\nu a^-_\lambda\right] \\
&+\frac{1}{2}\int d^3x \int d^3x' A^{\rm in}_0(x)V^{-1}(x-x')A^{\rm in}_0(x') \ ,
\end{aligned}
\tag{3.10}
$$

where the polarization tensors

$$
\Pi^{\mu\nu}_r(x,x') = \left.\frac{\delta^2 S}{\delta\mathcal{A}^r_\mu\delta\mathcal{A}^r_\nu}\right|_{\langle a^\pm_\mu\rangle,\langle A^{\rm in}_0\rangle} , \tag{3.11}
$$

$$
= -i\langle j^\mu_r(x)j^\nu_r(x')\rangle_C - \left\langle\frac{\delta j^\mu_r(x)}{\delta\mathcal{A}^r_\nu(x')}\right\rangle , \tag{3.12}
$$

which is diagrammatically shown in Fig. (3.1). Here $\langle\cdots\rangle$ represents the expectation value in the MF ground state, and C refers to the connected diagrams of the two particle correlation functions. $\mathcal{A}^r_\mu$ is the sum of all gauge fields interacting with the spin species r, and $j^\mu_r(x)$ is the fermionic current operator corresponding to spin index r. Note that the field a^-_μ in Eq. (3.10) does *not* exist for unpolarized states (see case–I in the previous chapter) and hence Eq. (3.10) reduces accordingly. In the partially polarized case, we have $s_- = 0$ (see (i) of case–II in the previous chapter), *i.e.*, $\theta_- = \infty$, a condition which we impose at the end of the calculation.

The fermionic current operators are given by

$$
j^r_0(x) = e\psi^{r*}(x)\psi^r(x) , \tag{3.13}
$$

$$
\begin{aligned}
j^r_k(x) = & \ i\frac{e}{2m^*}\left[\psi^{r*}(x)D^r_k\psi^r(x) - \left(D^{r*}_k\psi^{r*}(x)\right)\psi^r(x)\right] \\
&+\frac{g}{2}\mu_B\epsilon_{kj}\partial_j\left(\psi^{r*}(x)\sigma\psi^r(x)\right) ,
\end{aligned}
\tag{3.14}
$$

where the index r is the labeling for spins. The single particle Green's function

$$G^r(x,\, x') = -i\langle T\psi^r(x)\psi^{r*}(x')\rangle \tag{3.15}$$

can be obtained by solving the differential equation

$$(i\partial_0 - H^r + \mu)G^r(x,\, x') = \delta^{(3)}(x,\, x')\ , \tag{3.16}$$

subject to appropriate boundary conditions. Here $H^r = -\frac{1}{2m^*}D_k^{r2} - \frac{g}{2}\mu_B B\sigma$ is the Hamiltonian. Note that Green's function $G(x,\, x')$ is diagonal in spin space:

$$G = \begin{bmatrix} G^{\uparrow} & 0 \\ 0 & G^{\downarrow} \end{bmatrix}\ . \tag{3.17}$$

Thus using a suitable limiting procedure, one can express the mean fermionic current and polarization tensors respectively in terms of $G^r(x,\, x')$ as follows:

$$\begin{aligned}
\langle j_0^r(x)\rangle &= ieG^r(x,x')\Big|_{X'=X\,,\,t'=t+0^+}\ , && (3.18)\\
\langle j_k^r(x)\rangle &= -\frac{e}{2m^*}(D_k^r - D_k^{r\prime *})G^r(x.\, x')\Big|_{X'=X\,,\,t'=t+0^+} \\
&\quad + i\frac{g}{2}\mu_B\sigma\epsilon_{kj}\left(\partial_j G^r(x,x') + \partial_j' G^r(x,x')\right)\Big|_{X'=X\,,\,t'=t+0^+}\ , && (3.19)
\end{aligned}$$

$$\begin{aligned}
\Pi_{00}^r(x,x') &= ie^2 G^r(x,x')G^r(x',x)\ , && (3.20)\\
\Pi_{0k}^r(x,x') &= -\frac{e^2}{2m^*}\left[G^r(x,x')D_k^{r\prime}G^r(x',x) - \left(D_k^{r\prime *}G^r(x,x')\right)G^r(x',x)\right] \\
&\quad + ie\frac{g}{2}\mu_B\sigma\epsilon_{kj}\partial_j'\left[G^r(x,x')G^r(x',x)\right]\ , && (3.21)\\
\Pi_{kl}^r(x,x') &= -i\frac{e^2}{4m^{*2}}\left[D_k^r G^r(x,x')D_l^{\prime}G^r(x',x) - \left(D_k^r D_l^{r\prime *}G^r(x,x')\right)G^r(x',x)\right. \\
&\quad \left. + D_l^{r\prime *}G^r(x,x')D_k^{r*}G^r(x',x) - G^r(x,x')D_k^{r*}\ D_l^{r\prime}G^r(x',x)\right] \\
&\quad + i\frac{e^2}{2m}\delta_{kl}\left(\delta(x-x') + \delta(x''-x')\right)G^r(x,x'')\Big|_{X''=X\,,\,t''=t+0^+} \\
&\quad + i\frac{g^2}{4}\mu_B^2\epsilon_{ki}\epsilon_{lj}\sigma^2\partial_i\partial_j'\left[G^r(x,x')G^r(x',x)\right] \\
&\quad + \frac{e}{2m^*}\left(\frac{g}{2}\right)\mu_B\sigma\epsilon_{jk}\partial_j\left[G^r(x,x')D_l^{r\prime}G^r(x',x) - \left(D_l^{r*\prime}G^r(x,x')\right)G(x',x)\right] \\
&\quad + \frac{e}{2m^*}\left(\frac{g}{2}\right)\mu_B\sigma\epsilon_{jl}\partial_j'\left[\left(D_k^r G^r(x,x')\right)G^r(x',x) - G^r(x,x')D_k^{r*}G(x',x)\right]\ .
\end{aligned} \tag{3.22}$$

Note also that $\Pi^{\mu\nu}(x, x')$ is diagonal in spin space. Also, by the gauge invariance of the one-loop effective action in Eq. (3.10), we have

$$\partial^x_\mu \Pi^{\mu\nu}_\tau(x, x') = 0\,. \tag{3.23}$$

The one-loop effective action in the Fourier space reads

$$\begin{aligned} S^{(1)} &= -\frac{1}{2}\int\frac{d^3q}{(2\pi)^3}(A^\uparrow_\mu + a^+_\mu + a^-_\mu + A^{\rm in}_0\delta_{\mu 0})\Pi^{\mu\nu}_\uparrow(\omega\,,\,\mathbf{q})(A^\uparrow_\nu + a^+_\mu + a^-_\mu + A^{\rm in}_0\delta_{\nu 0}) \\ &\quad -\frac{1}{2}\int\frac{d^3q}{(2\pi)^3}(A^\downarrow_\mu + a^+_\mu - a^-_\mu + A^{\rm in}_0\delta_{\mu 0})\Pi^{\mu\nu}_\downarrow(\omega\,,\,\mathbf{q})(A^\downarrow_\nu + a^+_\mu - a^-_\mu + A^{\rm in}_0\delta_{\nu 0}) \\ &\quad +\frac{i}{2}\int\frac{d^3q}{(2\pi)^3}\left[\frac{\theta_+}{2}\epsilon^{\mu\nu\lambda}a^+_\mu q_\nu a^+_\lambda + \frac{\theta_-}{2}\epsilon^{\mu\nu\lambda}a^-_\mu q_\nu a^-_\lambda\right] \\ &\quad +\frac{1}{2}\int\frac{d^3q}{(2\pi)^3}A^{\rm in}_0 V^{-1}(|\mathbf{q}|)A^{\rm in}_0\,. \end{aligned} \tag{3.24}$$

As a consequence of gauge, translational, and rotational invariances the polarization tensors $\Pi^{\mu\nu}_{\uparrow,\downarrow}(\omega,\,\mathbf{q})$ can be resolved as:

$$\begin{aligned} \Pi^{\mu\nu}_{\uparrow,\downarrow}(\omega,\,\mathbf{q}) &= \Pi^{\uparrow,\downarrow}_0(\omega,\,\mathbf{q})(q^2 g^{\mu\nu} - q^\mu q^\nu) + \left(\Pi^{\uparrow,\downarrow}_2(\omega,\,\mathbf{q}) - \Pi^{\uparrow,\downarrow}_0(\omega,\,\mathbf{q})\right) \\ &\quad \times\left(\mathbf{q}^2\delta^{ij} - q^i q^j\right)\delta^{\mu i}\delta^{\nu j} + i\Pi^{\uparrow,\downarrow}_1(\omega,\,\mathbf{q})\epsilon^{\mu\nu\lambda}q_\lambda\,, \end{aligned} \tag{3.25}$$

where $q^2 = \omega^2 - \mathbf{q}^2$. Here $\Pi^{\uparrow,\downarrow}_1$ are the $\mathcal{P}$, $\mathcal{T}$ violating form factors. An evaluation of the above form factors in the lowest order in $\mathbf{q}^2$ yields (see Appendix A for details)

$$\Pi^{\uparrow,\downarrow}_0(\omega,\,\mathbf{q}) = -\left(\frac{e^2}{2\pi}\right)\frac{\bar\omega_c}{\omega^2 - \bar\omega_c^2}p_{\uparrow,\downarrow}\,, \tag{3.26}$$

$$\Pi^{\uparrow,\downarrow}_1(\omega,\,\mathbf{q}) = -\left(\frac{e^2}{2\pi}\right)\frac{\bar\omega_c^2}{\omega^2 - \bar\omega_c^2}p_{\uparrow,\downarrow}\,, \tag{3.27}$$

$$\Pi^{\uparrow,\downarrow}_2(\omega,\,\mathbf{q}) = -\frac{e^2}{4\pi m^*}\bar\omega_c^2\left[\frac{3}{\omega^2 - \bar\omega_c^2} - \frac{4}{\omega^2 - 4\bar\omega_c^2}\right]p_{\uparrow,\downarrow}\left(p_{\uparrow,\downarrow} - \frac{g}{2}\frac{m^*}{m_e}\sigma\right)\,. \tag{3.28}$$

3.2.4 The effective action

Since the effective action $S^{(1)}$ in Eq. (3.24) is quadratic in a^+_μ, a^-_μ, and $A^{\rm in}_0$, we can integrate out these fields and obtain the effective action for the external probes $A^{\uparrow,\downarrow}_\mu$.

Performing the integrations[3] in Eq. (3.24), we obtain the effective action for external probes to be

$$S_{\text{eff}}\left[A_\mu^\uparrow, A_\mu^\downarrow\right] = \frac{1}{2}\int \frac{d^3q}{(2\pi)^3} A_\mu^r(q)\tilde{K}_{rr'}^{\mu\nu}(\omega, \mathbf{q})A_\nu^{r'}(-q) \,. \tag{3.29}$$

where the indices r, $r' = \uparrow, \downarrow$. Here $\tilde{K}_{rr'}^{\mu\nu}(\omega, \mathbf{q})$ is the effective polarization tensor, which is also the response functions. Note that, unlike $\Pi^{\mu\nu}$, $\tilde{K}_{rr'}^{\mu\nu}$ is not diagonal in spin space: the CS gauge field fluctuations mix up the spin degree of freedom in current correlations. It is sufficient for our purposes to evaluate the density-density correlation functions $\tilde{K}_{rr'}^{00}$. We find (for low $\mathbf{q}^2$)

$$\begin{aligned}
\tilde{K}_{\uparrow\uparrow}^{00} &= \frac{\mathbf{q}^2}{\Pi_0^\uparrow + \Pi_0^\downarrow}\left[\Pi_0^\uparrow\Pi_0^\downarrow - \frac{\Pi_0^{\uparrow 2}\theta_+^2}{\left(\Pi_0^\uparrow + \Pi_0^\downarrow\right)^2\omega^2 - \left(\Pi_1^\uparrow + \Pi_1^\downarrow + \theta_+\right)^2}\right] + \mathcal{O}(\mathbf{q}^4) \,, && (3.30)\\
\tilde{K}_{\downarrow\downarrow}^{00} &= \frac{\mathbf{q}^2}{\Pi_0^\uparrow + \Pi_0^\downarrow}\left[\Pi_0^\uparrow\Pi_0^\downarrow - \frac{\Pi_0^{\downarrow 2}\theta_+^2}{\left(\Pi_0^\uparrow + \Pi_0^\downarrow\right)^2\omega^2 - \left(\Pi_1^\uparrow + \Pi_1^\downarrow + \theta_+\right)^2}\right] + \mathcal{O}(\mathbf{q}^4) \,, && (3.31)\\
\tilde{K}_{\uparrow\downarrow}^{00} &= -\frac{\mathbf{q}^2}{\Pi_0^\uparrow + \Pi_0^\downarrow}\left[\Pi_0^\uparrow\Pi_0^\downarrow + \frac{\Pi_0^\uparrow\Pi_0^\downarrow\theta_+^2}{\left(\Pi_0^\uparrow + \Pi_0^\downarrow\right)^2\omega^2 - \left(\Pi_1^\uparrow + \Pi_1^\downarrow + \theta_+\right)^2}\right] + \mathcal{O}(\mathbf{q}^4) , && (3.32)\\
\tilde{K}_{\downarrow\uparrow}^{00} &= \tilde{K}_{\uparrow\downarrow}^{00} \,, && (3.33)
\end{aligned}$$

subject to the condition $\lim_{\mathbf{q}^2\to 0} V(\mathbf{q})\mathbf{q}^2 = 0$. In other words, we assume the inter fermion potential is more short ranged compared to $\ln 1/r$. Here $\tilde{K}_{\uparrow\uparrow}^{00}$, $\tilde{K}_{\uparrow\downarrow}^{00}$, $\tilde{K}_{\downarrow\uparrow}^{00}$ and $\tilde{K}_{\downarrow\downarrow}^{00}$ represent the density-density correlations among spin up-up, up-down, down-up and down-down species of the particles respectively.

Recall that a_μ^- field is dynamically absent for unpolarized QHS in Eq. (3.24): the integration is performed only over a_μ^+ field in this case. On the other hand, for partially polarized QHS, a_μ^- field is present at the fluctuation level. Therefore, in this case, the integrations are performed both for a_μ^+ and a_μ^- fields. At the end of the calculation, the limit $s = 0$ (*i.e.*, $\theta_- = \infty$) is taken for partially polarized QHS. The expressions (3.30)–(3.33) hold both for unpolarized as well as partially polarized QHS, although the procedures for evaluating them are different in two cases. The higher order terms in

[3] One convenient gauge choice is to chose the Coulomb gauge $q_i A_i^r = 0$, $q_i a_i^\pm = 0$.

q^2 which we have dropped in Eqs. (3.30–3.33) do not contribute in the thermodynamic limit.

3.3 The wave functions

As Fradkin [56] has shown, for deriving the absolute square of the many body wave function for the ground state of a field theory, one needs the generating functional of equal-time correlation functions. We consider here the density representation. The eigen states of the density operator, $\delta\hat{\rho}_r(X)$ provide a basis for (the subspace of) states with a fixed number of particles having spin index r. We project out the ground state of the system in this basis.

As we need only equal-time density-density correlations, the fields $A_0^\uparrow$ and $A_0^\downarrow$ of the probes need to act only at one time, say t_0. In other words, let

$$A_0^r(x) = A_0^r(X)\delta(x_0 - t_0) \tag{3.34}$$

and let the space-like components of $A_\mu^r(x)$ be zero. By substituting this in Eq. (3.29), we evaluate the generating functional for equal-time density-density correlation matrix $K_{rr'}^{00}$. This is given by

$$\mathcal{Z}\left[A_0^\uparrow, A_0^\downarrow\right] = \exp\left[-\frac{1}{2}\int\frac{d^2\mathbf{q}}{(2\pi)^2}A_0^r(\mathbf{q})\mathcal{K}_{rr'}(\mathbf{q})A_0^{r'}(-\mathbf{q})\right] \tag{3.35}$$

with

$$\mathcal{K}_{rr'}(\mathbf{q}) = \int\frac{d\omega}{2\pi i}K_{rr'}^{00}(\omega\,,\,\mathbf{q}) \tag{3.36}$$

which we obtain as

$$\mathcal{K} = \frac{\mathbf{q}^2}{2\pi}\left(\frac{e^2}{2}\right)\frac{1}{(p_\uparrow + p_\downarrow)}\begin{bmatrix} p_\uparrow p_\downarrow + \frac{p_\uparrow^2}{2s(p_\uparrow+p_\downarrow)+1} & -p_\uparrow p_\downarrow + \frac{p_\uparrow p_\downarrow}{2s(p_\uparrow+p_\downarrow)+1} \\ -p_\uparrow p_\downarrow + \frac{p_\uparrow p_\downarrow}{2s(p_\uparrow+p_\downarrow)+1} & p_\uparrow p_\downarrow + \frac{p_\downarrow^2}{2s(p_\uparrow+p_\downarrow)+1}\end{bmatrix}. \tag{3.37}$$

Using the same procedure as employed by LF [54], we write the square of the modulus of the ground state (non-degenerate) wave function for QHS of mixed spin as

$$|\Psi[\rho_\uparrow,\rho_\downarrow]|^2 = \int[dA_0^\uparrow][dA_0^\downarrow]\mathcal{Z}[A_0^\uparrow, A_0^\downarrow]\exp\left[-ie\int\frac{d^2\mathbf{q}}{(2\pi)^2}A_0^r(\mathbf{q})\delta\rho_r(-\mathbf{q})\right], \tag{3.38}$$

where $\delta\rho_r(\mathbf{q})$ is the Fourier transform of the density fluctuation

$$\delta\rho_r(X) = \sum_{i=1}^{N_r} \delta(X - X_i^r) - \rho_r \ , \tag{3.39}$$

which is the eigen value of $\delta\hat{\rho}_r(X)$. Here N_r is the number of particles with spin index $r(=\uparrow,\downarrow)$, ρ_r is the corresponding mean density, and $X_i(r)$ is the position of i-th particle. Now the integrations over $A_0^\uparrow$ and $A_0^\downarrow$ in Eq. (3.38) yield

$$|\Psi[\rho_\uparrow,\rho_\downarrow]|^2 = \exp\left[\frac{e^2}{2}\int \frac{d^2\mathbf{q}}{(2\pi)^2}\delta\rho_r(\mathbf{q})\mathcal{K}_{rr'}^{-1}(\mathbf{q})\delta\rho_{r'}(-\mathbf{q})\right] \ . \tag{3.40}$$

The following remarks are in order here before we evaluate (3.40) for various cases. Note that we determine only the modulus square of the many body wave function. The corresponding wave function would have a phase which is, in general, gauge dependent. The phase is further required to ensure proper symmetry under the exchange of particles. It may be seen that so long as the Jastrow form of the wave function is known to be a monomial in the relative coordinates, it is easy to project out the antisymmetric part by supplying the appropriate phases. To that extent, the wave function gets determined in this formalism. This procedure would, however, fail if the many particle density (and hence the wave function) is a multinomial expression in the relative coordinates. In such a case, there does not seem to be any procedure to construct the wave function with proper symmetry. One would then have to be contented with a determination of the density. We may also remark that the Jastrow form of the densities that we have obtained in this paper are proper monomials in relative coordinates.

An exception would occur when the antisymmetric projection identically vanishes. Clearly, this signifies an incorrect/incomplete evaluation of the density density correlator. We find (see below) that the $\nu = 1/2s$ states fall into this category. Presumably, the formalism employed to evaluate $K_{rr'}^{\mu\nu}$ is inadequate for these states. Not very surprisingly so since these states correspond to $\bar{B} = 0$, where the Landau level picture breaks down.

We shall continue to use the word wave function loosely to mean the densities in subsequent sections.

3.3.1 Unpolarized states

For the unpolarized states, both up and down spins are equally populated. Therefore, $\rho_\uparrow = \rho_\downarrow = \rho/2$ and $N_\uparrow = N_\downarrow = N/2$ where N is the total number of particles. We also have seen that $p_\uparrow = p_\downarrow \equiv p$ for unpolarized states. Plugging these values in Eq. (3.37) and employing it in Eq. (3.40), we obtain

$$\begin{aligned}
|\Psi[\rho_\uparrow, \rho_\downarrow]|^2 &= \exp\left[\frac{2sp+1}{p}\int d^2X \int d^2Y \delta\rho_\uparrow(X) \ln\frac{|X-Y|}{R}\delta\rho_\uparrow(Y)\right] \\
&\times \exp\left[\frac{2sp+1}{p}\int d^2X \int d^2Y \delta\rho_\downarrow(X) \ln\frac{|X-Y|}{R}\delta\rho_\downarrow(Y)\right] \\
&\times \exp\left[2(2s)\int d^2X \int d^2Y \delta\rho_\uparrow(X) \ln\frac{|X-Y|}{R}\delta\rho_\downarrow(Y)\right], \qquad (3.41)
\end{aligned}$$

where we have transformed back into the real space. We have further introduced a long-distance cut off R which is the system radius. Both the magnetic length and inter-particle distance are much less than R. From Eqs. (3.39 and 3.41), it follows that the modulus square of the many body wave function for the ground state of unpolarized QHS having filling fraction $\nu = 2p/(4sp+1)$ is

$$\begin{aligned}
\left|\Psi\left(X_1^\uparrow, \cdots, X_{N/2}^\uparrow, X_1^\downarrow, \cdots, X_{N/2}^\downarrow\right)\right|^2 &= \prod_{i<j}^{N/2} \left|X_i^\uparrow - X_j^\uparrow\right|^{2(2sp+1)/p} \\
&\times \prod_{k<l}^{N/2} \left|X_k^\downarrow - X_l^\downarrow\right|^{2(2sp+1)/p} \prod_{i,k}^{N/2} \left|X_i^\uparrow - X_k^\downarrow\right|^{2(2s)} \\
&\times \exp\left[-\frac{1}{2l^2}\left(\sum_{i=1}^{N/2}\left|X_i^\uparrow\right|^2 + \sum_{k=1}^{N/2}\left|X_k^\downarrow\right|^2\right)\right], \qquad (3.42)
\end{aligned}$$

where $X_i^\uparrow(X_i^\downarrow)$ represents the co-ordinate of i-th spin-up (down) particle and $l = (eB)^{-1/2}$ is the magnetic length of the system.

(i) Consider the unpolarized state with $\nu = 2$ which corresponds to the choice $s = 0$ and $p = 1$. Thus the $|\Psi|^2_{\nu=2}$ is given by

$$|\Psi|^2_{\nu=2} = \prod_{i<j}^{N/2} |X_i^\uparrow - X_j^\uparrow|^2 \prod_{k<l}^{N/2} |X_i^\downarrow - X_j^\downarrow|^2 \times \exp\left[-\frac{1}{2l^2}\left(\sum_{i=1}^{N/2}\left|X_i^\uparrow\right|^2 + \sum_{k=1}^{N/2}\left|X_k^\downarrow\right|^2\right)\right], \qquad (3.43)$$

which is well known (see Ref. [65]).

(ii) The spin unpolarized wave function of $\nu = 2/5$ state which corresponds to the choice $s = 1$ and $p = 1$ is obtained from Eq. (3.42) as

$$
\begin{aligned}
|\Psi|^2_{\nu=2/5} &= \prod_{i<j}^{N/2} |X_i^\uparrow - X_j^\uparrow|^6 \prod_{k<l}^{N/2} |X_i^\downarrow - X_j^\downarrow|^6 \prod_{i,k}^{N/2} |X_i^\uparrow - X_j^\downarrow|^4 \\
&\quad \times \exp\left[-\frac{1}{2l^2}\left(\sum_{i=1}^{N/2} \left|X_i^\uparrow\right|^2 + \sum_{k=1}^{N/2} \left|X_k^\downarrow\right|^2\right)\right] . \qquad (3.44)
\end{aligned}
$$

This is exactly the same wave function as proposed by Halperin [34] for unpolarized $\nu = 2/5$ state.

(iii) The Jastrow part of the $|\Psi|^2$ in Eq. (3.42) can be written as

$$
|\Psi|^2 \sim \left[\prod_{i<j}^{N/2} |X_i^\uparrow - X_j^\uparrow|^{2s} \prod_{k<l}^{N/2} |X_i^\downarrow - X_j^\downarrow|^{2s} \prod_{i,k}^{N/2} |X_i^\uparrow - X_j^\downarrow|^{2s}\right]^2 \chi_p^2 . \qquad (3.45)
$$

where

$$
\chi_p = \prod_{i<j}^{N/2} |X_i^\uparrow - X_j^\uparrow|^{1/p} \prod_{k<l}^{N/2} |X_i^\downarrow - X_j^\downarrow|^{1/p} \qquad (3.46)
$$

is the wave function for the integer filling state p. This Ψ is indeed the same wave function as proposed by Jain *et al* [48, 66] for unpolarized states with $\nu = 2p/(4sp + 1)$.

(iv) However, the wave functions (3.42) differ (except for the state $\nu = 2/5$) from the trial wave functions for the sequence $\nu = 2n/(3n + 2)$, proposed by Belkhir and Jain [51]. This is not surprising because their proposal regarding vortices associated with spins does not lead to unpolarized state, as we have seen in the previous chapter (see (iii) of Case–II).

(v) We now consider the states $\nu = 1/2s$. The wave functions are obtained, from Eq. (3.42) in the limit $p = \infty$, and read

$$
\begin{aligned}
|\Psi|^2_{\nu=1/2s} &= \left[\prod_{i<j}^{N/2} |X_i^\uparrow - X_j^\uparrow|^{2s} \prod_{k<l}^{N/2} |X_i^\downarrow - X_j^\downarrow|^{2s} \prod_{i,k}^{N/2} |X_i^\uparrow - X_j^\downarrow|^{2s}\right]^2 \\
&\quad \times \exp\left[-\frac{1}{2l^2}\left(\sum_{i=1}^{N/2} \left|X_i^\uparrow\right|^2 + \sum_{k=1}^{N/2} \left|X_k^\downarrow\right|^2\right)\right] . \qquad (3.47)
\end{aligned}
$$

These densities are clearly unphysical, since the antisymmetric projection of their corresponding wave functions vanishes identically. In fact, our result disagrees with the

ones determined by Haldane and Rezayi [67]. As we remarked earlier, this may be due to the breakdown of the Landau level picture for these states.

(vi) The $|\Psi|^2$ for spin unpolarized IQHE states, which correspond to the choice $s = 0$, is given by

$$|\Psi|^2_{\nu=2p} = \prod_{i<j}^{N/2} |X_i^\uparrow - X_j^\uparrow|^{2/p} \prod_{k<l}^{N/2} |X_i^\downarrow - X_j^\downarrow|^{2/p} \times \exp\left[-\frac{1}{2l^2}\left(\sum_{i=1}^{N/2}\left|X_i^\uparrow\right|^2 + \sum_{k=1}^{N/2}\left|X_k^\downarrow\right|^2\right)\right] . \tag{3.48}$$

Note that Unlike the FQHE states, the IQHE wave functions have vanishing exponent of the overlapping Jastrow factor $|X_i^\uparrow - X_k^\downarrow|$. Therefore particles with unlike spins are uncorrelated for the integer states. We can see it from Eq. (3.37) as well since the matrix $\mathcal{K}$ is diagonal for the choice $p_\uparrow = p_\downarrow$ and $s = 0$.

Clearly the wave functions (3.42) are analytic only for the states with $\nu = 2/(4s \pm 1)$ which corresponds to $p = \pm 1$. On the other hand, all the states with other finite p are non-analytic, in the sense that they become multivalued. The reason behind analyticity/non-analyticity will be discussed in section (3.3.4).

3.3.2 Partially/Fully polarized states

Partially polarized states have unequal population in spin species. As discussed earlier, for small Zeeman energy, let $p_\uparrow = p_\downarrow + 1$. The filling fraction and the corresponding spin densities are given in Eq. (3.9). Therefore, $\rho_{\uparrow,\downarrow} = \rho[p_{\uparrow,\downarrow}/(p_\uparrow + p_\downarrow)]$ and $N_{\uparrow,\downarrow} = N[p_{\uparrow,\downarrow}/(p_\uparrow + p_\downarrow)]$. Using the same procedure as discussed for unpolarized states in section (3.3.1), we obtain the wave function for the ground state of partially/fully polarized states from Eqs. (3.37)-(3.40),

$$\begin{aligned}\left|\Psi\left(X_1^\uparrow, \cdots, X_{N_\uparrow}^\uparrow, X_1^\downarrow, \cdots, X_{N_\downarrow}^\downarrow\right)\right|^2 &= \prod_{i<j}^{N_\uparrow}\left|X_i^\uparrow - X_j^\uparrow\right|^{2(2sp_\uparrow+1)/p_\uparrow} \\ &\quad\times \prod_{k<l}^{N_\downarrow}\left|X_k^\downarrow - X_l^\downarrow\right|^{2(2sp_\downarrow+1)/p_\downarrow} \prod_{i,k}^{N_\uparrow,N_\downarrow}\left|X_i^\uparrow - X_k^\downarrow\right|^{2(2s)} \\ &\quad\times \exp\left[-\frac{1}{2l^2}\left(\sum_{i=1}^{N_\uparrow}\left|X_i^\uparrow\right|^2 + \sum_{k=1}^{N_\downarrow}\left|X_k^\downarrow\right|^2\right)\right] .\end{aligned} \tag{3.49}$$

(i) Rearranging the Jastrow part of the $|\Psi|^2$ in Eq. (3.49), we write

$$|\Psi|^2 = \left(\prod_{i<j}^{N_\uparrow} \left|X_i^\uparrow - X_j^\uparrow\right|^{2(2s)} \prod_{k<l}^{N_\downarrow} \left|X_k^\downarrow - X_l^\downarrow\right|^{2(2s)} \prod_{i,k}^{N_\uparrow, N_\downarrow} \left|X_i^\uparrow - X_k^\downarrow\right|^{2(2s)} \right) \chi^2_{p_\uparrow, p_\downarrow} \cdot \tag{3.50}$$

where

$$\chi_{p_\uparrow; p_\downarrow} = \prod_{i<j}^{N_\uparrow} \left|X_i^\uparrow - X_j^\uparrow\right|^{1/p_\uparrow} \prod_{k<l}^{N_\downarrow} \left|X_k^\downarrow - X_l^\downarrow\right|^{1/p_\downarrow} \tag{3.51}$$

is the wave function for integer fillings— $p_\uparrow$ and $p_\downarrow$ for spin up and down particles respectively. Eq. (3.50) is exactly the one proposed wave functions by Wu, Dev, and Jain [48] for partially polarized states.

(ii) The choice $s = 0$ again corresponds to partially polarized IQHE states with

$$\begin{aligned} |\Psi|^2_{\nu=p_\uparrow+p_\downarrow} &= \prod_{i<j}^{N_\uparrow} \left|X_i^\uparrow - X_j^\uparrow\right|^{2/p_\uparrow} \prod_{k<l}^{N_\downarrow} \left|X_k^\downarrow - X_l^\downarrow\right|^{2/p_\downarrow} \\ &\times \exp\left[-\frac{1}{2l^2} \left(\sum_{i=1}^{N_\uparrow} \left|X_i^\uparrow\right|^2 + \sum_{k=1}^{N_\downarrow} \left|X_k^\downarrow\right|^2 \right) \right] . \end{aligned} \tag{3.52}$$

Note again that the particles with unlike spins are uncorrelated for partially polarized (like unpolarized) IQHE states, as also can be seen from Eq. (3.37).

(iii) The determination of $|\Psi|^2$ for fully polarized QHS from Eq. (3.49) requires a slightly special treatment. For fully polarized QHS, $p_\downarrow = 0$, All the form factors (3.26–3.28) corresponding to spin down particles vanish and hence the effective action (3.24) is entirely for the spin up species. We therefore drop the factors corresponding to spin-down particles in Eq. (3.49) and set $N_\uparrow = N$. Then

$$|\Psi|^2_{\nu=p_\uparrow/(2sp_\uparrow+1)} = \prod_{i<j}^{N} \left|X_i^\uparrow - X_j^\uparrow\right|^{2(2sp_\uparrow+1)/p_\uparrow} \times \exp\left[-\frac{1}{2l^2} \sum_{i=1}^{N} \left|X_i^\uparrow\right|^2 \right] , \tag{3.53}$$

which has been obtained by LF [54] in their pioneering work, considering spinless system from the very beginning. The $|\Psi|^2$ for fully polarized Laughlin sequence can be obtained for $p_\uparrow = 1$ from Eq. (3.53).

It is clear that the wave functions are non-analytic for $p_\uparrow > 1$, which is the case for partial polarization. However, for $p_\uparrow = 1$ and $p_\downarrow = 0$, which essentially gives fully polarized Laughlin sequence, (3.53) is analytic, in agreement with the result of LF [54] for spinless systems.

3.3.3 General remarks

While an infrared cut-off required to capture the exponential part of Eqs. (3.42) and (3.49), the Jastrow part of the wave functions is obtained unambiguously. The wave functions in Eqs. (3.42) and (3.49) are evaluated in the thermodynamic limit ($R \to \infty$) but not really for an infinite system, as a consequence these are not translationally invariant. At this juncture, we recall that the well known Laughlin wave functions have also broken translational symmetry.

As LF [54] have argued for fully polarized QHS, the above non-analytic nature of the wave functions suggests that in a general case, for unpolarized or fully polarized QHS, the wave functions cannot be written in terms of single particle states of the lowest LL, even in the limit $B \to \infty$.

Recall that we have derived the $|\Psi|^2$ at large distances compared to the effective magnetic length l_0. At length scale comparable with l_0, short distance effects become important. Details of the fermion-fermion interaction also will play some role. At these length scales, $|\Psi|^2$ may not have the Jastrow form. However, the procedure for evaluation of $|\Psi|^2$ will go through.

Finally, since we recover the well known wave functions: (i) Laughlin fully polarized wave function for $\nu = 1/(2n+1)$ states, (ii) Halperin wave function for unpolarized $\nu = 2/5$ state, it is our belief that the model employed here is viable.

3.3.4 Source of analyticity/non-analyticity

We have seen that the densities that we have determined involve, in general, fractional exponents in the relative coordinates. The corresponding wave functions (in the complex relative coordinate) will be non-analytic, *i.e.*, multivalued. The only exceptions occur when the exponent is an even integer, as it happen, *e.g.*, in the case of Laughlin states.

To gain further insight, let us write the Jastrow part of the wave function for

unpolarized states (3.42) in the form,

$$
\begin{aligned}
|\Psi|^2 \;\approx\; & \prod_{i<j}^{N/2} \left|X_i^{\uparrow} - X_j^{\uparrow}\right|^{2\left((1/\theta)+(1/\Pi_1^{\uparrow})\right)e^2/(2\pi)} \prod_{k<l}^{N/2} \left|X_k^{\downarrow} - X_l^{\downarrow}\right|^{2\left((1/\theta)+(1/\Pi_1^{\downarrow})\right)e^2/(2\pi)} \\
& \times \prod_{i,k}^{N/2} \left|X_i^{\uparrow} - X_k^{\downarrow}\right|^{2(1/\theta)e^2/(2\pi)} \quad ,
\end{aligned}
\tag{3.54}
$$

where $\Pi_1^{\uparrow,\downarrow}$ are evaluated at $\omega = 0\,,\ \mathrm{q}^2 = 0$. Note that the exponents of the Jastrow forms are determined by the parity and time reversal violating factors of the effective action given by Eqs. (3.24) and (3.25) . $1/\theta$ is always an even integral multiple of $(2\pi/e^2)$, and depending on the effective filling factor p, $1/\Pi_1^{\uparrow,\downarrow}$ should either be an integral or fractional multiple of $(2\pi/e^2)$. Therefore the wave function becomes analytic when $1/\Pi_1^{\uparrow,\downarrow}$ is an integral multiple of $(2\pi/e^2)$, *i.e.*, only for $p = \pm 1$, while for other values of p, $1/\Pi_1^{\uparrow,\downarrow}$ is fractional multiple of $(2\pi/e^2)$ and hence the wave function becomes non-analytic.

Indeed, the exponents describe the number of effective vortices associated with a particle which is seen by others and therefore the exponents of the Jastrow form between like spin particles differ from the same between unlike spins. It is natural that Ψ should reflect the nature of vortices associated with the fermion. Ψ is determined from the density-density correlations which represent, in fact, the change in local density of the system and hence the change in CS magnetic field. This causes a change in the local current which is represented by the vortices.

A similar argument for analyticity/non-analyticity also holds for partially/fully polarized QHS.

3.4 Kohn's mode and Hall conductivity

We have introduced the external probes $A_\mu^{\uparrow,\downarrow}$, purely for computational purposes, *viz.*, for determining the mixed spin density-density correlations which are used to determine the ground state wave functions of QHS. All the electromagnetic responses of the system are determined by the physical electromagnetic probe A_μ which couples to both the spins. It is not necessary to compute the response function *de novo*, since,

the correlations found from the probes $A_\mu^{\uparrow,\downarrow}$ are related to that from the probe A_μ. If we write

$$S_{\text{eff}}[A_\mu] = \frac{1}{2}\int \frac{d^3q}{(2\pi)^3} A_\mu(q) K^{\mu\nu}(\omega,\, \mathbf{q}) A_\nu(-q)\ , \tag{3.55}$$

the electromagnetic response tensor $K^{\mu\nu}$ is related to $K^{\mu\nu}_{rr'}$ (which we have evaluated with the probes $A_\mu^{\uparrow,\downarrow}$), through

$$K^{\mu\nu} = \sum_{r,r'} K^{\mu\nu}_{rr'}\ . \tag{3.56}$$

Having thus determined $K^{\mu\nu}$, considering translational and gauge invariance, we write

$$K^{\mu\nu} = K_0(q^2 g^{\mu\nu} - q^\mu q^\nu) + (K_2 - K_0)(\mathbf{q}^2\delta^{ij} - q^i q^j)\delta^{\mu i}\delta^{\nu j} + iK_1\epsilon^{\mu\nu\lambda}q_\lambda\ , \tag{3.57}$$

where K_0, K_1 and K_2 are functions of ω and $\mathbf{q}^2$.

3.4.1 Kohn's mode

The density-density correlation function can then be evaluated in the limit $\mathbf{q}^2 \to 0$ as

$$K^{00}(\omega\,,\, \mathbf{q}^2) \equiv -K_0\mathbf{q}^2 = -\left(\frac{e^2\rho}{m^*}\right)\frac{\mathbf{q}^2}{\omega^2 - \omega_c^2} + \mathcal{O}((\mathbf{q}^2)^2) \tag{3.58}$$

which is the same for both the cases, *i.e.*, unpolarized and polarized states.

Note that Eq. (3.58) depends only on ω_c, the actual cyclotron frequency. Indeed, while magnetic invariance is broken due to attachment of fluxes to particles, for translationally invariant system, the magnetic symmetry must be restored. Therefore the centre of mass of the particles should move with the actual cyclotron frequency ω_c, in accordance with Kohn's theorem [55]. Thus while the form factors in (3.26–3.28) with a dependence on $\bar{\omega}_c$ seem to violate Kohn's theorem, we see that the fluctuations of the CS gauge fields in fact do restore it.

3.4.2 Saturation of f-sum rule

The long wave length form of $K^{00}(\omega,\, \mathbf{q})$ in Eq. (3.58), calculated in the MF ansatz, saturates the f-sum rule, *i.e.*,

$$\int \frac{d\omega}{2\pi i}\omega K^{00}(\omega,\, \mathbf{q}) = \frac{e^2\rho}{m^*}\mathbf{q}^2\ . \tag{3.59}$$

Therefore the higher order fluctuations ('non Gaussian') in the gauge fields do not contribute to the correlation functions at very low q^2.

3.4.3 Hall conductivity

Finally, We obtain the Hall conductivity of the system to be

$$\sigma_H \equiv K_1(0,0) = \frac{\left(\Pi_1^{\uparrow}(0,0) + \Pi_1^{\downarrow}(0,0)\right)\theta_-}{\left(\Pi_1^{\uparrow}(0,0) + \Pi_1^{\downarrow}(0,0)\right) + \theta_-} . \tag{3.60}$$

which on substitution yields

$$\sigma_H = \nu(e^2/2\pi) , \tag{3.61}$$

with the value of ν given by Eq. (3.9). We have thus verified that σ_{xy} does indeed get quantized at the filling factors obtained from the MF ansatz.

3.5 Comparison with bilayered systems

Before we end, we note that recently Lopez and Fradkin (LF) [52] have studied QHE in bilayered systems with complete spin polarization. There is a close resemblance between their approach with the one we have taken here: The Lagrangians are formally the same, with a fermion doublet (while there is layered index in LF, we have the spin index here) and a matrix valued CS strength. In bilayered system the interlayer and intralayer interaction potentials are different, unlike in the case of spin-1/2 fermions for which the interaction potential does not depend on spin. However, this aspect is not important as long as we consider short-range interactions.

The crucial difference, in fact, is in the (physical) choice of Θ. In their work, LF [52] have chosen the Θ matrix as

$$\Theta_{\rm LF} = \frac{e^2}{2\pi}\frac{1}{4s_1s_2 - n^2}\begin{pmatrix} 2s_2 & -n \\ -n & 2s_1 \end{pmatrix} , \tag{3.62}$$

where s_1, s_2 and n are integers. Clearly $\Theta_{\rm LF}$ has more parameters compared to our choice of Θ in Eq. (2.2) since LF [52] have assumed more generically that the particles

in two different layers feel unequal number of flux quanta which is, in fact, not possible for spin-1/2 fermions in a single layer. In contrast, our case corresponds to $s_1 = s_2$. Note that this choice is a strict requirement that the parity operation transforms the up-spin to down-spin electron and vice versa. There is no such requirement in the LF [52] case. More importantly, note that $\Theta_{\rm LF}$ is ill-defined for $s_1 = s_2 = n/2$. As a consequence, there are fundamental differences in results and interpretation in the two approaches which we discuss below.

Consider the spin unpolarized state first. The corresponding sequence of states obtained by LF [52] for equal population in the two layers is identical to Eq. (2.11) here for the choice of $s_1 = s_2 = n/2$ in Eq. (3.62). A closer look however shows that it is precisely for these states, (characterized by the filling fractions $\nu_1 = \nu_2$ in the two layers and the number of particles $N_1 = N_2$ in two layers in Ref.[52]) that the CS strength $\Theta_{\rm LF}$ becomes ill-defined. The ensuing dynamics is also ill-defined. Indeed as we have quoted earlier, LF [52] point out in their paper "the spin singlet state (3,3,2), which has filling fraction $\nu = 2/5$, cannot be described within the Abelian Chern-Simons approach". In fact, no spin unpolarized states given by filling fraction in (2.11), can be described in the approach of LF [52]. In contrast, our Θ is given by

$$\Theta = \frac{e^2}{2\pi}\frac{1}{2s}\begin{pmatrix} 1 & 1 \\ 1 & 1 \end{pmatrix}, \tag{3.63}$$

corresponding to $\theta_1 = \theta_2$, with eigen values $\theta_+ = (e^2/2\pi)(1/2s)$ and $\theta_- = 0$, which keeps the composite fermion picture intact. This well defined matrix naturally leads to unpolarized states (see chapter 2). The dynamics is also well defined, allowing us to obtain quantization of Hall conductivity (3.61) and many-body wave functions (3.42) for these states. Again, as we have stated earlier, we recover Halperin wave function for spin unpolarized $\nu = 2/5$ state. Note that since all the elements in Θ in Eq. (3.63) are same, the flux seen by all the particles are same irrespective of their spins, unlike $\Theta_{\rm LF}$ for which flux seen by particles in the same layer are different from particles in different layers.

In our approach, $\nu = 1/m$ (m odd) states (which are the Laughlin sequence) are

always fully polarized (see Eq. 2.20). This, in fact, is true as it is seen both in the experiment and numerical calculations in a single layer. Contrarily in the work of LF [52], these states can also be obtained for equal population of particles in the two layers corresponding to filling fractions $\nu_1 = \nu_2 = 1/2m$ (where 1 and 2 refer to two different layers). The wave functions for fully polarized $\nu = 1/m$ states are well known Laughlin wave functions which is also derived here (See Eq. (3.49) for fully polarized limit). On the other hand, LF [52] have obtained the wave functions for $\nu = 1/m$ states, in their above construction, as (m, m, m) Halperin wave functions with an extra non-analytic piece (which we do not encounter) due to the presence of a gapless mode in the spectrum of collective excitations for these states.

The $\nu = 1/2$ state in bilayered systems corresponds to the assignment of filling fractions $\nu_1 = \nu_2 = 1/4$ in two layers which yield the gaps $\bar{\omega}_c^{1,2} = \omega_c/4$. With their choice, LF [52] obtain the wave function for which coincides with the one obtained by numerical computation in double layers. On the other hand, the present model yields $\bar{\omega}_c^{\uparrow,\downarrow} = 0$. This is again closer to several experiments which have unambiguously verified that $\bar{\omega}_c = 0$ for $\nu = 1/2$ in a single layer.

It is of course not that the two models are entirely different in all aspects. Indeed, the double layered systems with dissimilar gaps in two layers are exact analogues of the spin systems with dissimilar gaps for spin up and down states because Θ_{LF} becomes identical to Θ here, provided one puts $s_1 = s_2$ in Eq. (3.62). Note, however, that spin unpolarized states (which are seen experimentally can never arise if $\bar{\omega}_c^{\uparrow} \neq \bar{\omega}_c^{\downarrow}$. Experimentally observed partially polarized or fully polarized states which are given by Eq. (2.20) also correspond to $\bar{\omega}_c^{\uparrow} = \bar{\omega}_c^{\downarrow}$. It will be interesting to observe experimentally whether there is any such states for which $\bar{\omega}_c^{\uparrow} \neq \bar{\omega}_c^{\downarrow}$ in which case there would be a one-to-one correspondence between the two models.

Finally, we remark that LF [52] have also studied spin unpolarized states in a single layer by employing a non-abelian CS interaction. In their picture, electrons are composite of holons and spinons. Charged spinless holons interact with *U(1)* CS gauge field where as neutral spin-1/2 spinons interact with *SU(2)* CS gauge field. They both

obey semionic statistics — which indicates a departure from composite fermion model (where spin and charge are not separated) to which we completely adhere.

3.6 Conclusion

In conclusion, we have, in this chapter, developed a theory for arbitrarily polarized quantum Hall states by employing a doublet of CS gauge fields. We have confirmed by an explicit one-loop computation that the Hall conductivity does indeed get quantized at those filling fractions that follow from the model. We have further derived the absolute square of the many body wave functions for these states. We recover the fully polarized Laughlin wave functions and the Halperin (3,3,2) wave function for unpolarized $\nu = 2/5$ state. The wave functions agree with that of Jain *et al* [66, 48]. We have further given a physical picture of the analytic/non-analytic nature of the wave functions in terms of attachment of effective number of vortices to each particle. Finally, we have shown that quantum fluctuations of CS gauge fields restore the Kohn mode.

In short, the doublet model not only yields correctly the bulk properties like quantization of Hall conductivity for arbitrarily polarized QHS, but also captures important microscopic features of the many body system: (i) the correct wave function of the ground state and (ii) restoration of Kohn's mode. These features make the doublet model quite viable.

In the next two chapters, we study the applications of the model. In the next chapter, we shall show the model provides direct tests for the confirmation of the CFM.

Chapter 4

Direct test of the composite fermion model

4.1 Introduction

In the previous two chapters, we have discussed the doublet model and demonstrated its viability. In this chapter and in the following one, we shall discuss the application of the model. This chapter is devoted for a discussion on the possible direct tests, which are provided by the doublet model, for the existence of composite fermions.

It was first emphasized by Halperin, Lee, and Read (HLR) [20] that the single particle excitation gap of CF, corresponding to the state with filling fraction $\nu = p/(2sp+1)$, is the effective cyclotron energy $\bar{\omega}_c$ which is determined by the effective magnetic field $\bar{B}$. More significantly, the CFM makes the remarkable prediction that at $\nu = 1/2s$, the effective field $\bar{B}_{1/2s} = 0$. HLR have thus argued that at $\nu = 1/2$, the CF form a Fermi sea. Subsequently, Rezayi and Read [68] have found numerically in a spherical geometry [57] that CF at half filled Landau level form a Fermi liquid. A set of recent experiments [21–33] provide good experimental support for the existence of CF in FQHE systems. We review the main features of the experiments below.

(i) Du *et al* [21] find that the excitation gap, which is obtained from the activation in diagonal resistivity ρ_{xx}, is proportional to $\bar{B}$, in agreement with the prediction of the CFM, for the states which are away from half filling. They further find that the effective mass m^* is independent of $\bar{B}$. Recall that on the other hand, HLR have

argued that m^* diverges logarithmically for Coulomb interaction and that it has a power law divergence for other short range interactions as $\nu \rightarrow 1/2$, where CF form a Fermi liquid. (ii) Three experiments [22–24] have treated the oscillations in diagonal resistivity ρ_{xx} around $\nu = 1/2$ as Shubnikov-de Haas oscillations (SDHO) of CF, in analogy with SDHO of free electrons near $B = 0$. The effective mass of CF m^* is then determined from SDHO. Though all these experiments are in favour of CF, they are mutually conflicting: while Leadley *et al* [22] have reported a finite mass m^* at $\bar{B} = 0$, and that m^* increases linearly with $|\bar{B}|$, Du *et al* [23] and Manoharan *et al* [24] have observed 'drastic enhancement' of CF mass as $\nu \rightarrow 1/2$, indicating a novel Frmi liquid at $\nu = 1/2$. Although both Du *et al* [23] and Manoharan *et al* [24] have observed diverging m^* as $\nu \rightarrow 1/2$, the former have obtained much faster divergence compared to the latter. (iii) The 'anomaly' in surface accoustic wave (SAW) propagation at $\nu = 1/2$ was studied theoretically by HLR at half field landau level, who find good qualitative agreement with the SAW experiments [25, 26]. In the SAW experiments, Willett *et al* [25, 26] determine the finite wave vector dependent conductivity $\sigma_{xx}(q)$ to be proportional to q. This behaviour is deduced from the attenuation of the amplitude and deviation of the velocity of SAW (at even denominator ν). This behaviour is found to persist up to high temperature, even after FQHE has generally disappeared. (iv) There is yet another interesting aspect of the SAW experiments. As we know, electrons in a metal geometrically resonate with a sound wave when a magnetic field is applied perpendicular to the sound wave propagation. Willett *et al* [27] have observed a similar resonance of SAW at $\nu = 1/2$ with cyclotron orbits of CF, with a cyclotron radius $R_c = K_F/e\bar{B}$, where the Fermi wave vector $K_F = \sqrt{4\pi\rho}$. Kang *et al* [28] also have reported the existence of cyclotron motion of CF with radius R_c at $\nu = 1/2$ by their transport measurement in an antidot supperlattice. (v) Goldman *et al* [29] have performed a transverse magnetic focussing experiment and observed quasiperiodic resistance peaks near $\nu = 1/2$. Moreover, they have observed that the quasiperiodic structure occurs on one side of $\nu = 1/2$, describing the negatively charged CF. They have also found that the charge carriers experience an effective magnetic field $\bar{B}$, in

agreement with the CF picture.

(vi) Apart from the above transport measurements, there are plenty of data available in thermal measurements. Ying *et al* [30] have reported that thermopower measurements at $\nu = 1/2$ and $3/2$ are consistent with the presence of a CF Fermi surface. Based on their data on thermopower, Bayot *et al* [31] have concluded that CF exhibits IQHE. (vii) There also exists a time-resolved magneto-luminescence experiment to study the hierarchy of FQHE states. Kukushkin *et al* [32] have observed a striking symmetry in the dependence of chemical potential discontinuity on the filling factor for different families (different s) of Jain sequence. They find a linear dependence of chemical potential discontinuity on magnetic fields starting at $\nu = 1/2, 1/4, 1/6$. (viii) Finally, Kukushkin *et al* [33] have studied the influence of disorder on the properties of 2DEG in the vicinity of $\nu = 1/2$. They have observed that ρ_{xx} at $\nu = 1/2$ is very sensitive to the disorder level in 2DEG. This observation is in agreement with the theory of half filled Landau level in CF picture. It is noteworthy that the results are obtained for fully polarized samples.

All the above experiments which are strongly in favour of the existence of CF are still rather incomplete in the sense that none of them determines either of the composite fermion parameters, *viz.*, the effective number of LL (p) or the number of flux quanta ($2s$) attached to each electron directly. In that sense the evidence for the CF is yet indirect. Apart from the activation [21] and magneto-luminescence [32] experiments, the measurements which are in the vicinity of $\nu = 1/2s$ essentially verify that $\bar{B} \approx 0$. The gap determination which is done by the activation experiments does not determine p unambiguously as the parametrization of activation of ρ_{xx} is not unique. There is the additional complication that m^* also changes with $\bar{B}$. It would therefore be desirable to have experiments which can circumvent these complications, and also be not necessarily restricted to the vicinity of $\nu = 1/2s$. Indeed, we propose such experiments and show how $|p|$ can be determined unambiguously. (The other parameter $2s$ can then be found out from the knowledge of filling fraction $\nu = |p|/(2s|p| \pm 1)$.) We do so by employing FQHE states which are either partially polarized or more preferably

unpolarized. Indeed, they are central to our analysis because the wave functions for fully polarized QHS depend solely on ν, while on the other hand, as we have shown in the previous chapter, the wave functions for unpolarized (3.42) or partially polarized (3.49) QHS depend on any two parameters among p, s, and ν.

The main result is that neutron scattering and Raman scattering experiments in partially polarized or unpolarized QHS can unambiguously determine $|p|$ and $\bar{\omega}_c$ respectively. To that end, we need to evaluate the charge density and spin density correlation functions. Recall that in the previous chapter, we calculated the density-density correlation functions among different spin species by considering Gaussian fluctuation of the gauge fields, *i.e.*, in the random phase approximation (RPA). In this chapter, we improve upon RPA by the time dependent Hartree-Fock approximation (TDHFA) by taking into account the Coulomb interaction between CF. It is worthwhile to note that this improved RPA will not alter the final results obtained in the previous chapter since any correction due to Coulomb interaction corresponds to higher order in $\mathbf{q}^2$. For example, the wave functions remain same as we have determined them in the thermodynamic limit. The correlation functions can be evaluated from the effective action (in terms of external probes) for the system.

4.2 The effective action

In the previous chapter, we have determined the effective action (3.29) for the external probes in the arbitrarily polarized QHS. We rewrite the same as

$$S_{\text{eff}}\left[A_\mu^{\uparrow}, A_\mu^{\downarrow}\right] = \frac{1}{2}\int \frac{d^3q}{(2\pi)^3} A_\mu^r(q) K_{rr'}^{\mu\nu}(\omega, \mathbf{q}) A_\nu^{r'}(-q) \ , \tag{4.1}$$

where the indices $r, r' = \uparrow, \downarrow$. $K_{rr'}^{\mu\nu}$ measures linear response of the system to weak external probes. Recall that $K_{\uparrow\uparrow}^{00}$, $K_{\uparrow\downarrow}^{00}$, $K_{\downarrow\uparrow}^{00}$ and $K_{\downarrow\downarrow}^{00}$ represent the density-density correlations among spin up-up, up-down, down-up and down-down species of the particles respectively. We derived these correlations in the lowest order in $\mathbf{q}^2$ [see Eqs. (3.30)–(3.33)]. If we do not make this approximation, the response function has the general

form

$$K^{00}_{\uparrow\uparrow} = \frac{\mathbf{q}^2}{\Pi_0^{\uparrow} + \Pi_0^{\downarrow}} \left[\Pi_0^{\uparrow}\Pi_0^{\downarrow} - \frac{\left(\Pi_0^{\uparrow}\Pi_1^{\downarrow} - \Pi_0^{\downarrow}\Pi_1^{\uparrow} + \Pi_0^{\uparrow}\theta_-\right)^2}{\mathcal{D}(\omega, \mathbf{q})} \right] . \tag{4.2}$$

$$K^{00}_{\downarrow\downarrow} = \frac{\mathbf{q}^2}{\Pi_0^{\uparrow} + \Pi_0^{\downarrow}} \left[\Pi_0^{\uparrow}\Pi_0^{\downarrow} - \frac{\left(\Pi_1^{\uparrow}\Pi_0^{\downarrow} - \Pi_1^{\downarrow}\Pi_0^{\uparrow} + \Pi_0^{\downarrow}\theta_-\right)^2}{\mathcal{D}(\omega, \mathbf{q})} \right] . \tag{4.3}$$

$$K^{00}_{\uparrow\downarrow} = -\frac{\mathbf{q}^2}{\Pi_0^{\uparrow} + \Pi_0^{\downarrow}} \left[\Pi_0^{\uparrow}\Pi_0^{\downarrow} + \frac{\left(\Pi_0^{\uparrow}\Pi_1^{\downarrow} - \Pi_0^{\downarrow}\Pi_1^{\uparrow} + \Pi_0^{\uparrow}\theta_-\right)\left(\Pi_1^{\uparrow}\Pi_0^{\downarrow} - \Pi_1^{\downarrow}\Pi_0^{\uparrow} + \Pi_0^{\downarrow}\theta_-\right)}{\mathcal{D}(\omega, \mathbf{q})} \right] . \tag{4.4}$$

$$K^{00}_{\downarrow\uparrow} = K^{00}_{\uparrow\downarrow} , \tag{4.5}$$

with

$$\begin{aligned} \mathcal{D}(\omega, \mathbf{q}) = {} & \left(\Pi_0^{\uparrow} + \Pi_0^{\downarrow}\right)^2 \omega^2 - \left(\Pi_1^{\uparrow} + \Pi_1^{\downarrow} + \theta_+\right)^2 \\ & - \left(\Pi_0^{\uparrow} + \Pi_0^{\downarrow}\right)\left(\Pi_2^{\uparrow} + \Pi_2^{\downarrow}\right) \mathbf{q}^2 - \left(\Pi_0^{\uparrow} + \Pi_0^{\downarrow}\right) \theta_+^2 V(\mathbf{q}^2)\mathbf{q}^2 . \end{aligned} \tag{4.6}$$

It may be observed that the form factors Π_i here are not merely in the lowest order in $\mathbf{q}^2$ (as in Eqs. 3.26–3.28). We shall determine them in the next section.

4.3 Evaluation of form factors

Kallin and Halperin [69] have determined charge density and spin density response functions using a diagrammatic approach, which is equivalent to the time dependent Hartree Fock approximation (TDHFA) employed by MacDonald [70] for studying IQHE. Girvin, MacDonald, and Platzmann [71] have studied collective excitations of FQHE in the single mode approximation in which the correlation effects in a partially filled are taken into account. Here we shall employ TDHFA, and adopt the method of Kallin and Halperin [69] to evaluate form factors for effective filled Landau levels. In this approximation, only diagrams with one exciton present at a time are considered. In other words, the Coulomb energy $e^2/\epsilon l_0$ is taken to be smaller than $\overline{\omega}_c$, where $l_0 = (e\overline{B})^{-1/2}$ is the effective magnetic length of the system and ϵ is the background dielectric constant. This assumption is, therefore, not valid at or near $\nu = 1/2s$. We

consider the states which are far away from even denominator filling factors. In other words, the condition on the validity of our assumption is $e^{3/2}m^*/\epsilon \ll \sqrt{\overline{B}}$.

Using TDHFA, we obtain (see Appendix B) the component $\Pi^{00}_{\uparrow,\downarrow}$ of the polarization tensor (3.25) as

$$\Pi^{00}_{\uparrow,\downarrow}(\omega, \mathbf{q}) = e^2$$
$$\times \left[\sum_{n_2<p_{\uparrow,\downarrow}} \sum_{n_1\geq p_{\uparrow,\downarrow}} \frac{|M_{n_1n_2}(\mathbf{q})|^2}{\omega + \epsilon^{\uparrow,\downarrow}_{n_2} - \epsilon^{\uparrow,\downarrow}_{n_1} - E^{\uparrow,\downarrow}_{n_1n_2} + \tilde{V}^{(1)}_{n_1n_2n_2n_1}(\mathbf{q}) - \gamma\tilde{V}^{(2)}_{n_1n_2n_1n_2}(\mathbf{q}) + i\eta} \right.$$
$$\left. - \sum_{n_1<p_{\uparrow,\downarrow}} \sum_{n_2\geq p_{\uparrow,\downarrow}} \frac{|M_{n_1n_2}(\mathbf{q})|^2}{\omega + \epsilon^{\uparrow,\downarrow}_{n_2} - \epsilon^{\uparrow,\downarrow}_{n_1} - E^{\uparrow,\downarrow}_{n_1n_2} - \tilde{V}^{(1)}_{n_1n_2n_2n_1}(\mathbf{q}) + \gamma\tilde{V}^{(2)}_{n_1n_2n_1n_2}(\mathbf{q}) - i\eta} \right], \tag{4.7}$$

where n_1, n_2 represent the effective Landau level indices. Here $\epsilon^r_n = (n + 1/2)\overline{\omega}_c - (1/2)g\mu_B\overline{B}\sigma$ is the energy on n th LL with spin index r. $\sigma = (\pm 1)$ for up(down) states. $E^r_{n_1n_2} = \Sigma^r_{n_1} - \Sigma^r_{n_2}$ represents the exchange energy, *i.e.*, the difference in self energy between two LL having same spin index r. Σ^r_n is independent of momentum $\mathbf{q}$. The interaction between an excited electron and hole (*i.e.*, the ladder diagrams) is represented by $\tilde{V}^{(1)}_{n_1n_2n_2n_1}(\mathbf{q})$. The contribution of the bubble diagrams is represented by $\tilde{V}^{(2)}_{n_1n_2n_1n_2}(\mathbf{q})$ in which an electron hole pair recombines, exciting simultaneously another electron hole pair. The expressions for Σ^r_n, $\tilde{V}^{(1)}_{n_1n_2n_2n_1}(\mathbf{q})$, and $\tilde{V}^{(2)}_{n_1n_2n_1n_2}(\mathbf{q})$ read (see Appendix B)

$$\Sigma^r_n = -\int \frac{d^2r}{2\pi l_0^2} V(r) e^{-r^2/2l_0^2} L^1_{p_r-1}\left(\frac{r^2}{2l_0^2}\right) L^0_n\left(\frac{r^2}{2l_0^2}\right), \tag{4.8}$$

$$\tilde{V}^{(1)}_{n_1n_2n_2n_1}(\mathbf{q}) = \frac{2^{n_2}n_2!}{2^{n_1}n_1!} \int \frac{d^2r}{2\pi l_0^2} V(\mathbf{r} - l_0^2\mathbf{q}\times\hat{z}) e^{-r^2/2l_0^2} \left(\frac{r^2}{l_0^2}\right)^{n_1-n_2} \left[L^{n_1-n_2}_{n_2}\left(\frac{r^2}{2l_0^2}\right)\right]^2, \tag{4.9}$$

$$\tilde{V}^{(2)}_{n_1n_2n_1n_2}(\mathbf{q}) = \frac{2^{n_2}n_2!}{2^{n_1}n_1!} e^{-\overline{q}^2} \frac{V(\mathbf{q})}{2\pi l_0^2} (2\overline{q}^2)^{n_1-n_2} \left[L^{n_1-n_2}_{n_2}\left(\overline{q}^2\right)\right]^2, \tag{4.10}$$

for $n_1 \geq n_2$. On the other hand for $n_2 \geq n_1$, the right hand sides of the expressions in Eqs. (4.9 and 4.10) are expressed by interchanging n_1 and n_2. Therefore, $\tilde{V}^{(1)}_{n_2n_1n_1n_2} = \tilde{V}^{(1)}_{n_1n_2n_2n_1}$ and $\tilde{V}^{(2)}_{n_2n_1n_2n_1} = \tilde{V}^{(2)}_{n_1n_2n_1n_2}$. The factor $\gamma = 2$ when Landau level n_1 for both

up and down spins are occupied and $\gamma = 1$ otherwise. The matrix element $M_{n_1 n_2}(\mathrm{q})$ in (4.7) is given by

$$M_{n_1 n_2}(\mathrm{q}) = \left(\frac{2^{n_2} n_2!}{2^{n_1} n_1!}\right)^{1/2} e^{-\overline{\mathrm{q}}^2/2}\left[l_0(q_x + iq_y)\right]^{n_1-n_2} L_{n_2}^{n_1-n_2}\left(\overline{\mathrm{q}}^2\right) . \tag{4.11}$$

where $\overline{\mathrm{q}}^2 = \mathrm{q}^2 l_0^2/2$ and the associated Laguerre polynomial $L_n^m(x)$ is given by

$$L_n^m(x) = \frac{1}{n!} e^x x^{-m} \frac{d^n}{dx^n}\left(e^{-x} x^{n+m}\right) . \tag{4.12}$$

We, therefore, obtain

$$\begin{aligned}
\Pi_0^{\uparrow,\downarrow} \quad = \quad & -\frac{e^2}{4\pi} \sum_{n_2 < p_{\uparrow,\downarrow}} \sum_{n_1 \geq p_{\uparrow,\downarrow}} \left(\frac{n_2!}{n_1!}\right) e^{-\overline{\mathrm{q}}^2} \left(\overline{\mathrm{q}}^2\right)^{n_1-n_2-1} \left\{L_{n_2}^{n_1-n_2}(\overline{\mathrm{q}}^2)\right\}^2 \\
\times & \left[\frac{1}{\omega - (n_1 - n_2)\overline{\omega}_c - E_{n_1 n_2}^{\uparrow,\downarrow} + \tilde{V}_{n_1 n_2 n_2 n_1}^{(1)}(\mathrm{q}) - \gamma \tilde{V}_{n_1 n_2 n_1 n_2}^{(2)}(\mathrm{q}) + i\eta}\right. \\
- & \left.\frac{1}{\omega + (n_1 - n_2)\overline{\omega}_c + E_{n_1 n_2}^{\uparrow,\downarrow} - \tilde{V}_{n_1 n_2 n_2 n_1}^{(1)}(\mathrm{q}) + \gamma \tilde{V}_{n_1 n_2 n_1 n_2}^{(2)}(\mathrm{q}) - i\eta}\right] .
\end{aligned} \tag{4.13}$$

In a similar manner, by the calculation of other components of $\Pi_{\uparrow,\downarrow}^{\mu\nu}$, say, $\Pi_{\uparrow,\downarrow}^{01}$ and $\Pi_{\uparrow,\downarrow}^{11}$, we obtain

$$\begin{aligned}
\Pi_1^{\uparrow,\downarrow} = & -\frac{e^2 \overline{\omega}_c}{8\pi} \sum_{n_2 < p_{\uparrow,\downarrow}} \sum_{n_1 \geq p_{\uparrow,\downarrow}} \left(\frac{n_2!}{n_1!}\right) e^{-\overline{\mathrm{q}}^2} \left(\overline{\mathrm{q}}^2\right)^{n_1-n_2-1} L_{n_2}^{n_1-n_2}(\overline{\mathrm{q}}^2) \\
\times & \left[(n_2+1) L_{n_2+1}^{n_1-n_2-1}(\overline{\mathrm{q}}^2) + n_1 L_{n_2}^{n_1-n_2-1}(\overline{\mathrm{q}}^2) - \overline{\mathrm{q}}^2 \left\{L_{n_2}^{n_1-n_2}(\overline{\mathrm{q}}^2) + 2L_{n_2-1}^{n_1-n_2+1}(\overline{\mathrm{q}}^2)\right\}\right] \\
\times & \left[\frac{1}{\omega - (n_1 - n_2)\overline{\omega}_c - E_{n_1 n_2}^{\uparrow,\downarrow} + \tilde{V}_{n_1 n_2 n_2 n_1}^{(1)}(\mathrm{q}) - \gamma \tilde{V}_{n_1 n_2 n_1 n_2}^{(2)}(\mathrm{q}) + i\eta}\right. \\
- & \left.\frac{1}{\omega + (n_1 - n_2)\overline{\omega}_c + E_{n_1 n_2}^{\uparrow,\downarrow} - \tilde{V}_{n_1 n_2 n_2 n_1}^{(1)}(\mathrm{q}) + \gamma \tilde{V}_{n_1 n_2 n_1 n_2}^{(2)}(\mathrm{q}) - i\eta}\right]
\end{aligned} \tag{4.14}$$

and

$$\begin{aligned}
\Pi_2^{\uparrow,\downarrow} = & -\frac{e^2 \overline{\omega}_c}{16\pi m^*}\left(1 - \sigma \frac{g}{2} \frac{m^*}{m_e}\right) \sum_{n_2 < p_{\uparrow,\downarrow}} \sum_{n_1 \geq p_{\uparrow,\downarrow}} \left(\frac{n_2!}{n_1!}\right) e^{-\overline{\mathrm{q}}^2} \left(\overline{\mathrm{q}}^2\right)^{n_1-n_2-1} \\
\times & \left\{L_{n_2}^{n_1-n_2}(\overline{\mathrm{q}}^2) + 2L_{n_2-1}^{n_1-n_2+1}(\overline{\mathrm{q}}^2)\right\} \left[2(n_2+1) L_{n_2+1}^{n_1-n_2-1}(\overline{\mathrm{q}}^2)\right. \\
& \left. + 2n_1 L_{n_2}^{n_1-n_2-1}(\overline{\mathrm{q}}^2) - \overline{\mathrm{q}}^2 \left\{L_{n_2}^{n_1-n_2}(\overline{\mathrm{q}}^2) + 2L_{n_2-1}^{n_1-n_2+1}(\overline{\mathrm{q}}^2)\right\}\right] \\
\times & \left[\frac{1}{\omega - (n_1 - n_2)\overline{\omega}_c - E_{n_1 n_2}^{\uparrow,\downarrow} + \tilde{V}_{n_1 n_2 n_2 n_1}^{(1)}(\mathrm{q}) - \gamma \tilde{V}_{n_1 n_2 n_1 n_2}^{(2)}(\mathrm{q}) + i\eta}\right. \\
- & \left.\frac{1}{\omega + (n_1 - n_2)\overline{\omega}_c + E_{n_1 n_2}^{\uparrow,\downarrow} - \tilde{V}_{n_1 n_2 n_2 n_1}^{(1)}(\mathrm{q}) + \gamma \tilde{V}_{n_1 n_2 n_1 n_2}^{(2)}(\mathrm{q}) - i\eta}\right] .
\end{aligned} \tag{4.15}$$

In obtaining (4.13)–(4.15), we have included all the contributions up to order $e^2/\epsilon l_0$, and so the form factors are essentially exact in the strong effective field limit. In the absence of Coulomb interaction, $E^r_{n_1 n_2}$, $\tilde{V}^{(1)}_{n_1 n_2 n_2 n_1}(\mathbf{q})$, and $\tilde{V}^{(2)}_{n_1 n_2 n_1 n_2}(\mathbf{q})$ are zero and then the form factors reduce to their pure RPA form. Note that in the small $\mathbf{q}$ limit, introduction of TDHFA is not very important. Indeed Kallin and Halperin [69] have already observed that the charge density collective excitations for IQHE states in the small $\mathbf{q}$ regime to be similar both in the pure RPA and in TDHFA. The effect of TDHFA, as we shall show below, will however be seen clearly in the spin density excitations.

4.4 Results and experimental consequences

4.4.1 Correlations

The charge density correlation can now be obtained as

$$K^{00}(\omega\,,\,\mathbf{q}^2) \equiv \sum_{r,r'} K^{00}_{rr'}(\omega\,,\,\mathbf{q}^2) = -\mathbf{q}^2 \frac{\left(\Pi_0^{\uparrow} + \Pi_0^{\downarrow}\right)\theta_+^2}{\mathcal{D}(\omega\,,\,\mathbf{q}^2)}\,. \tag{4.16}$$

On the other hand the spin density correlation is given by

$$\Sigma(\omega\,,\,\mathbf{q}^2) = \sum_{r,r'} \left[K^{00}_{rr'}\delta_{rr'} - K^{00}_{rr'}(1-\delta_{rr'})\right] \tag{4.17}$$

For unpolarized states, $\Pi_0^{\uparrow} = \Pi_0^{\downarrow} \equiv \Pi_0$. Thus Σ gets the simpler form,

$$\Sigma_{\mathsf{unp}}(\omega\,,\,\mathbf{q}^2) = 2\Pi_0(\omega\,,\,\mathbf{q}^2)\mathbf{q}^2\,. \tag{4.18}$$

Note at the outset that the charge density excitations (CDE) will be very different from spin density excitations (SDE) ($\delta S_z = 0$ excitations) especially for unpolarized states. This is so, because CDE are determined by the poles of $K^{00}(\omega\,,\,\mathbf{q}^2)$, while SDE are determined by the poles of Π_0. The collective CDE and SDE will be discussed below. We note that the leading order term in $\mathbf{q}^2$ of K^{00} saturates the f-sum rule.

The above results are valid in the thermodynamic limit. For as LF [72] have argued in a similar case, we note that we have evaluated the effective action by neglecting

higher order response functions, *viz*, the correlations of three or more currents or densities. These higher order correlations are of higher order in q^2 compared to the quadratic term in Eqs. (4.2–4.5 and 4.16–4.18). They would not be negligible for a finite system since the minimum allowed value of the momentum is then determined by the linear size of the system L, *i.e.*, $|\mathbf{q}| > 1/L$. On the other hand, in the thermodynamic limit, $L \to \infty$ and the minimum allowed value of $|\mathbf{q}|$ goes to zero. Therefore one is allowed to keep only the quadratic term in effective action and neglect the higher order corrections for an infinite system.

In the limit of low $\mathbf{q}^2$, CDC and SDC are respectively given by

$$K^{00}(\omega\,,\,\mathbf{q}^2) = -\left(\frac{e^2\rho}{m^*}\right)\frac{1}{\omega^2-\omega_c^2}\mathbf{q}^2 + \mathcal{O}(\mathbf{q}^4)\,. \tag{4.19}$$

$$\Sigma(\omega\,,\,\mathbf{q}^2) = -\left(\frac{e^2\rho}{m^*}\right)\left[\frac{(p_\uparrow-p_\downarrow)^2}{(p_\uparrow+p_\downarrow)^2}\frac{1}{\omega^2-\omega_c^2} + \frac{4p_\uparrow p_\downarrow}{(p_\uparrow+p_\downarrow)^2}\frac{1}{\omega^2-\overline{\omega}_c^2}\right]\mathbf{q}^2 + \mathcal{O}(\mathbf{q}^4)\,. \tag{4.20}$$

We see from Eq. (4.19) that CDC preserves the Kohn mode [55] of excitation. On the other hand, SDC in Eq. (4.20) shows a new mode of excitation at $\overline{\omega}_c$ apart from the actual cyclotron energy ω_c. Interestingly, in the case of unpolarized QHS for which $p_\uparrow = p_\downarrow$, *only* the mode at $\overline{\omega}_c$ survives at $\mathbf{q}$=0. This, in fact, gives the measure of energy scale for CF. Equations (4.19) and (4.20) are the same as the pure RPA result since we are in the regime of very low $\mathbf{q}$.

4.4.2 The spin transitions

At $\omega = 0$, SDC (4.20) can be written as

$$\Sigma(0,\mathbf{q}^2) = \mathbf{q}^2\left(\frac{e^2 m^*}{4\pi^2\rho}\right)\left[\frac{(p_\uparrow-p_\downarrow)^2}{(p_\uparrow+p_\downarrow)^2}\nu^2 + 4p_\uparrow p_\downarrow\right]\,. \tag{4.21}$$

We see that $\Sigma(0,\,\mathbf{q}^2)$ given by the above expression plays an important role in the spin transitions. Experimentally, Eisenstein *et al* [37] and Engel *et al* [38] have observed spin transitions in QHS with filling fractions $\nu = 2/3$ and $3/5$. By the increase of Zeeman energy, QHS at $\nu = 2/3$ ($p_\uparrow = p_\downarrow = -1$, $s = 1$) and $\nu = 3/5$ ($p_\uparrow = -2$, $p_\downarrow = -1$, $s = 1$) undergo a spin transition from their respective phase of no polarization and partial

polarization to fully polarized phase ($p_\downarrow = 0$) keeping $p_\uparrow + p_\downarrow$ fixed. It is clear that the effective number of LL filled by up (or down) spins $p_\uparrow$ ($p_\downarrow$) acts as an order parameter in the spin transitions. The value of Σ, accordingly, changes discontinuously in the spin transitions. Indeed, the ratio of the values of Σ between the unpolarized and fully polarized phases is given by $\Sigma_{\mathrm{unp}}/\Sigma_{\mathrm{p}} = 4p_\uparrow^2/\nu^2$. Therefore, the ratio of $\Sigma(0, \mathbf{q}^2)$ in unpolarized and fully polarized phase would determine $p_\uparrow (= p_\downarrow)$ in the unpolarized phase unambiguously. Significantly, the ratio does *not* depend on other parameters such as m^* which has a complicated dependence on the value of the magnetic field [22–24]. Similarly, the ratio of $\Sigma(0, \mathbf{q}^2)$ in partially polarized and fully polarized phases would also determine $p_\uparrow$ and $p_\downarrow$ in partially polarized phase unambiguously. The order parameter shows a discontinuity in the spin transitions.

4.4.3 Neutron scattering

We shall now show that neutron scattering can determine p unambiguously. In the standard neutron scattering experiments [73], (in this case, the scattering is in the plane of the sample), the differential scattering cross section is given by

$$\frac{d\sigma}{d\Omega} \propto \frac{k_f}{k_i}\left[S_c(q) + \frac{\sigma_\Sigma}{\sigma_c} S_\Sigma(q)\right] , \tag{4.22}$$

where $\mathbf{k}_i$ and $\mathbf{k}_f$ are the momentum of the incident and scattered neutrons, $\mathbf{q} = \mathbf{k}_i - \mathbf{k}_f$ is the momentum transfer. In Eq. (4.22), $S_c(q)$ and $S_\Sigma(q)$ are static charge and spin structure factors which are frequency integrated imaginary parts of the corresponding correlation functions. In Eq. (4.22), σ_Σ/σ_c is the ratio of the spin and charge dependent total cross sections.

In our case, the static structure factors are evaluated from Eqs. (4.19 and 4.20), as

$$\begin{aligned} S_c(q) &= \mathbf{q}^2\left(\frac{e^2}{2}\right)\nu , & (4.23)\\ S_\Sigma(q) &= \mathbf{q}^2\left(\frac{e^2}{2}\right)\left[\left|\frac{4p_\uparrow p_\downarrow}{p_\uparrow + p_\downarrow}\right| + \frac{(p_\uparrow - p_\downarrow)^2}{(p_\uparrow + p_\downarrow)^2}\nu\right] . & (4.24)\end{aligned}$$

Note that unlike the parent expressions in Eqs. (4.19 and 4.20), the above expressions are free from any dependence on ρ, and m^* which by now is known to possess a depen-

dence on the magnetic field [22–24]. Note that $S_c(q)$ is proportional to ν irrespective of the spin phase. The form of $S_\Sigma(q)$ depends on the spin phase, however. In the fully polarized phase, $S_c(q) \equiv S_\Sigma(q)$. In the unpolarized phase, $S_\Sigma(q) \propto p_*$ while, in general, for a partially polarized phase, it depends on both p_* and ν.

What is then required is a determination of $S_\Sigma(q)$ in unpolarized or partially polarized phases which may be accomplished by two different ways: (i) By the measurement of neutron scattering cross section in fully polarized phase, one will be able to extract $S_c(q)$ since the cross section is proportional to $S_c(q)$. This remains same in all phases. The same experiment then in the unpolarized or partially polarized phase, whichever is the relevant one, has to be performed to determine $S_\Sigma(q)$ in the corresponding phase, with the previous knowledge of $S_c(q)$. Since structure factors are independent of the particle density ρ, their determination is unambiguous, no matter how the different spin phases are obtained — be it by changing the particle density or by a tilting angle experiment. (ii) The second method corresponds to the experiments entirely in unpolarized or partially polarized phase, whichever is the relevant one. However, here one needs two probes — X-ray and neutron. X-ray scattering experiment will determine $S_c(q)$ and then neutron scattering experiment can be used to determine $S_\Sigma(q)$, with the knowledge of $S_c(q)$.

Thus in both the unpolarized and partially polarized phases, $S_\Sigma(q)$ determines the composite fermion parameter $p_\uparrow$ which is identified as an order parameter in the spin transition, and can be measured experimentally by neutron scattering experiments. Therefore, neutron scattering experiment provides a *direct unambiguous* test of CF. The accuracy of Eqs. (4.23 and 4.24) lie on the region of small angle scattering as it is valid only for low $\mathbf{q}^2$.

4.4.4 Collective excitations

It is also intersting to study the collective modes of CDE and SDE and determine their respective spectral weights, which can be probed by Raman scattering experiments. In this context, we note that in inelastic light scattering experiments, the magnetoplasmon

modes of IQHE, and FQHE state at $\nu = 1/3$, have been observed [74, 75]. While Raman scattering experiments do not determine p as directly neutron scattering experiments, they will measure the CF energy scale parameter $\overline{\omega}_c$ as we shall show below, and they remain on par with the current experiments in testing the CFM.

A determination of the collective modes requires both polarized and depolarized Raman scattering. It is further necessary (as we shall see below) that the momentum transfer $\mathbf{q}$ have a non-zero component in the plane of the system. We look for the collective excitations in the small $\mathbf{q}$ regime for both unpolarized and fully polarized phases of the QHS. We shall study the $\nu = 2/3$ state in detail, as the state is observed in both the phases [37, 38]. However, the determination of collective excitations for other states is equally straight forward and follows the same procedure. We shall make general qualitative observations on the other states wherever possible.

We first consider CDE for fully polarized phase of $\nu = 2/3$ ($p_\uparrow = -2,\ p_\downarrow = 0,\ s = 1$) state. The collective modes are determined by the poles of $K^{00}(\omega, \mathbf{q})$. There are two perturbing parameters — $\overline{\mathbf{q}}$ and $\lambda = e^2/\epsilon l_0 \overline{\omega}_c$ since in TDHFA, the coulomb energy is smaller than $\overline{\omega}_c$. We thus expand both numerator and denominator of K^{00} in powers of $\overline{\mathbf{q}}$ and up to order λ. We then look for solutions of the form

$$\omega_k^2 = (k\overline{\omega}_c)^2 + \lambda\beta_1 + \beta_2(\overline{\mathbf{q}}^2)^{\gamma_1} + \lambda\beta_3(\overline{\mathbf{q}}^2)^{\gamma_2} , \tag{4.25}$$

where β_i and γ_i are constants to be determined for the corresponding modes which are characterized by k (an integer). The value of k runs from 1 to 3. For the state $\nu = 2/3$, $k = 3$ gives the mode corresponding to the actual cyclotron energy ω_c.

We find that there is no mode whose zero momentum gap is at $\overline{\omega}_c$. The mode at $k = 2$ is found to have a dispersion relation which is given by

$$\omega_2^2 = (2\overline{\omega}_c)^2 + \frac{32}{5}\overline{\omega}_c^2\overline{\mathbf{q}}^2 \tag{4.26}$$

with the corresponding residue in K^{00} being

$$\mathrm{Res}(K^{00})|_{\omega_2} = -e^2\omega_c\frac{\nu}{25\pi}\mathbf{q}^2\overline{\mathbf{q}}^2 . \tag{4.27}$$

Finally, the mode corresponding to $k = 3$ is given by

$$\omega_3^2 = \omega_c^2 - 2\sqrt{2}e^2\left(\frac{e^2}{\epsilon l_0}\right)\overline{\omega}_c\overline{\mathrm{q}} + 15\sqrt{2}\lambda\overline{\omega}_c^2\overline{\mathrm{q}} \tag{4.28}$$

with the residue,

$$\mathrm{Res}(K^{00})|_{\omega_3} = -e^2\omega_c\frac{\nu}{2\pi}\mathrm{q}^2 \,. \tag{4.29}$$

The last mode has a higher spectral weight compared to that of the mode ω_2. It may be noted that the second term of right hand side of Eq. (4.28) is the contribution from $V(\mathrm{q})$ in the expression of $\mathcal{D}(\omega,\ \mathrm{q})$ in (4.6), and comes from pure RPA. The last term is due to TDHFA and dominates over the RPA contribution. At $\mathrm{q} = 0$, there is only one mode at $\omega = \omega_c$ (see Eq. 4.19) in accordance with the Kohn's theorem.

We now consider the unpolarized phase of $\nu = 2/3$ ($p_\uparrow = p_\downarrow = -1$, $s = 1$) state. The CDE mode at $\overline{\omega}_c$ is again absent. The mode for $k = 2$ is given by

$$\omega_2^2 = (2\overline{\omega}_c)^2 + \frac{16}{5}\overline{\omega}_c^2\overline{\mathrm{q}}^2 \tag{4.30}$$

with the residue in K^{00},

$$\mathrm{Res}(K^{00})|_{\omega_2} = -e^2\omega_c\frac{\nu}{50\pi}\mathrm{q}^2\overline{\mathrm{q}}^2 \,. \tag{4.31}$$

The other mode for which the zero momentum gap is at ω_c follows the dispersion relation

$$\omega_3^2 = \omega_c^2 - 2\sqrt{2}e^2\left(\frac{e^2}{\epsilon l_0}\right)\overline{\omega}_c\overline{\mathrm{q}} + 30\sqrt{2}\lambda\overline{\omega}_c^2\overline{\mathrm{q}} \tag{4.32}$$

with the corresponding spectral weight (proportional to q^2), given by

$$\mathrm{Res}(K^{00})|_{\omega_3} = -e^2\omega_c\frac{\nu}{2\pi}\mathrm{q}^2 \,. \tag{4.33}$$

So far we have discussed CDE and we now study the SDE. In the fully polarized phase, SDE are same as CDE. However, SDE in the unpolarized phase of $\nu = 2/3$ state are very different. Indeed they are determined by the poles of $\Pi_0(\omega,\ \mathbf{q})$ (see Eq. (4.18)). The spin density excitation modes are obtained as

$$\omega_n = n\overline{\omega}_c + E_{n0}^{\uparrow} - \tilde{V}_{n00n}^{(1)}(\mathrm{q}) + 2\tilde{V}_{n0n0}^{(2)}(\mathrm{q}) \,. \tag{4.34}$$

Interestingly, the mode near $\overline{\omega}_c$ *survives* in the unpolarized phase which is otherwise absent in the fully polarized phase. The dispersion relations of the first three modes (*i.e.*, $n = 1$, 2, and 3) of SDE are shown in Figs. (4.1, 4.2, and 4.3) respectively in the low $\mathbf{q}$ regime. For very low $\mathbf{q}$, they have the form

$$\omega_1 = \overline{\omega}_c + \frac{e^2}{\epsilon l_0}\left[\sqrt{2}\overline{\mathbf{q}} - \frac{1}{4}\sqrt{\frac{\pi}{2}}\overline{\mathbf{q}}^2\right] , \tag{4.35}$$

$$\omega_2 = 2\overline{\omega}_c + \frac{e^2}{\epsilon l_0}\left[\frac{1}{4}\sqrt{\frac{\pi}{2}} - \frac{11}{128}\sqrt{\frac{\pi}{2}}\overline{\mathbf{q}}^2\right] , \tag{4.36}$$

$$\omega_3 = \omega_c + \frac{e^2}{\epsilon l_0}\left[\frac{3}{8}\sqrt{\frac{\pi}{2}} + \frac{955}{768}\sqrt{\frac{\pi}{2}}\overline{\mathbf{q}}^2\right] \tag{4.37}$$

with the respective residues in $\Sigma_{\rm unp}$ given by

$$\mathrm{Res}(\Sigma_{\rm unp})|_{\omega_1} = -e^2\mathbf{q}^2\omega_c\frac{\nu}{2\pi}\left[1 + \lambda\sqrt{2}\overline{\mathbf{q}}\right] , \tag{4.38}$$

$$\mathrm{Res}(\Sigma_{\rm unp})|_{\omega_2} = -e^2\mathbf{q}^2\overline{\mathbf{q}}^2\omega_c\frac{\nu}{2\pi}\left[1 + \lambda\frac{1}{8}\sqrt{\frac{\pi}{2}}\right] , \tag{4.39}$$

$$\mathrm{Res}(\Sigma_{\rm unp})|_{\omega_3} = -e^2\mathbf{q}^2\overline{\mathbf{q}}^4\omega_c\frac{\nu}{4\pi}\left[1 + \lambda\frac{1}{8}\sqrt{\frac{\pi}{2}}\right] . \tag{4.40}$$

It may be seen from (4.35–4.37) that the electron correlation effects do not change the zero momentum gap energy for the lowest energy excitation ω_1, but do affect the excitation gap for other higher excitations. It is significant that all these modes acquire their dispersive character entirely from TDHFA contribution. At the pure RPA level, the dispersive character would not be revealed. The spectral weight for the modes ω_n are proportional to $\mathbf{q}^{2n}$.

A few general observations: We find that, irrespective of the spin phases of quantum Hall states, the CDE have several universal characteristics: (i) The mode at $\overline{\omega}_c$ does not exist. (ii) The mode corresponding to the highest spectral weight (proportional to $\mathbf{q}^2$) is the plasmon mode at ω_c. We also find that SDE in the fully polarized phase is the same as CDE. We further find that for all unpolarized QHS, the SDE have a mode whose gap energy is $\overline{\omega}_c$ and with spectral weight proportional to $\mathbf{q}^2$. The spectral weights for all the other higher modes ω_n ($n \neq 1$) are down by a factor $\mathbf{q}^{2(n-1)}$. The gap energies for these higher modes change very much the same as $\nu = 2/3$ state due to the electron correlation effects. In the partially polarized quantum Hall states, the SDE

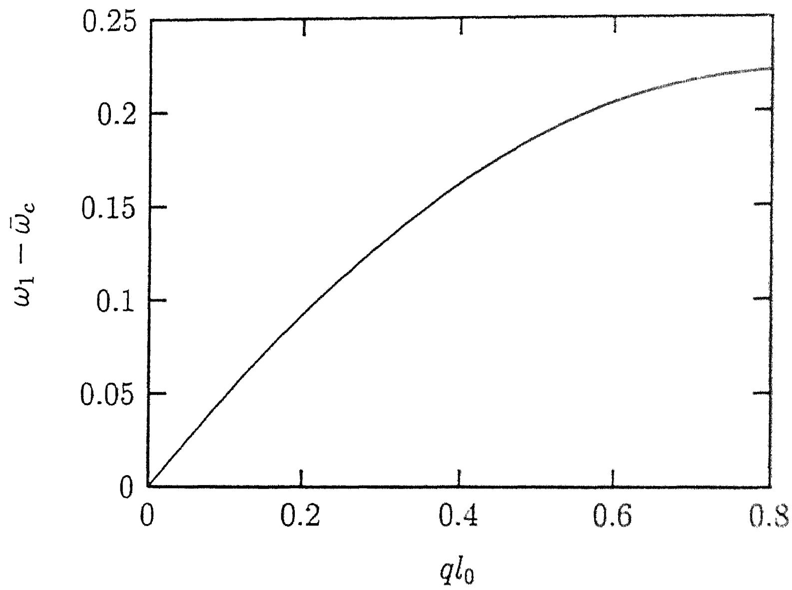

Figure 4.1: The spin density excitation mode $\omega_1 - \bar{\omega}_c$ in the units of $e^2/\epsilon l_0$ for unpolarized $\nu = 2/3$ state.

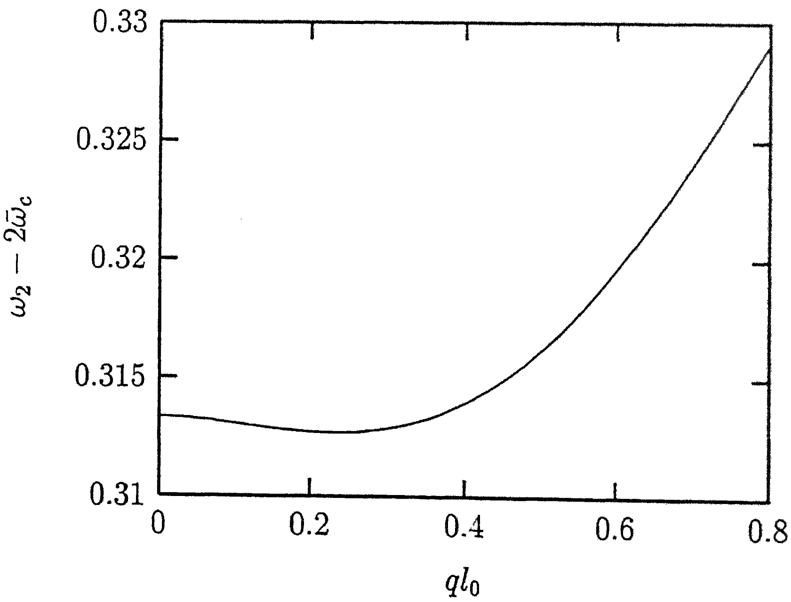

Figure 4.2: The spin density excitation mode $\omega_2 - 2\bar{\omega}_c$ in the units of $e^2/\epsilon l_0$ for unpolarized $\nu = 2/3$ state.

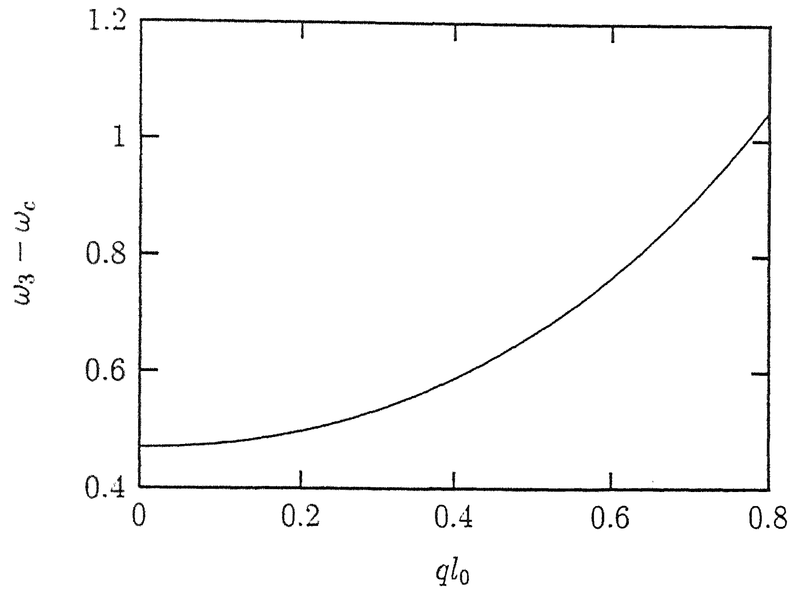

Figure 4.3: The spin density excitation mode $\omega_3 - \omega_c$ in the units of $e^2/\epsilon l_0$ for unpolarized $\nu = 2/3$ state.

mode at $\overline{\omega}_c$ acquires two branches, *i.e.*, there exists two modes with the spectral weights proportional to $\mathbf{q}^2$ which coincide at $\mathbf{q}^2 = 0$. The mode at ω_c for partially polarized phase has a spectral weight proportional to $\mathbf{q}^2$ which is unlike the unpolarized case. Thus the SDE behave very differently from CDE, in both unpolarized and partially polarized phases. This difference has been seen by Kallin and Halperin [69] in IQHE as well.

4.4.5 Raman scattering

By polarized and depolarized Raman scattering experiments, the modes of CDE and SDE (discussed in the previous subsection) can respectively be found out. The Raman intensity $I(\omega)$ is proportional to the imaginary part of the corresponding correlation functions which are known as spectral functions [76]. We are interested in that geometry of Raman scattering where the contributions of CDE and SDE in the cross sections get separated out. It corresponds to $\hat{e}_i \parallel \hat{e}_s$ for CDE and $\hat{e}_i \perp \hat{e}_s$ for SDE, where $\hat{e}_i$ and $\hat{e}_s$ are the direction of the polarization of the incident and scattered beam respectively.

The respective separated cross sections are given by [76]

$$\frac{d^2\sigma_c}{d\Omega d\omega} \propto (\hat{e}_i \cdot \hat{e}_s)^2 S_c(\omega, q) ; \tag{4.41}$$

$$\frac{d^2\sigma_\Sigma}{d\Omega d\omega} \propto (\hat{e}_i \times \hat{e}_s)^2 S_\Sigma(\omega, q) . \tag{4.42}$$

Here $S_c(\omega, q)$ and $S_\Sigma(\omega, q)$ are the spectral functions for CDE and SDE respectively. The geometry in which only CDE are determined is known as *polarized* Raman scattering geometry, while SDE are determined in *depolarized* Raman scattering geometry.

In the limit $q^2 l_0^2 \ll 1$, most of the weight of CDC is in the plasmon mode *i.e.*, at ω_c (4.28 and 4.32) for both fully polarized and unpolarized phases. The pole in CDC for excitation energy ω_2 for $\nu = 2/3$ state may be read off from Eqs. (4.26) or (4.30). The intensities corresponding to the mode ω_2 will be suppressed by a factor of q^2 relative to the plasmon mode. Polarized Raman scattering will determine these modes of excitations.

Consider now depolarized Raman scattering experiment. In the *fully polarized* phase, it creates spectra very similar to the one in the polarized Raman scattering experiment because CDE and SDE are same in this phase. On the other hand, in the *unpolarized* phase, the highest intensity will be observed for the mode whose energy gap is $\overline{\omega}_c$, and would signal the existence of composite fermions. We note that the intensity corresponding to the next higher mode at $2\overline{\omega}_c$ is suppressed by a factor of $\overline{q}^2$. The intensity for other modes are further down by successive factors of $\overline{q}^2$, here as well.

Although we have discussed depolarized Raman spectra only for $\nu = 2/3$ state in unpolarized phase, it is easy to check that the characteristics of the spectra will be similar for all other unpolarized QHS. The depolarized Raman spectra continue to have the highest intensity corresponding to the mode at $\overline{\omega}_c$. For partially polarized states, such as $\nu = 3/5$, there will be three highest intensity peaks (in the same order of q^2) corresponding to one mode at ω_c and two modes at $\overline{\omega}_c$. Since $\overline{\omega}_c$ is thus directly measured in depolarized Raman scattering both for unpolarized or partially polarized QHS — it follows that $p_\uparrow + p_\downarrow$, the effective number of filled LL, will also be known

provided m^* is given.

4.5 Conclusion

In summary, we state the most important results. The effective number of filled Landau levels by composite fermions of up (or down) spin is identified as an order parameter in the spin transitions from unpolarized or partially polarized phases to the fully polarized phase of the quantum Hall states. The static spin density correlation undergoes a discontinuous change in its value in the spin transitions. The static charge and spin structure factors are independent of carrier density and effective mass of the particles. While the static charge structure factor is a function of the filling factor, the static spin structure factor, in general, is a function of effective Landau levels filled by both up and down spins and the filling factor as well. The mode corresponding to the highest spectral weights in the charge density excitations is the plasmon mode at ω_c, irrespective of the spin phases. The spin density excitations for fully polarized quantum Hall states are same as the charge density excitations, but they differ from each other in the unpolarized or partially polarized phases. The mode at $\overline{\omega}_c$ corresponds to the highest spectral weight in the spin density excitations of unpolarized quantum Hall states. In the partially polarized phase, there are three modes of almost equal (in the same order of q^2) spectral weights — one at ω_c and two at $\overline{\omega}_c$. Neutron scattering scattering experiments would unambiguously determine one of the composite fermion parameters, *viz*, the effective number of filled Landau levels by the composite fermions. The other parameter (number of flux quanta attached to each particle) may be determined from the knowledge of the former. Depolarized Raman scattering experiments can directly determine $\overline{\omega}_c$, the energy scale for the composite fermions. The composite fermion parameters also will be determined by the latter experiment if the effective mass of the composite fermions is given.

Finally, LF [52] have studied recently the bilayered QHS employing a similar model as ours. However, the two models leads to certain different physical consequences. (For detailed comparison between the two models, see section 3.5). It might be of

interest to examine whether there is some experimental procedure that can determine the composite fermion parameters in bilayered systems as well.

Chapter 5

Spin-wave and spin-flip excitations in arbitrarily polarized quantum Hall states

5.1 Introduction

As the second application of the doublet model, we shall study the spin-wave and spin-flip excitations in arbitrarily polarized QHS in this chapter. In other words, we shall study the spin density excitations (SDE) ($\delta S_z = \pm 1$) in the ground state of arbitrarily polarized QHS.

Stein *et al* [46] were the first to observe experimentally electron spin resonance corresponding to spin wave excitations in odd integer QHS. This type of excitations is possible only for odd integer QHS, for in that case when g is small, for a given LL one spin state is fully occupied while the other remains completely empty in the same LL for small g values. Theoretically, Kallin and Halperin [69] have studied spin-wave and spin-flip excitations in IQHE in a diagrammatic approach which is equivalent to TDHFA for the Coulomb interactions. Longo and Kallin [77] have extended the analysis of spin-flip excitations to partial filling factors. They argue that the change in energy of excitations due to the Coulomb interactions is simply the filling factor times the value for fully filled lowest LL. This is, in fact, not so, as we shall show below. Longo and Kallin [77] have further studied the spin-flip excitations in the single

mode approximation (SMA) which includes the correlation effects in the partially filled LL. They find entirely different results for the TDHFA and SMA: the gap calculated from SMA is much less than that from TDHFA and the dispersion relation behaves differently. Nakajima and Aoki [78] have numerically found spin-wave excitations in Laughlin states using CF picture. They have used a reduced Haldane Pseudo potential [57] for CF to carry out the calculation. In this chapter, we shall develop a generalized procedure for obtaining spin-wave and spin-flip excitations both for integer QHS, and fractional QHS in the lowest LL. We treat Coulomb interaction between CF in TDHFA, within the doublet model.

5.2 The formalism

To study the spin-wave and spin-flip excitations, we introduce additional spin sources $h_\pm$, which can flip the spin, to the system. Therefore the new Lagrangian reads [see Eq. (3.1)]

$$\begin{aligned}\mathcal{L} &= \psi_\uparrow^* \mathcal{D}(a_\mu^\uparrow)\psi_\uparrow + \psi_\downarrow^* \mathcal{D}(a_\mu^\downarrow)\psi_\downarrow + \frac{1}{2}\tilde{a}_\mu \epsilon^{\mu\nu\lambda}\Theta\partial_\nu a_\lambda - eA_0^{\text{in}}\rho \\ &+\frac{1}{2}\int d^3x' A_0^{\text{in}}(x)V^{-1}(x-x')A_0^{\text{in}}(x') + e\psi^\dagger(\sigma_+ h_+ + \sigma_- h_-)\psi\,. \qquad (5.1)\end{aligned}$$

Here $\psi \equiv (\psi_\uparrow\,,\,\psi_\downarrow)$ is the doublet of fermionic field. The potential for interactions between CF is considered to be Coulombic, *i.e.*, $V(r) = e^2/\epsilon r$, where ϵ is the background dielectric constant of the system. $\sigma_\pm = \frac{1}{2}(\sigma_x \pm i\sigma_y)$ are the spin raising and lowering operators respectively.

5.2.1 Mean field results (a brief resume)

As discussed in chapter 2, for the QHS at hand, mean magnetic field for all the particles, irrespective of their spin, is given by $\bar{B} = B + \langle b^+\rangle$. Let $p_\uparrow(p_\downarrow)$ be the number of LL, which are formed by effective field $\bar{B}$, filled by spin up (down) particles. This leads to the actual filling fraction and spin density [see Eqs. (2.11), (2.19)–(2.21)] to be

$$\nu = \frac{p_\uparrow + p_\downarrow}{2s(p_\uparrow + p_\downarrow)+1}\,,\quad \Delta\rho = \rho\left(\frac{p_\uparrow - p_\downarrow}{p_\uparrow + p_\downarrow}\right)\,. \qquad (5.2)$$

Note that $p_\uparrow$ and $p_\downarrow$ can be negative integers as well in which case $\bar{B}$ is antiparallel to B. The effective cyclotron frequency $\bar{\omega}_c$ is related to the actual cyclotron frequency $\omega_c = \frac{e}{m^*}B$ by $\omega_c = \bar{\omega}_c[2s(p_\uparrow + p_\downarrow) + 1]$. For unpolarized QHS, $p_\uparrow = p_\downarrow = p$ (say) and therefore the states with filling fraction $v = 2p/(4sp+1)$ are spin unpolarized in the limit of small Zeeman energy. In this limit, $p_\uparrow = p_\downarrow + 1$ for partially polarized states with $\Delta\rho/\rho = 1/(p_\uparrow + p_\downarrow)$. Fully polarized Laughlin states are obtained for $p_\uparrow = 1$, $p_\downarrow = 0$. The IQHE states correspond to the choice $s = 0$ (*i.e.*, $\theta_+ = \infty$), in which case mean CS magnetic field is zero.

5.2.2 Effective action

Employing the above MF ansatz, we then evaluate one-loop effective action for the gauge fields and probes to be

$$
\begin{aligned}
S_{\rm eff} \;=\; & -\frac{1}{2}\int d^3x \int d^3x' \Big[(a_\mu^+ + a_\mu^- + A_0^{\rm in}\delta_{\mu 0})(x)\,\Pi_\uparrow^{\mu\nu}(x,x')\,(a_\nu^+ + a_\nu^- + A_0^{\rm in}\delta_{\nu 0})(x') \\
& + (a_\mu^+ - a_\mu^- + A_0^{\rm in}\delta_{\mu 0})(x)\,\Pi_\downarrow^{\mu\nu}(x,x')\,(a_\nu^+ + a_\nu^- + A_0^{\rm in}\delta_{\nu 0})(x') \\
& - A_0^{\rm in}(x)V^{-1}(x-x')A_0^{\rm in}(x') + 2h^a(x)\Gamma_\uparrow^{a\mu}(x,x')(a_\mu^+ + a_\mu^- + A_0^{\rm in}\delta_{\mu 0})(x') \\
& + 2h^a(x)\Gamma_\downarrow^{a\mu}(x,x')(a_\mu^+ - a_\mu^- + A_0^{\rm in}\delta_{\mu 0})(x') + h_a(x)\chi^{ab}(x,x')h_b(x')\Big] \\
& + \frac{1}{2}\int d^3x \left\{\theta_+\epsilon^{\mu\nu\lambda}a_\mu^+\partial_\nu a_\lambda^+ + \theta_-\epsilon^{\mu\nu\lambda}a_\mu^-\partial_\nu a_\lambda^-\right\} . \qquad (5.3)
\end{aligned}
$$

Here $a_\mu^\pm$ and $A_0^{\rm in}$ are fluctuating part of the corresponding gauge fields. Note that the field a_μ^- does not exist for unpolarized states and hence Eq. (5.3) reduces accordingly. The indices a, b in (5.3) represent $\pm$ indices of spin raising and lowering operators. The correlation functions $\Pi_\tau^{\mu\nu}(x,x')$, $\chi^{ab}(x,x')$, and $\Gamma_\tau^{a\mu}(x,x')$ have to be evaluated at the prescribed MF state. Their explicit forms are as follows:

$$
\Pi_\tau^{\mu\nu}(x,x') = -i\,\langle j_\tau^\mu(x) j_\tau^\nu(x')\rangle_C - \left\langle \frac{\delta j_\tau^\mu(x)}{\delta A_\nu(x')}\right\rangle , \qquad (5.4)
$$

$$
\chi^{ab}(x,x') = -i\left\langle j^a(x) j^b(x')\right\rangle_C , \qquad (5.5)
$$

$$
\Gamma_\tau^{a\mu}(x,x') = -i\,\langle j^a(x) j_\tau^\mu(x')\rangle_C . \qquad (5.6)
$$

Here $\langle\cdots\rangle$ represents the expectation value in the ground state of the system. $\langle\cdots\rangle_C$ corresponds to the connected diagrams which contribute to the expectation value. $\mathcal{A}_\mu$

represents the sum of all the gauge fields. The current operators in (5.4–5.6) are given by

$$
\begin{aligned}
j_r^0(x) &= e\psi_r^*\psi_r \,, &(5.7)\\
j_r^k(x) &= e\frac{e}{2m^*}\left[\psi_r^* D^k\psi_r - \left(D^{k*}\psi_r^*\right)\psi_r\right] + \frac{g}{2}\sigma\mu_B\epsilon^{kj}\partial_j\psi_r^*\psi_r \,. &(5.8)\\
j^a(x) &= e\psi^\dagger\sigma_a\psi \,. &(5.9)
\end{aligned}
$$

It is easy to see that

$$\Gamma_r^{a\mu}(x,x') \equiv 0 \,, \tag{5.10}$$

since $\langle\sigma_a\rangle \equiv 0$. Therefore, the terms in (5.3) corresponding to the probe h_a completely decouple from the fluctuation of the gauge fields. In other words, gauge field fluctuations do not change the correlation $\chi^{ab}(x,x')$. Further, $\chi^{++}(x,x') = \chi^{--}(x,x') \equiv 0$ since $\langle\sigma_+^2\rangle = \langle\sigma_-^2\rangle \equiv 0$. We, thus, obtain

$$S_{\text{eff}}[h^+, h^-] = -\frac{1}{2}\int d^3x \int d^3x' \left[h^+(x)\chi^{+-}(x,x')h^-(x') + h^-(x)\chi^{-+}(x,x')h^+(x')\right] \,. \tag{5.11}$$

$\chi^{+-}(x,x') \equiv \delta^2 S_{\text{eff}}/\delta h^+(x)\delta h^-(x')$ is the spin correlation function where a particle of up spin is destroyed at the point x' and a particle of spin down is created at the point x. In other words, this is the correlation function for producing a spin up quasihole at the point x' and a spin down quasiparticle at the point x. Similarly, $\chi^{-+}(x,x')$ represents the spin correlation function for producing a spin down quasihole at the point x' and a spin up quasiparticle at the point x. These correlation functions are the response functions for SDE ($\delta S_z = \pm 1$) which we shall evaluate below.

5.3 Response functions

In terms of the single particle Green function

$$G(x,x') = -i\langle T\psi(x)\psi^\dagger(x')\rangle \,, \tag{5.12}$$

the linear response functions can be written as

$$
\begin{aligned}
\chi^{+-}(x,\,x') &= ie^2\,\mathrm{Tr}\left[\sigma_+ G(x,\,x')\sigma_- G(x',\,x)\right] \,, &(5.13)\\
\chi^{-+}(x,\,x') &= ie^2\,\mathrm{Tr}\left[\sigma_- G(x,\,x')\sigma_+ G(x',\,x)\right] \,. &(5.14)
\end{aligned}
$$

Let G be the single particle Green's function evaluated by switching off the Coulomb interaction. Then χ^{+-} and χ^{-+} that emerge are in pure RPA. We shall go beyond RPA and determine χ^{+-} and χ^{-+} in the TDHFA.

We now determine the response functions (in momentum space) in the TDHFA as a generalization to the RPA. Recall that in TDHFA, the Green's functions are Hartree Fock Green's functions (see appendix B) and incorporate self energy due to the Coulomb interactions. In this approximation, as we have discused in the previous chapter, only diagrams with one exciton present at a time are considered. In other words, the Coulomb energy $e^2/\epsilon l_0$ is taken to be smaller than $\bar{\omega}_c$, where $l_0 = (e\bar{B})^{-1/2}$ is the effective magnetic length of the system and ϵ is the background dielectric constant. This assumption is, therefore, not valid at or near $\nu = 1/2s$. In other words, the condition on the validity of our assumption is $e^{3/2}m^*/\epsilon \ll \sqrt{\bar{B}}$.

The TDHFA response functions are determined in appendix B. They are

$$
\begin{aligned}
\chi^{+-}(\omega, \mathbf{q}) &= \frac{e^2}{4\pi}\mathbf{q}^2 e^{-\bar{\mathbf{q}}^2/2} \\
&\times \left[\sum_{n_2<p_\uparrow} \sum_{n_1 \geq p_\downarrow} \left(\frac{n_2!}{n_1!}\right) \frac{(\bar{\mathbf{q}}^2)^{n_1-n_2-1}\left\{L_{n_2}^{n_1-n_2}(\bar{\mathbf{q}}^2)\right\}^2}{\omega - (\epsilon_{n_1}^{\downarrow} - \epsilon_{n_2}^{\uparrow}) - E_{n_1 n_2}^{\downarrow\uparrow} + \tilde{V}_{n_1 n_2 n_2 n_1}^{(1)}(q) + i\eta} \right. \\
&\left. - \sum_{n_2<p_\downarrow} \sum_{n_1 \geq p_\uparrow} \left(\frac{n_2!}{n_1!}\right) \frac{(\bar{\mathbf{q}}^2)^{n_1-n_2-1}\left\{L_{n_2}^{n_1-n_2}(\bar{\mathbf{q}}^2)\right\}^2}{\omega + (\epsilon_{n_1}^{\uparrow} - \epsilon_{n_2}^{\downarrow}) + E_{n_1 n_2}^{\uparrow\downarrow} - \tilde{V}_{n_1 n_2 n_2 n_1}^{(1)}(q) - i\eta} \right],
\end{aligned}
\tag{5.15}
$$

$$
\begin{aligned}
\chi^{+-}(\omega, \mathbf{q}) &= \frac{e^2}{4\pi}\mathbf{q}^2 e^{-\bar{\mathbf{q}}^2/2} \\
&\times \left[\sum_{n_2<p_\downarrow} \sum_{n_1 \geq p_\uparrow} \left(\frac{n_2!}{n_1!}\right) \frac{(\bar{\mathbf{q}}^2)^{n_1-n_2-1}\left\{L_{n_2}^{n_1-n_2}(\bar{\mathbf{q}}^2)\right\}^2}{\omega - (\epsilon_{n_1}^{\uparrow} - \epsilon_{n_2}^{\downarrow}) - E_{n_1 n_2}^{\uparrow\downarrow} + \tilde{V}_{n_1 n_2 n_2 n_1}^{(1)}(q) + i\eta} \right. \\
&\left. - \sum_{n_2<p_\uparrow} \sum_{n_1 \geq p_\downarrow} \left(\frac{n_2!}{n_1!}\right) \frac{(\bar{\mathbf{q}}^2)^{n_1-n_2-1}\left\{L_{n_2}^{n_1-n_2}(\bar{\mathbf{q}}^2)\right\}^2}{\omega + (\epsilon_{n_1}^{\downarrow} - \epsilon_{n_2}^{\uparrow}) + E_{n_1 n_2}^{\downarrow\uparrow} - \tilde{V}_{n_1 n_2 n_2 n_1}^{(1)}(q) - i\eta} \right],
\end{aligned}
\tag{5.16}
$$

where n_1, n_2 represent the indices of the LL formed by effective magnetic field $\bar{B}$. Here $\epsilon_n^r = (n + 1/2)\bar{\omega}_c - (1/2)g\mu_B\overline{B}\sigma$ is the energy of n th LL with spin index r.

$\sigma = +1(-1)$ for up (down) states. $E^{rr'}_{n_1 n_2} = \Sigma^r_{n_1} - \Sigma^{r'}_{n_2}$ represents the exchange energy, *i.e.*, the difference in self energy of particles in two different LL with unequal spin indices. Σ^r_n is independent of momentum q, and is given by Eq. 4.8. The interaction between an excited particle and hole (*i.e.*, the ladder diagrams) is represented by the matrix element $\tilde{V}^{(1)}_{n_1 n_2 n_2 n_1}(q)$ which is expressed in Eq. 4.9. We note that the bubble diagrams in which a particle-hole pair recombines to form another particle-hole pair do not contribute to the response functions considered here. This is because particle and hole possess different spin.

In obtaining Eqs. (5.15) and (5.16), we have included all the contributions up to order $e^2/\epsilon l_0$ and so the form factors are essentially exact in the strong effective magnetic field limit. In the absence of Coulomb interaction, Σ^r_n and $\tilde{V}^{(1)}_{n_1 n_2 n_2 n_1}(q)$ are zero and hence the response functions acquire their pure RPA form. We shall see below that the coulomb interaction between composite fermions plays a decisive role in the excitations considered in this chapter.

5.4 The excitations

As we have seen above, the response functions χ^{+-} and χ^{-+} remain unchanged by the fluctuation of the gauge fields. They depend only on the mean effective magnetic field. Therefore, the corresponding SDE depend solely on effective magnetic length l_0 which is related to actual magnetic length of the system $l = (eB)^{-1/2}$ via $l_0 = (|p_\uparrow + p_\downarrow|/\nu)^{1/2} l$. The excitations for the fractional states with $\nu = |p_\uparrow + p_\downarrow|/(2s|p_\uparrow + p_\downarrow| \pm 1)$ are equivalent to that of integer states with $\nu = |p_\uparrow + p_\downarrow|$, since the states have same l_0.

The dispersion relation for the excitation of a spin down particle and a spin up hole is obtained from Eq. (5.15) as

$$\omega = (n_1 - n_2)\bar{\omega}_c + g\mu_B \overline{B} + E^{\downarrow\uparrow}_{n_1 n_2} - \tilde{V}^{(1)}_{n_1 n_2 n_2 n_1}(q)\ , \tag{5.17}$$

with $n_2 < p_\uparrow$ and $n_1 \geq p_\downarrow$. In these SDE, the z component of the spin changes as $\delta S_z = -1$. Similarly the SDE with a spin up particle and a spin up hole ($\delta S_z = +1$)

have dispersion relation (see Eq. (5.16))

$$\omega = (n_1 - n_2)\bar{\omega}_c - g\mu_B\overline{B} + E^{\uparrow\downarrow}_{n_1 n_2} - \tilde{V}^{(1)}_{n_1 n_2 n_2 n_1}(q) \,, \tag{5.18}$$

with $n_2 < p_\downarrow$ and $n_1 \geq p_\uparrow$.

5.4.1 Spin-flip excitations

In the spin-flip excitations, a particle changes Landau level as well as flipping its spin. The excitation modes can have energy different from $(n_1 - n_2)\bar{\omega}_c + g\mu_B\bar{B}(\delta S_z)$ at $q = 0$, since the Coulombic interaction may change the gap energy, in general. There are three types of ground state to consider: (i) fully polarized states ($p_\uparrow = 1$, $p_\downarrow = 0$); (ii) unpolarized states ($p_\uparrow = p_\downarrow$); and (iii) partially polarized states ($p_\uparrow = p_\downarrow + 1$). We discuss the spin-flip excitations of each of these ground states.

Case-I: For fully polarized states, the dispersion relation, corresponding to spin down particle and spin up hole excitations, from Eq. (5.17), is given by

$$\begin{aligned} \omega_m - m\bar{\omega}_c - g\mu_B\overline{B} &= \Delta E_m(q) \\ &= E^{\downarrow\uparrow}_{m0} - \tilde{V}^{(1)}_{m00m}(q) \,, \end{aligned} \tag{5.19}$$

where m is an integer. The change in energy, due to Coulomb interaction between the fermions, corresponding to the two lowest modes with $m = 1$ and $m = 2$, are respectively obtained as

$$\Delta E_1(q) = \frac{e^2}{\epsilon l_0}\frac{1}{2}\sqrt{\frac{\pi}{2}}\left\{2 - e^{-\bar{q}^2/2}\left[(1+\bar{q}^2)I_0\left(\frac{\bar{q}^2}{2}\right) - \bar{q}^2 I_1\left(\frac{\bar{q}^2}{2}\right)\right]\right\} \,, \tag{5.20}$$

$$\begin{aligned} \Delta E_2(q) = \frac{e^2}{\epsilon l_0}\frac{1}{8}\sqrt{\frac{\pi}{2}}\Bigg\{8 - e^{-\bar{q}^2/2}\Bigg[&(3 + 2\bar{q}^2 + 2\bar{q}^4)I_0\left(\frac{\bar{q}^2}{2}\right) \\ &-(4\bar{q}^2 + 2\bar{q}^4)I_1\left(\frac{\bar{q}^2}{2}\right)\Bigg]\Bigg\} \,. \end{aligned} \tag{5.21}$$

Here I_0 and I_1 are the modified Bessel's functions whose integral representations are given by

$$I_0(z) = \frac{1}{4\pi}\int_0^{4\pi} e^{-z\cos\theta} d\theta \,, \tag{5.22}$$

$$\frac{1}{z}I_1(z) = \frac{1}{4\pi}\int_0^{4\pi} e^{-z\cos\theta}\sin^2\theta \, d\theta \,. \tag{5.23}$$

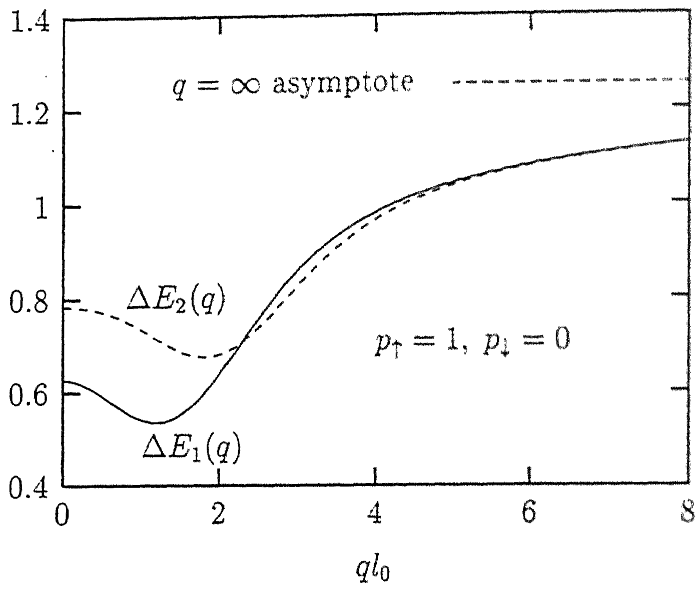

Figure 5.1: $\Delta E_1(q)$ and $\Delta E_2(q)$ are plotted in the units of $e^2/\epsilon l_0$ against ql_0. $q = \infty$ asymptotes are same for both the cases.

These two dispersion relations are shown in Fig. (5.1). For very low ql_0, these energies behave as

$$\Delta E_1(q) \approx \frac{e^2}{\epsilon l_0}\frac{1}{2}\sqrt{\frac{\pi}{2}}\left[1 - \frac{\bar{\mathrm{q}}^2}{2}\right], \tag{5.24}$$

$$\Delta E_2(q) \approx \frac{e^2}{\epsilon l_0}\frac{1}{8}\sqrt{\frac{\pi}{2}}\left[5 - \frac{\bar{\mathrm{q}}^2}{2}\right]. \tag{5.25}$$

Thus the Coulomb interaction has changed the gap energy for these spin-flip excitations. At low momentum, the exchange in self energy dominates over the interaction energy between excited particle and hole pair. On the other hand, their contributions reverse for higher momentum. Thus the dispersion relations show a minima in their spectra (see Fig. (5.1)).

There is no mode corresponding to the dispersion relation (5.18), since the population of down spins is zero in the fully polarized ground state.

Note that the above dispersion relations of the spin-flip excitations hold for the Laughlin states with $\nu = \frac{1}{2s+1}$ because they all have same l_0. All these states acquire non vanishing gap energies due to the Coulomb interaction, contrary to the result

of Kallin and Halperin[69] for $\nu = 1$ state ($s = 0$). The reason for the mismatch between the two results is that they have calculated exchange self energy wrongly. This drawback was corrected by Longo and Kallin[77], who have further calculated dispersion relations using the SMA to obtain finite gap energies due to the Coulomb interaction in partially filled Landau levels. As we have seen, the present model allows for spin-flip excitation at $\bar{\omega}_c + g\mu_B\overline{B}$, while the lowest spin-flip mode in the SMA is at $\omega_c + g\mu_B B$.

Case–II: For unpolarized QHS, equal number of LL filled by particles of up and down spins. Consider the simplest case $|p_\uparrow| = |p_\downarrow| = 1$. The dispersion relations for the spin flip excitations with $\delta S_z = \mp 1$ are respectively given by

$$\begin{aligned} \omega_m - n\bar{\omega}_c - g\mu_B\overline{B} &= \Delta E_m^- \\ &= E_{m0}^{\downarrow\uparrow} - \tilde{V}_{m00m}^{(1)}(q) \,, \qquad (5.26) \\ \omega_m - m\bar{\omega}_c + g\mu_B\overline{B} &= \Delta E_m^+ \\ &= E_{m0}^{\uparrow\downarrow} - \tilde{V}_{m00m}^{(1)}(q) \,. \qquad (5.27) \end{aligned}$$

Here $\Delta E_m^+ = \Delta E_m^-$ as $E_{m0}^{\downarrow\uparrow} = E_{m0}^{\uparrow\downarrow}$ due to the equal population of both the spins. The change in energy due to the Coulomb interaction for the two lowest modes ($m = 1, 2$) are given by

$$\Delta E_1^\pm(q) = \frac{e^2}{\epsilon l_0}\frac{1}{2}\sqrt{\frac{\pi}{2}}\left\{1 - e^{-\bar{q}^2/2}\left[(1+\bar{q}^2)I_0\left(\frac{\bar{q}^2}{2}\right) - \bar{q}^2 I_1\left(\frac{\bar{q}^2}{2}\right)\right]\right\} \,, \qquad (5.28)$$

$$\begin{aligned} \Delta E_2^\pm(q) = \frac{e^2}{\epsilon l_0}\frac{1}{8}\sqrt{\frac{\pi}{2}}\Bigg\{5 - e^{-\bar{q}^2/2}\Bigg[&(3 + 2\bar{q}^2 + 2\bar{q}^4)I_0\left(\frac{\bar{q}^2}{2}\right) \\ &-(4\bar{q}^2 + 2\bar{q}^4)I_1\left(\frac{\bar{q}^2}{2}\right)\Bigg]\Bigg\} \qquad (5.29) \end{aligned}$$

respectively. These are shown in Fig. (5.2). Note that the Coulomb interaction does not contributes to the $m = 1$ mode. The unpolarized states with $\nu = 2/(4s \pm 1)$, *i.e.*, the states with 2 as a numerator such as $2, 2/3, 2/5$ have similar spin flip excitations as above since they all have same l_0.

Case-III: Consider the simplest case $|p_\uparrow| = 2$ and $|p_\downarrow| = 1$ as an example of partially polarized QHS. The dispersion relation corresponding to $\delta S_z = +1$ excitations is given

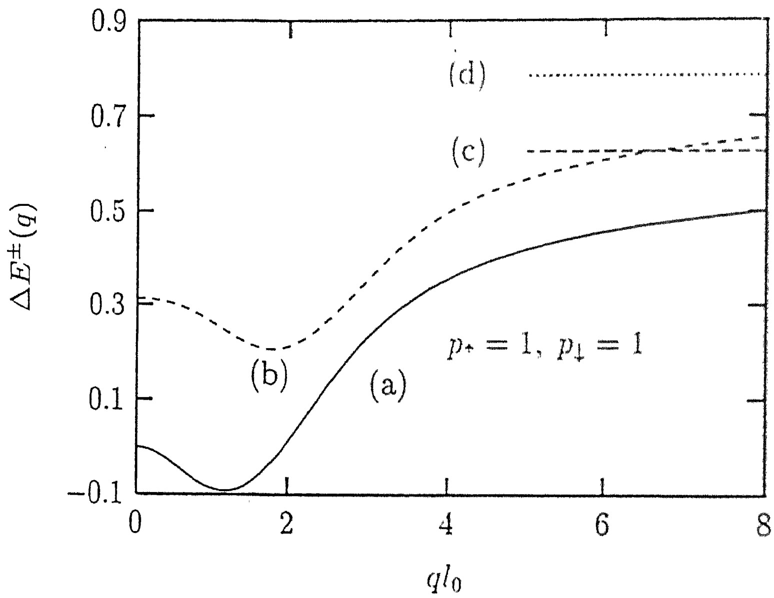

Figure 5.2: (a) $\Delta E_1^{\pm}(q)$ and (b) $\Delta E_2^{\pm}(q)$ are plotted in the units of $e^2/\epsilon l_0$ against ql_0. The lines (c) and (d) are the respective $q = \infty$ asymptotes.

by

$$\omega_m - m\bar{\omega}_c + g\mu_B\overline{B} = \delta E_m^- = E_{m0}^{\uparrow\downarrow} - \tilde{V}_{m00m}^{(1)}(q). \tag{5.30}$$

with $m > 1$. Therefore there is no mode at $\bar{\omega}_c - g\mu_B\bar{B}$ in this case. $\delta S_z = -1$ type of spin flip excitations may occur from any of the two filled LL by up spins. They have two classes if dispersion relations given by

$$\begin{aligned} \omega_m - m\bar{\omega}_c - g\mu_B\overline{B} &= \Delta E_m^{(1)-} = E_{m0}^{\downarrow\uparrow} - \tilde{V}_{m00m}^{(1)}(q)\ ;\ m > 0\ , & (5.31)\\ \omega_m - (m-1)\bar{\omega}_c - g\mu_B\overline{B} &= \Delta E_m^{(2)-} = E_{m1}^{\downarrow\uparrow} - \tilde{V}_{m11m}^{(1)}(q)\ ;\ m > 1\ . & (5.32)\end{aligned}$$

The energies $\Delta E_1^{(1)-}(q)$, $\Delta E_2^{(1)-}(q)$, and $\Delta E_2^{(2)-}(q)$ are shown in Fig. (5.3). Figure (5.4) represents $\Delta E_1^{+}(q)$. The states with $\nu = 3/(6s \pm 1)$, *i.e.*, all the states with numerator 3 such as 3, 3/5, 3/7 have the similar spin-flip excitations as shown above.

5.4.2 Spin-wave excitations

When Fermi energy lies between two spin split levels in the same LL, the particles may be excited within the same LL by flipping the spin. This excitation is possible only

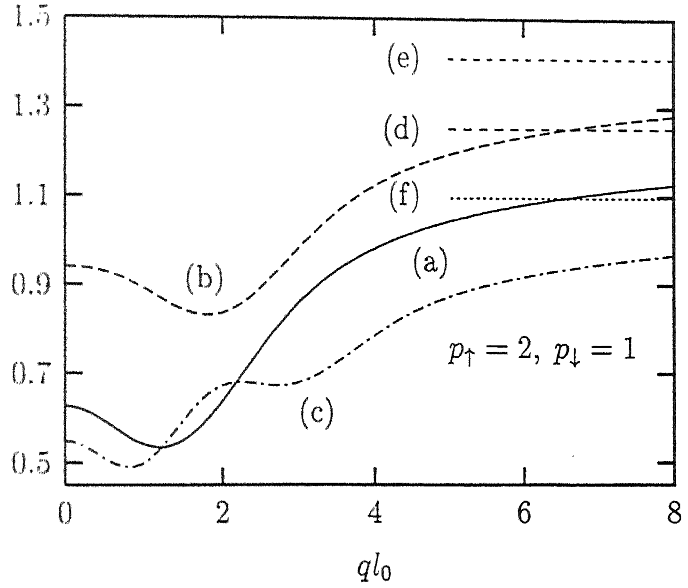

Figure 5.3: (a) $\Delta E_1^{(1)-}(q)$, (b) $\Delta E_2^{(1)-}(q)$, and (c) $\Delta E_1^{(2)-}(q)$ are plotted in the units of $e^2/\epsilon l_0$ against ql_0. The lines (d), (e), and (f) are the respective $q = \infty$ asymptotes.

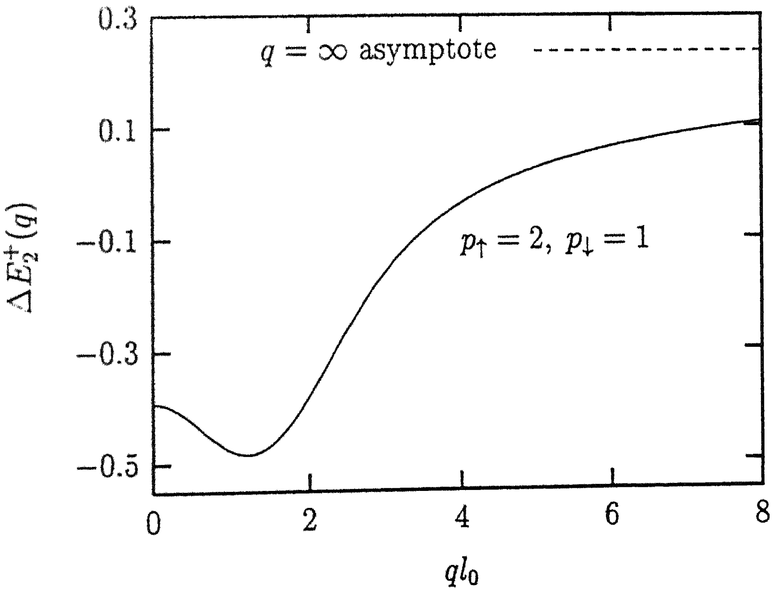

Figure 5.4: The spin flip mode, corresponding to flipping the spin from down to up, $\Delta E_1^+(q)$ is shown in the unit of $e^2/\epsilon l_0$.

in the ferromagnetic ground state. Therefore, fully polarized and partially polarized QHS are possible candidates to observe this kind of excitations. We shall see below that the Coulomb interactions do not change the spin-wave excitation energy at $q = 0$, as required by Larmor's theorem. The long wave length spin wave becomes gapless at $g = 0$.

Fully polarized states: Consider the fully polarized ($p_\uparrow = 1$, $p_\downarrow = 0$) QHS first. The spin wave dispersion relation is obtained as

$$\omega - g\mu_B\bar{B} = \Delta E(q) = E^{\downarrow\uparrow}_{\bar{0}\bar{0}} - \tilde{V}^{(1)}_{0000}(q) \ . \tag{5.33}$$

The explicit form of $\Delta E(q)$ is given by

$$\Delta E(q) = \frac{e^2}{\epsilon l_0}\sqrt{\frac{\pi}{2}}\left[1 - e^{-\bar{q}^2/2} I_0\left(\frac{\bar{q}^2}{2}\right)\right] \ . \tag{5.34}$$

The dispersion energy $\Delta E(q)$ is shown in Fig. (5.5). The states $\nu = 1$ and $\nu = 1/(2s+1)$ follow the above dispersion relation in their spin wave excitations. At very low ql_0, the spin wave is quadratically dispersed as

$$\omega = g\mu_B\bar{B} + \frac{e^2}{\epsilon l_0}\frac{1}{2}\sqrt{\frac{\pi}{2}}(ql_0)^2 \ . \tag{5.35}$$

The energy cost to excite a spin down quasi-particle and a spin up quasihole is $\sqrt{\frac{\pi}{2}}\frac{e^2}{\epsilon l_0}$. This excitation corresponds to $\bar{q}^2 \to \infty$ in Eq. (5.34).

Partially polarized states: For the simplest case of partially polarized QHS, $|p_\uparrow| = 2$ and $|p_\downarrow| = 1$. In this case, the spin wave dispersion relation is given by

$$\omega - g\mu_B\bar{B} = \Delta E = E^{\downarrow\uparrow}_{\bar{1}\bar{1}} - \tilde{V}^{(1)}_{1111}(q) \ . \tag{5.36}$$

We find the dispersion energy to be

$$\Delta E(q) = \frac{e^2}{\epsilon l_0}\frac{1}{4}\sqrt{\frac{\pi}{2}}\left[3 - e^{-\bar{q}^2/2}\left\{(3 - 2\bar{q}^2 + 2\bar{q}^4)I_0\left(\frac{\bar{q}^2}{2}\right) - 2\bar{q}^2 I_1\left(\frac{\bar{q}^2}{2}\right)\right\}\right] \tag{5.37}$$

which is shown in Fig. (5.6). The spin wave excitations of the states with $\nu = 3$, and $\nu = 3/(6s \pm 1)$ such as 3, 3/5, 3/7 have the above dispersion relation. Ar very low ql_0, this is again quadratically dispersed. The dispersion relation then is given by

$$\omega = g\mu_B\bar{B} + \frac{e^2}{\epsilon l_0}\frac{7}{16}\sqrt{\frac{\pi}{2}}(ql_0)^2 \ . \tag{5.38}$$

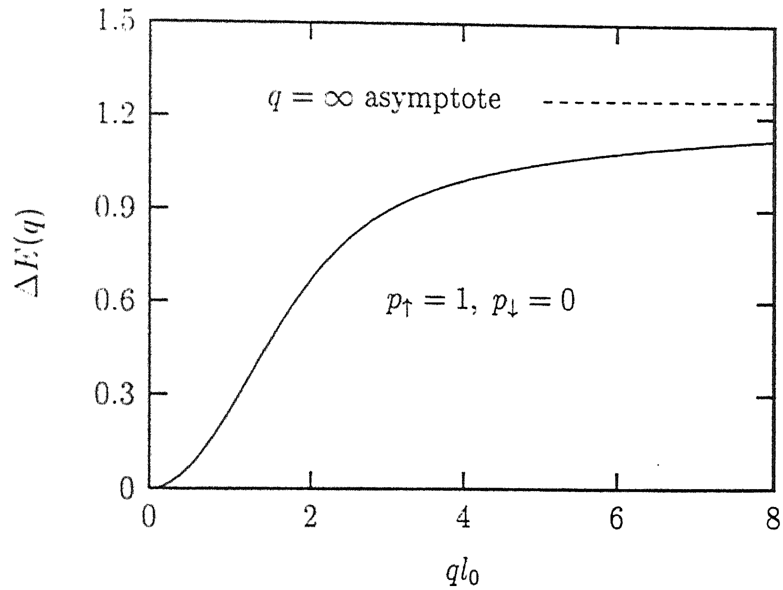

Figure 5.5: The spin-wave mode is shown in the unit of $e^2/\epsilon l_0$ for $p_\uparrow = 1$, $p_\downarrow = 0$, with the omission of Zeeman energy.

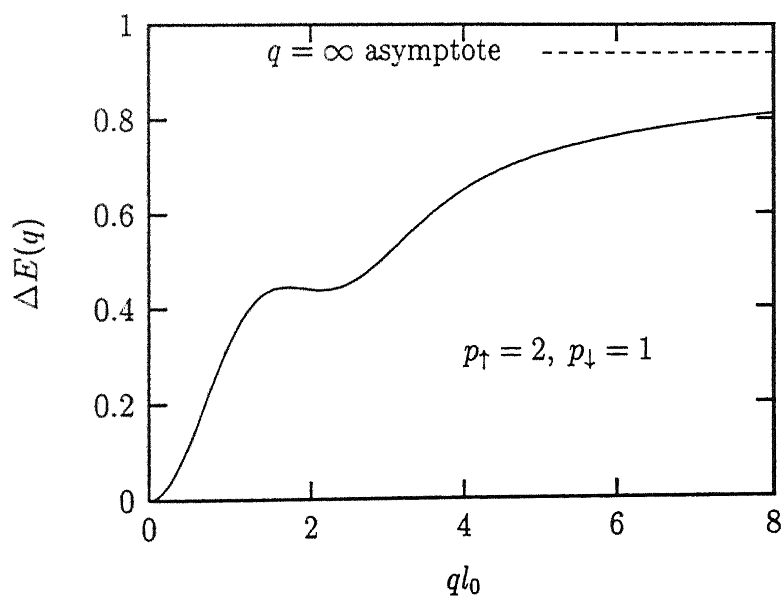

Figure 5.6: The spin-wave mode is shown in the unit of $e^2/\epsilon l_0$ for $p_\uparrow = 2$, $p_\downarrow = 1$, with the omission of Zeeman energy.

In this case, the energy necessary to create a spin up quasiparticle and a spin down quasihole pair is $\frac{3}{4}\sqrt{\frac{\pi}{2}}\frac{e^2}{\epsilon l_0}$ (see Eq. 5.37).

Similarly other partially polarized QHS such as $\nu = 5, 5/9, 5/11$ also possess spin wave excitations.

Chapter 6

Activated resistivities in integer quantum Hall effect

6.1 Introduction

It was first observed by von Klitzing *et al* [1] that two dimensional electron gas at low temperatures and in the presence of high magnetic field B perpendicular to the plane can exhibit quantization of the Hall resistivity at integer fillings, with a high accuracy (one part in 10^5). Subsequently, it has been observed that the precision of this quantization could be much higer (one part in 10^9) [79]. The essence of this IQHE is that the quantization of Hall resistivity $\rho_{xy} = \frac{1}{i}(2\pi/e^2)$ at integer filling factor $\nu = i$ exists for a wide range of physical parameters, *viz*, of B and of the carrier density ρ. At the same time the diagonal resistivity ρ_{xx} shows a sharp minimum. Prange [8], Laughlin [9], and Halperin [10] have argued that as long as the Fermi level lies in the region of localized states between two current carrying regions of extended states, the Hall conductivity σ_{xy} is quantized and σ_{xx} vanishes. It has been observed that the measured value of ρ_{xy} approaches the universal value $\frac{1}{i}(2\pi/e^2)$ as the temperature is lowered.

In his pioneering work, Laughlin [9] has shown that the edge effects are not important for the accuracy of quantization. He further speculates that the only significant source of error in quantization is the thermal activation. In fact, there exists a fairly good number of experiments [12, 13, 80–89] which study the effect of temperature on

the quantization. Speaking broadly, there are two important aspects regarding these studies, viz, (i) the flatness of the plateaus formed in ρ_{xy} and the critical transition between the plateaus, (ii) the value of quantization at the central point of the plateaus, *i.e.*, the points at which ρ_{xx} show minima and for which ν are exactly integers.

The present chapter is principally concerned with the latter aspect, *i.e.*, the behaviour of ρ_{xy} and ρ_{xx} with changing temperature and disorder. We shall study this at the centre of the plateau, *i.e.*, we look at the point at which the filling factor ν is an integer.

Let us now briefly review the pertinent experimental situation. Early studies by Yoshihiro *et al* [12] and Cage *et al* [13] show that ρ_{xy} decreases with increase in temperature at the minimum of ρ_{xx}. They also find a linear relationship $\Delta\rho_{xy} = -S\rho_{xx}^{\min}$ between the deviation $\Delta\rho_{xy} \equiv \rho_{xy}(T) - \rho_{xy}(0)$ from the zero temperature value of ρ_{xy}, and the minimum value of ρ_{xx}. Cage *et al* [13] have further found that the value of S varies from 0.06 to 0.51 for different GaAs samples. In Si MOSFETs, Yoshihiro *et al* [12] have found $S \simeq 0.1$. Although the values of S are device dependent and also on how the system is cooled, the linear relationship is itself universal. Cage [90] has pointed out that sample size effects which have been calculated by Rendell and Girvin [91], Hall probe misallignment, and variable range hopping conduction are not responsible for the linear relation between $\Delta\rho_{xy}$ and $\rho_{xx}^{\min}$. Moreover, Cage *et al* [13] have surprisingly observed that even when the Hall steps are flat to within 0.01 ppm instrumental resolution, the temperature dependent error $\Delta\rho_{xy}$ is still quite large. This suggests the loss of universality at finite temperatures. However, it is not always true that ρ_{xy} decreases with the increase of temperature, as Wel *et al* [80] have observed a positive slope between $\Delta\rho_{xy}$ and $\rho_{xx}^{\min}$ in their GaAs samples. Finally, Weiss *et al* [81] have fitted the temperature dependent prefactor in the activation of $\rho_{xx}^{\min}$ by a form $\rho_{xx}^{\min} \sim \frac{1}{T}\exp[-\omega_c/2T]$ in the leading order, where ω_c is the cyclotron frequency.

We remark here the fact that the value of S depends not only on T but also on its prior history, hinders any explicit comparison between theory and experiment. Nevertheless, we show that the present model yields a linear relationship between $\Delta\rho_{xy}$

and ρ_{xx}^{min} and can accommodate both positive and negative values of S. The linearity is in a smaller range of temperatures for the case of positive values of S. A further estimation of effective mass m^* which follows thereof is also not unrealistic, and is of the same order of magnitude as the experimental number.

The experimental results are quite ambiguous regarding the prefactor of σ_{xx}. Clark *et al* [82] have measured the prefactor of σ_{xx} for fractional quantum Hall states and find a universal value $e^2/2\pi$, independent even of the filling factors. In contrast, in a recent experiment by Katayama *et al* [83], the prefactor is found to be proportional to $1/T$. On the theoretical side, Fogler and Shklovskii [92] have found that for the case of long range random potential, the prefactor is indeed universal and is given by $e^2/2\pi$, but only above a certain critical temperature, and that it decays according to a power law below the critical temperature. On the other hand, Polyakov and Shklovskii [93] obtain the prefactor to be $2e^2/2\pi$. Here we study the case of short range potential and we find the prefactor to be temperature dependent, in agreement with that of Katayama *et al* [83].

To be sure, there is more experimental information available largely related to the aspect (i) mentioned above and not studied in the present chapter. For instance, Wei *et al* [84] have observed a similarity between ρ_{xx} and $\frac{d\rho_{xy}}{dB}$ with the only difference that while the maximum value of ρ_{xx} decreases, the maximum value of $\frac{d\rho_{xy}}{dB}$ increases with decreasing temperature over the range of temperatures from 0.1 K to 4.2 K. They have also found the power law behaviour $(\frac{d\rho_{xy}}{dB})^{\max} \propto T^{-k}$ and the width of the ρ_{xx} peak $\Delta B \propto T^k$ with $k = 0.42 \pm 0.04$. Further measurements by Wei *et al* [85] show that the extrema of $\frac{d^2\rho_{xy}}{dB^2}$ and $\frac{d^3\rho_{xy}}{dB^3}$ diverge like T^{-2k} and T^{-3k} respectively. Huckestein *et al* [86] also have measured the temperature dependence of the plateau and obtain a value $k = 0.42$ in agreement with Wei *et al* [84]. The above observations are for fully polarized quantum Hall states. When the Landau levels are spin degenerate, Wei *et al* [85] and Hwang *et al* [87] have reported that $(\frac{d\rho_{xy}}{dB})^{\max}$ and $(\Delta B)^{-1}$ diverge like $T^{-k/2}$. However, Wakabayashi *et al* [88] and Koch *et al* [89] find no evidence for the universality of the exponent k. All these aspects are discussed in a recent review by

Huckestein [94]. These mutual conflicting experimental results lie outside the scope of the present study.

On the theoretical side, Ando *et al* [95] computed σ_{xx} and σ_{xy} at $T = 0$ using a simple Lorentzian density of states (DOS) approximated from the self consistent Born approximation (SCBA) density of states; they have not considered the frequency dependent imaginary part of the SCBA self energy of the single particle Green function. In this chapter, we make the full use of frequency dependent self energy.

6.2 The formalism

Consider a system of (weakly) interacting electrons in two space dimensions in the presence of a uniform external magnetic field of strength B, confined to the direction perpendicular to the plane. The electrons also experience a short ranged impurity potential $U(X)$. The strength of magnetic field is fine tuned such that N Landau levels (LL) are exactly filled. In the presence of a sufficiently high magnetic field (as is relevant to our case), the spins of the fermions would be 'frozen' in the direction of magnetic field. Therefore, one may treat the fermions as spinless. The study of such a *spinless* system can be accomplished with the Lagrangian density,[1]

$$\mathcal{L} = \psi^* iD_0\psi - \frac{1}{2m^*}|D_k\psi|^2 + \psi^*\mu\psi - \psi^* U\psi - eA_0^{\text{in}}\rho + \frac{1}{2}\int d^3x' A_0^{\text{in}}(x)V^{-1}(x-x')A_0^{\text{in}}(x'). \tag{6.1}$$

Here $D_\nu = \partial_\nu - ie(A_\nu + A_0^{\text{in}}\delta_{\nu,0})$ (where A_ν is the external Maxwell gauge field and A_0^{in} is identified as internal scalar potential), μ is the chemical potential, and m^* and ρ are the effective mass and the mean density of electrons respectively. The fifth term in Eq.(6.1) describes the charge neutrality of the system. Finally, $V^{-1}(x - x')$ represents the inverse of the instantaneous charge interaction potential (in the operator sense). The above Lagrangian density is equivalent to the usual interaction term with quartic form of Fermi fields, which can be obtained by an integration of A_0^{in} field in Eq. (6.1).

[1]Alternatively, one may also use Hamiltonian formalism in the frame work of random phase approximation (RPA). The Gaussian fluctuation in the Lagrangian formalism is equivalent to RPA in Hamiltonian formalism.

Note also that the electrons interact with each other via $1/r$ or some other short range potential, *i.e.*, the internal dynamics is governed by the (3+1)-dimensional Maxwell Lagrangian as is appropriate for the medium.

We now construct the partition function ($\beta = 1/T$ being the inverse temperature) of the system,

$$\mathcal{Z} = \int [dA_\tau^{\text{in}}][d\psi][d\psi^*] \exp\left[-\int_0^\beta d\tau \int d^2X \mathcal{L}^{(E)}\right] , \tag{6.2}$$

which on integration over the fermionic fields, (by fixing of the saddle point at the uniform background magnetic field B), factors into the form $\mathcal{Z} = \mathcal{Z}_B \mathcal{Z}_I$. Here $\mathcal{L}^{(E)}$ is the Euclidean version of $\mathcal{L}$ in Eq. (6.1). For the transformation into the Euclidean space, we make a substitution $t \to -i\tau$ and consider the real parameter τ as a coordinate on a circle of circumference β. Fermionic fields are antiperiodic on this circle while the bosonic fields are periodic. The time component of the vector field A_μ is redefined as $A_0 \to iA_\tau$. The back ground part of the partition function is given by

$$\mathcal{Z}_B = Tr\, e^{-\beta(H-\mu\rho)} , \tag{6.3}$$

which is obtained from the fermion determinant, found by the integration of fermionic fields. The finite temperature back ground properties of the system can be studied using $\mathcal{Z}_B$. Here

$$H = -\frac{1}{2m^*} D_k^2 + U(X) \equiv H_0 + U(X) \tag{6.4}$$

is the single particle Hamiltonian. $\mathcal{Z}_I$ is the partition function corresponding to the external probe, which will be determined later below.

6.3 Single particle Green's function

6.3.1 Disorder free Green's function

The spectrum of disorder free Hamiltonian H_0 for the system is a set of LL with energy eigen value for the n-th LL,

$$\epsilon_n = (n + \frac{1}{2})\omega_c \; ; \; n = 0, 1, 2, \cdots , \tag{6.5}$$

where $\omega_c = eB/m^*$ is the cyclotron frequency. In the Landau gauge

$$\vec{A} = (-BX_2, 0) , \tag{6.6}$$

the eigen function corresponding to the eigen value ϵ_n is

$$\psi_{nk}(X) = \frac{1}{\sqrt{l}} e^{ikX_1} v_n \left(\frac{X_2}{l} + kl \right) , \tag{6.7}$$

where $v_n(x)$ is the appropriate harmonic oscillator wave function. Here $l = (eB)^{-1/2}$ is the magnetic length of the system and is also the classical cyclotron radius in the lowest LL ($n = 0$). Each level is infinitely degenerate with a degeneracy $\rho_l = 1/2\pi l^2$ per unit area.

The single particle Green function $G_0(x, x')$ for the disorderless system can be obtained by solving

$$(\delta_\tau + H_0 - \mu) G_0(x, x') = \delta^{(3)}(x - x') \tag{6.8}$$

subject to the requirement of antiperiodicity under the translation $\tau \to \tau + \beta$. $G_0(x, x')$ can be expanded in the normal modes of discrete frequencies $\xi_s = (2s + 1)\pi/\beta$; $s \epsilon Z$, as

$$G_0(x, x') = -\frac{1}{\beta} \sum_s e^{-i\xi_s(\tau - \tau')} \langle X | G_0(i\xi_s) | X' \rangle , \tag{6.9}$$

where the operator $G_0(i\xi_s)$ is given by

$$G_0(i\xi_s) = \frac{1}{i\xi_s + \mu - H_0} . \tag{6.10}$$

with eigen value $G_0^n(i\xi_s) = [i\xi_s + \mu - \epsilon_n]^{-1}$. By analytical continuation $i\xi_s \to \epsilon \pm i\eta$, we obtain this eigen value in the real space as

$$G_0^n(\epsilon) = \frac{1}{\epsilon + \mu - \epsilon_n \pm i\eta} . \tag{6.11}$$

Here $+(-)$ refers to retarded(advanced) Green's function.

The density of the particles is obtained in terms of the Green's function as

$$\rho(X) = - G_0(x, x')|_{X'=X, \tau'=\tau+0} . \tag{6.12}$$

The density is independent of the spatial coordinate, *i.e.*, the density is uniform, and is given by

$$N \equiv \frac{\rho}{\rho_l} = \sum_n f_n \,, \tag{6.13}$$

where the Fermi function corresponding to n-th LL, $f_n = [1+\exp(\beta[\epsilon_n - \mu])]^{-1}$ and N is the number of fully filled LL at $T = 0$.

At low temperatures characterized by $\beta\omega_c \gg 1$, we shall determine the chemical potential for fixed density. To this end, we write [99]

$$e^{\beta(\epsilon_n-\mu)} = w^{\mu/\omega_c - 1/2 - n} \,, \tag{6.14}$$

where $w = \exp[-\beta\omega_c]$ is the perturbative expansion parameter. We expand the right-hand side of Eq. (6.14) to obtain

$$\sum_n (1 + w^{\mu/\omega_c - 1/2 - n})^{-1} = \left[\frac{\mu}{\omega_c} + \frac{1}{2}\right] + \sum_{r\geq 1} (-1)^r \frac{w^{r\delta} - w^{r(1-\delta)} - w^{r(\mu/\omega_c + 1/2)}}{1 - w^r} \,, \tag{6.15}$$

where $[\mu/\omega_c + 1/2]$ denotes the (positive) integer part:

$$\frac{\mu}{\omega_c} + \frac{1}{2} = \left[\frac{\mu}{\omega_c} + \frac{1}{2}\right] + \delta \,, \; 0 < \delta < 1 \,. \tag{6.16}$$

Since w is very small, Eq. (6.13) takes the form

$$N = \left[\frac{\mu}{\omega_c} + \frac{1}{2}\right] - w^\delta + w^{1-\delta} + w^{\mu/\omega_c + 1/2 + \delta} + \cdots \,. \tag{6.17}$$

The solution of (6.17) in the leading order is obtained as

$$\left[\frac{\mu}{\omega_c} + \frac{1}{2}\right] = N \,, \; \delta = \frac{1}{2} + \frac{w^N}{2\ln w} \,. \tag{6.18}$$

Therefore, the chemical potential is given by

$$\mu = \frac{2\pi\rho}{m^*} - \frac{1}{2\beta} e^{-N\beta\omega_c} + \cdots \,, \tag{6.19}$$

which is an exponentially small temperature correction to the Fermi energy at $T = 0$. On substitution of the value of μ on Eq. (6.14) we obtain

$$e^{\beta(\epsilon_n-\mu)} = \exp\left[\beta\omega_c(n - N + 1/2)\right]\left(1 + \frac{1}{2} e^{-\beta\omega_c(N+1/2)} + \cdots\right) \,, \tag{6.20}$$

which will be needed later.

6.3.2 Impurity averaged Green's function

We assume a random distribution of white noise disorder potential $U(X)$ all over the space with probability distribution

$$P[U] = \mathcal{N} \exp\left[-\frac{1}{2\lambda^2}\int d^2X|U(X)|^2\right] . \tag{6.21}$$

where $\mathcal{N}$ is the renormalization constant. The average potential

$$\overline{U(X)} = 0 . \tag{6.22}$$

Hereafter overbar denotes the average with respect to the distribution $P[U]$ (Eq. (6.21)) of the disorder potential. The correlation between the potentials at two points is given by

$$\overline{U(X)U(X')} = \lambda^2\delta(X - X') . \tag{6.23}$$

The scattering potentials are short ranged.

The single particle Green's function for the disordered system in terms of the free Green's function (6.9) is given by

$$\begin{aligned} G(x,x') &\equiv \langle x|G|x'\rangle = \langle x|G_0 + G_0UG|x'\rangle \\ &= \langle x|G_0|x'\rangle + \langle x|G_0UG_0|x'\rangle + \langle x|G_0UG_0UG_0|x'\rangle + \cdots . \end{aligned} \tag{6.24}$$

When we average over the distribution in disorder, the terms with odd number of U operators vanish. Further, due to the condition (6.23), each scattering centre is responsible for an even number of scatterings.

If $G_0^n(\epsilon)$ be the free Green's function for n-th LL, then the corresponding impurity averaged Green's function is given by

$$\overline{G^n(\epsilon)} = G_0^n(\epsilon) + G_0^n(\epsilon)\Sigma_n(\epsilon)\overline{G^n(\epsilon)} . \tag{6.25}$$

In other words,

$$\overline{G^n(\epsilon)} = \frac{1}{\epsilon + \mu - \epsilon_n - \Sigma_n(\epsilon)} . \tag{6.26}$$

$\overline{G^n(\epsilon)}$ has the diagrammatic representation as in Fig. 6.1(a). Here Σ_n is the corresponding self energy. For the evaluation of $\Sigma_n(\epsilon)$, we make the self consistent Born

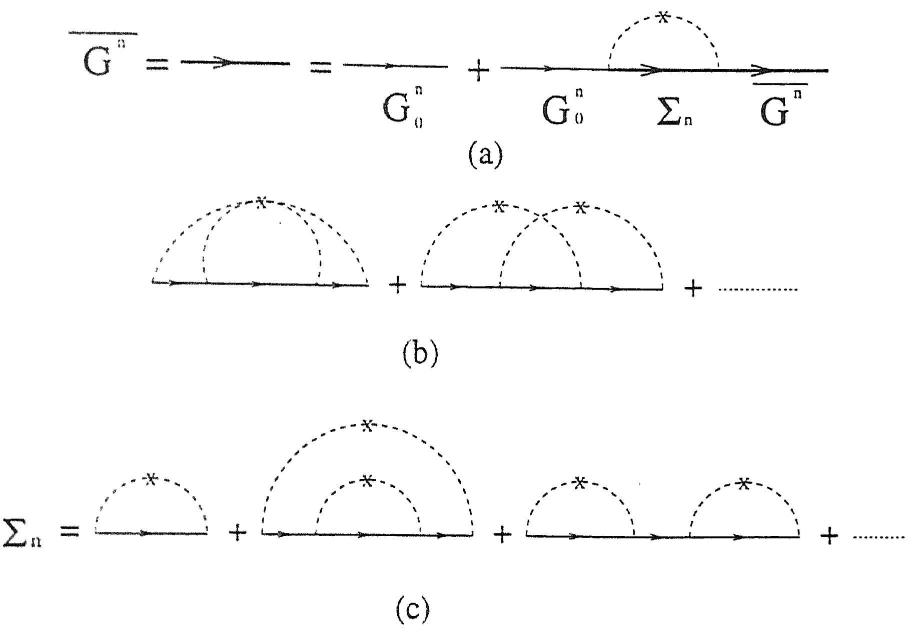

Figure 6.1: The thick (thin) lines with arrows represent disordered (disorderless) single particle Green's functions. The symbol X denotes the scattering centre and the dashed lines represent the scatterings. (a) The propagator (impurity averaged) for n-th LL $\overline{G^n}$ is shown. Here Σ_n is the corresponding self energy. (b) The diagrams which are not taken into account in the SCBA — the diagrams corresponding to multiple scatterings at a given scattering centre and the cross diagrams. (c) The diagrams which have been considered for the evaluation of self energy.

approximation (SCBA). In SCBA, one neglects multiple scattering at any point and the cross scatterings which are shown in Fig. 6.1(b). The diagrams which contribute to SCBA are shown in Fig. 6.1(c).

We find that Σ_n (see Fig. 6.1(a)) is

$$\Sigma_n(\epsilon) = \lambda^2 \rho_l \sum_{m \geq -n} \frac{1}{\epsilon + \mu - \epsilon_{n+m} - \Sigma_{n+m}(\epsilon)} . \tag{6.27}$$

The solution of Eq. (6.27) can be obtained self consistently [96]. This is given by

$$\Sigma_n(\epsilon) = -\frac{1}{2}(\epsilon + \mu - \epsilon_n) + \frac{1}{2}\sqrt{(\epsilon + \mu - \epsilon_n)^2 - \Gamma^2} , \tag{6.28}$$

where $\Gamma^2 = 4\lambda^2 \rho_l$.

For a disorderless system, $\Gamma = 0$ and hence the self energy Σ_n also vanishes. In the range of energy ϵ for which $|\epsilon + \mu - \epsilon_n| > \Gamma$, Σ_n is real; it merely changes the energy of the particles. On the other hand, for the range $|\epsilon + \mu - \epsilon_n| < \Gamma$, Σ_n has both real and imaginary parts, and is given by

$$\Sigma_n^{\pm}(\epsilon) = -\frac{1}{2}(\epsilon + \mu - \epsilon_n) \pm \frac{i}{2}\sqrt{\Gamma^2 - (\epsilon + \mu - \epsilon_n)^2}\,. \tag{6.29}$$

Therefore in this range, the impurity averaged retarded and advanced Green's functions are given by

$$\overline{G^n_{r,a}(\epsilon)} = \frac{2}{\epsilon + \mu - \epsilon_n \pm i\sqrt{(\epsilon + \mu - \epsilon_n)^2 - \Gamma^2}}\,. \tag{6.30}$$

The DOS for the n-th Landau band,

$$\begin{aligned}\mathcal{D}_n(\epsilon) &\equiv -\frac{\rho_l}{\pi}\,\mathrm{Im}\,\overline{G^n_r(\epsilon)} \\ &= \frac{1}{2\pi l^2}\frac{2}{\pi\Gamma}\left[1 - \left(\frac{\epsilon + \mu - \epsilon_n}{\Gamma}\right)^2\right]^{1/2}.\end{aligned} \tag{6.31}$$

This is the well known SCBA DOS which is semi circular in nature. This will be used to determine the linear response of the system.

Alternatively, one may also consider the Gaussian DOS which is given by

$$\mathcal{D}_n(\epsilon) = \frac{1}{2\pi l^2}\sqrt{\frac{2}{\pi\Gamma}}\,e^{-2(\epsilon+\mu-\epsilon_n)^2/\Gamma^2}\,. \tag{6.32}$$

A brief comparison between the above two DOS will be made later.

6.4 Response functions

The partition function corresponding to the external electromagnetic probe A_μ is

$$\mathcal{Z}_I[A_\mu] = \int [dA^{\rm in}_\tau]\exp[-S^E]\,, \tag{6.33}$$

where S^E is identified as the Euclidean one-loop effective action of the gauge fields. It is given by

$$\begin{aligned}S^E &= \frac{1}{2}\int d^3x\int d^3x'\left(A_\mu(x) + A^{\rm in}_\tau\delta_{\mu\tau}(x)\right)\Pi^E_{\mu\nu}(x,x')\left(A_\nu(x') + A^{\rm in}_\tau\delta_{\nu\tau}(x')\right) \\ &\quad -\frac{1}{2}\int d^3x\int d^3x' A^{\rm in}_\tau(x)V^{-1}(x-x')A^{\rm in}_\tau(x')\,.\end{aligned} \tag{6.34}$$

Here the integration over the imaginary time τ runs from 0 to β. The effective action is obtained by expanding the fermionic determinant up to quadratic terms in powers of fields A_μ and $A_\tau^{\rm in}$. The polarization tensor $\Pi^E_{\mu\nu}(x,\, x')$ is evaluated at the saddle point mentioned. Since $\Pi^E_{\mu\nu}$ is evaluated in the path integral formalism, τ-ordering is implied for the correlations, *i.e.*,

$$\Pi^E_{\mu\nu}(x,\, x') = -\overline{\langle T_\tau j_\mu(x) j_\nu(x')\rangle} - \overline{\left\langle \frac{\delta j_\mu(x)}{\delta A_\nu(x')} \right\rangle} \,. \tag{6.35}$$

The overbar implies the average over the distribution of random disorder in Eq. (6.21). In terms of the thermal single particle Green's function, the components of $\Pi^E_{\mu\nu}$ are given by

$$\begin{aligned}
\Pi^E_{\tau\tau}(x,x') &= -e^2\overline{G(x,x')G(x',x)}\,, && (6.36)\\
\Pi^E_{k\tau}(x,x') &= \frac{e^2}{2m^*}\left[\overline{D_k G(x,x')G(x',x)} - \overline{G(x,x')D_k^* G(x',x)}\right]\,, && (6.37)\\
\Pi^E_{kl}(x,x') &= -\frac{e^2}{4m^{*2}}\left[\overline{D_k G(x,x')D_l' G(x',x)} - \overline{\left(D_k D_l'^* G(x,x')\right) G(x',x)}\right.\\
&\quad \left. + \overline{D_l'^* G(x,x')D_k^* G(x',x)} - \overline{G(x,x')D_k^* D_l' G(x',x)}\right]\\
&\quad + \frac{e^2}{m^*}\delta_{kl}\delta(x-x')\overline{G(x,x')}\Big|_{X'=X\,,\,\tau'=\tau+0+}\,. && (6.38)
\end{aligned}$$

We remark here that once we average over the distribution of the impurity potential, the translational invariance gets restored. Therefore, the polarization tensor can be represented by Fourier expansion

$$\Pi^E_{\mu\nu}(x,x') = \frac{1}{\beta}\sum_j \int \frac{d^2\mathbf{q}}{(2\pi)^2} e^{-i\mathbf{q}\cdot(X-X')} e^{-i\omega_j(\tau-\tau')} \Pi^E_{\mu\nu}(\omega_j,\mathbf{q})\,, \tag{6.39}$$

where Matsubara frequency $\omega_j = 2\pi j/\beta$. Due to rotational symmetry and gauge invariance, there are three independent form factors. One thus obtains the polarization tensor in the form (in momentum space)

$$\begin{aligned}
\Pi^E_{\mu\nu}(\omega_j,\mathbf{q}) &= \Pi_0(\omega_j,\mathbf{q})(q^2\delta_{\mu\nu} - q_\mu q_\nu) + (\Pi_2(\omega_j,\mathbf{q}) - \Pi_0(\omega_j,\mathbf{q}))\\
&\quad \times(\mathbf{q}^2\delta_{ij} - q_i q_j)\delta_{\mu i}\delta_{\nu j} + \Pi_1(\omega_j,\mathbf{q})\varepsilon_{\mu\nu\lambda}q^\lambda\,, && (6.40)
\end{aligned}$$

where $q^2 = \omega_j^2 + \mathbf{q}^2$. Here Π_0, Π_1 and Π_2 are the form factors. Note that Π_1 is a $\mathcal{P}.\mathcal{T}$ violating form factor. The one loop effective action then acquires the form

$$\begin{aligned} S_{\text{eff}}^E &= \frac{1}{2\beta}\sum_j \int \frac{d^2\mathbf{q}}{(2\pi)^2}\left[\left(A_\mu(q) + A_\tau^{\text{in}}(q)\delta_{\mu\tau}\right)\Pi_{\mu\nu}^E(\omega_j,\mathbf{q})\left(A_\nu(-q) + A_\tau^{\text{in}}(-q)\delta_{\nu\tau}\right)\right. \\ &\quad \left. - A_\tau^{\text{in}}(q)V^{-1}(\mathbf{q})A_\tau^{\text{in}}\right] , \end{aligned} \quad (6.41)$$

which will be used below for determining the linear responses of the system.

6.4.1 Off-diagonal conductivity

A straight forward linear response analysis from Eqs. (6.40) and (6.41), yields the expression for off-diagonal conductivity to be

$$\sigma_{xy} = \lim_{\omega\to 0} \operatorname{Re}\Pi_1(\omega, 0) , \quad (6.42)$$

subject to the condition $\lim_{\mathbf{q}\to 0} V(\mathbf{q})\mathbf{q}^2 = 0$. $\Pi_1(\omega, 0)$ is obtained by the analytical continuation: $i\omega_j \to \omega + i\delta$.

The form factor Π_1 can be determined from the evaluation of the component, say $\Pi_{1\tau}^E$ of the polarization tensor (6.40). The impurity average over two Green's functions in Eq. (6.37) is not equal to the product of two averaged Green's functions (Fig. 6.2(a)), in general. It has an additional contribution coming from vertex corrections (see Fig. 6.2(b)). We shall determine the contributions from Figs. 6.2(a) and 6.2(b) separately.

Considering figure 6.2(a), we get

$$\Pi_1^{(0)}(\omega_j, 0) = \frac{e^2}{2m^*}\frac{1}{2\pi l^2}\sum_{n=0}^{\infty}\sum_{m=0}^{\infty} I_{nm}(\omega_j)[(n+1)\delta_{m,n+1} + n\delta_{m,n-1} - (2n+1)\delta_{mn}] , \quad (6.43)$$

where

$$I_{nm}(\omega_j) = -\frac{1}{\beta}\sum_{s=-\infty}^{\infty} \overline{G^n(i\xi_s)}\;\overline{G^m(i\xi_s - i\omega_j)} . \quad (6.44)$$

The evaluation of I_{nm} is done in the Appendix C. Performing analytical continuation: $i\omega_j \to \omega + i\delta$, we obtain the real part of I_{nm} (see Eq. C.9),

$$\begin{aligned} \operatorname{Re} I_{nm}(w) &= 2\int_{\epsilon_n-\mu-\Gamma}^{\epsilon_n-\mu+\Gamma} \frac{d\epsilon}{2\pi} n_F(\epsilon)\operatorname{Im}\overline{G_r^n(\epsilon)}\operatorname{Re}\overline{G_a^m(\epsilon-\omega)} \\ &\quad +2\int_{\epsilon_m-\mu-\Gamma}^{\epsilon_m-\mu+\Gamma} \frac{d\epsilon}{2\pi} n_F(\epsilon)\operatorname{Im}\overline{G_r^m(\epsilon)}\operatorname{Re}\overline{G_r^n(\epsilon+\omega)} . \end{aligned} \quad (6.45)$$

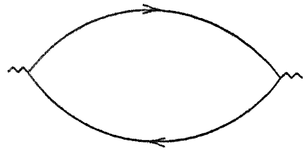

(a)

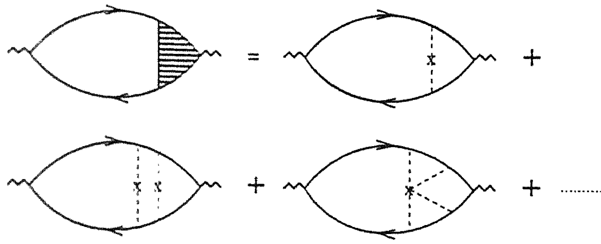

(b)

Figure 6.2: The thick lines with the arrows represent the single particle Green's function. The wiggly lines represent the external electromagnetic probe. (a) The response function $\Pi_{\mu\nu}$ within the SCBA is shown. (b) The diagrams corresponding to the vertex corrections for the response function.

Here $n_f(\epsilon)$ represents the Fermi function,

$$n_F(\epsilon) = \frac{1}{1+e^{\beta\epsilon}} \,. \tag{6.46}$$

By Taylor expansion of Eq. (6.45) in powers of Γ/ω_c, we obtain, with the use of Eqs. (6.42) – (6.46), the off-diagonal conductivity (without vertex correction)

$$\sigma_{xy}^{(0)} = -\frac{e^2}{2\pi}\left[\sum_{n=0}^{\infty} f_n - \frac{1}{2}\beta\omega_c \sum_{n=0}^{\infty}(2n+1)f_n(1-f_n)\right] + \mathcal{O}\left(\frac{\Gamma}{\omega_c}\right)^2 . \tag{6.47}$$

Vertex correction: We next consider the contribution to σ_{xy} due to vertex corrections shown in Fig. 6.2(b). For the lowest order vertex correction, the contribution $\sigma_{xy}^{(1)}$ is suppressed by a factor $(\Gamma/\omega_c)^2$ in the limit $\Gamma/\omega_c \ll 1$, since two more scatterings take place in the virtual process. The vertex corrections due to more and more number of scatterings lead to the contributions which are further suppressed by a factor Γ/ω_c for each scattering. Therefore, in the limit $\Gamma/\omega_c \ll 1$, the total off-diagonal conductivity is essentially given by

$$\sigma_{xy} \simeq \sigma_{xy}^{(0)}$$

$$= -\frac{e^2}{2\pi}\left[\sum_{n=0}^{\infty} f_n - \frac{1}{2}\beta\omega_c \sum_{n=0}^{\infty}(2n+1) f_n(1-f_n) + O\left(\frac{\Gamma}{\omega_c}\right)^2\right] \quad (6.48)$$

In agreement with Ando *et al* [95], the impurity contribution to σ_{xy} is of the order of $(\Gamma/\omega_c)^2$ which is small in the strong field and small broadening approximation.

Starting with the result of Ando *et al* [95] which was obtained at $T = 0$ using a simple Lorentzian DOS, Levine *et al* [97] have shown that after successive renormalizations, there is a renormalization group flow towards $\sigma_{xx} = 0$, $\sigma_{xy} =$ (an integer)$\frac{e^2}{h}$, corresponding to the widening of the plateaus. They find another flow towards an unstable fixed point which corresponds to $\sigma_{xy} = (N + 1/2)\frac{e^2}{h}$ where the transition between the plateaus occur. The group flows have been observed experimentally [98]. Thus at $T = 0$, the stable group flow is towards the point for which filling factor ν is an integer and $(\sigma_{xx}, \sigma_{xy}) = (0, \nu)\frac{e^2}{2\pi}$ which is the value of $(\sigma_{xx}, \sigma_{xy})$ at $\Gamma = 0$. Recall that we are considering those specific values of B (or ρ) for which $\nu = N$ is an integer. We have computed here σ_{xy} more rigorously within SCBA and also at $T \neq 0$. It is therefore reasonable to expect the present improved treatment to be capable of explaining the behaviour of plateaus, *a la* the Levine *et al* [97] analysis. It would indeed be interesting to examine whether the stable renormalization group flow at finite T occurs towards the point $(\sigma_{xx}, \sigma_{xy})$, which we evaluate here, for which ν is an integer and $\Gamma = 0$. This analysis would explain the behaviour of plateau at finite temperatures in σ_{xy} given by Eq. (6.48).

The leading order contribution to σ_{xy} in Eq. (6.48) is in the zero-th order of Γ/ω_c, and has a temperature dependent term. It may be noted that this temperature dependent contribution[2] owes its origin to intra LL transitions, which would contribute in the thermodynamic limit only if degeneracy grows with area.

It is interesting that the above mentioned intra Landau level transition which is unique to this case also contributes to the specific heat, as was derived by Zawadzki and Lassnig [105]. This has been experimentally verified later by Gornik *et al* [106].

At low temperatures ($\beta\omega_c \gg 1$), we perturbatively evaluate σ_{xy} with the expansion

[2] A similar temperature dependent contribution is also obtained in the allied context of anyon superconductivity [99–104].

parameter $e^{-\beta\omega_c/2}$, as we have discussed in the section (6.3.1). We thus find

$$\sigma_{xy}(T) = -\frac{e^2 N}{2\pi}[1 - 4y] \,, \tag{6.49}$$

with

$$y = \frac{T_0}{T} \exp\left[-\frac{T_0}{T}\right] \,, \tag{6.50}$$

where $T_0 = \omega_c/2$. The temperature correction to the σ_{xy} is exponentially weak. This leads to some interesting consequences as we shall show in the next section.

6.4.2 Diagonal conductivity

Again, a linear response analysis of Eq. (6.41) provides the diagonal conductivity to be

$$\sigma_{xx} = -\lim_{\omega \to 0} \mathrm{Im}\, \Pi_{11}^{r}(\omega, 0) \,. \tag{6.51}$$

Here r represents the retarded part of the correlation function which is obtained from Eq. (6.40) by analytical continuation. Equation (6.51) is derived in the limit $\lim_{\mathbf{q}\to 0} V(\mathbf{q})\mathbf{q}^2 = 0$. Therefore Eq. (6.51) is true for all those potentials which are short ranged compared to $\ln r$.

We evaluate $\Pi_{11}^{E}(\omega_j, 0)$ using the same procedure employed in determining Π_{1r}^{E} discussed above. It may again be shown that vertex corrections are suppressed by an extra factor of Γ/ω_c. We therefore only need to evaluate the contribution arising from Fig. 6.2(a). We thus obtain

$$\begin{aligned} \Pi_{11}^{E}(\omega_j, 0) &= \frac{e^2}{4m^{*2}} \frac{1}{2\pi l^4} \sum_{n=0}^{\infty} \sum_{m=0}^{\infty} I_{nm}(\omega_j)[(n+1)\delta_{m,n+1} + n\delta_{m,n-1} - (2n+1)\delta_{mn}] \\ &\quad - \frac{e^2}{m^*} \frac{1}{2\pi l^2} \sum_{n=0}^{\infty} I_n \,. \end{aligned} \tag{6.52}$$

where

$$I_n = -\frac{1}{\beta} \sum_{s=-\infty}^{\infty} \overline{G^n(i\xi_s)} \,. \tag{6.53}$$

The term I_n is independent of ω_j; it does not have any imaginary part. Using Eq.(C.9), we write

$$\mathrm{Im}\, I_{nm}(w) = -2 \int_{\epsilon_n - \mu - \Gamma}^{\epsilon_n - \mu + \Gamma} \frac{d\epsilon}{2\pi} n_F(\epsilon)\, \mathrm{Im}\, \overline{G_r^n(\epsilon)}\, \mathrm{Im}\, \overline{G_a^m(\epsilon - \omega)}$$

$$+2\int_{\epsilon_m-\mu-\Gamma}^{\epsilon_m-\mu+\Gamma}\frac{d\epsilon}{2\pi}n_F(\epsilon)\,\mathrm{Im}\,\overline{G_r^m(\epsilon)}\,\mathrm{Im}\,\overline{G_r^n(\epsilon+\omega)}\,. \tag{6.54}$$

The diagonal conductivity is thus given by

$$\sigma_{xx} = -\lim_{\omega\to 0}\frac{e^2}{4m^{*2}}\frac{1}{2\pi l^4}\sum_{n=0}^{\infty}\sum_{m=0}^{\infty}\mathrm{Im}\,I_{nm}(\omega)\,\left[(n+1)\delta_{m,n+1}+n\delta_{m,n-1}-(2n+1)\delta_{mn}\right]\,. \tag{6.55}$$

In the limit $\Gamma\to 0$ (disorder free), σ_{xx} vanishes, as may easily be checked. For Γ finite, there are some interesting consequences. Recall that according to SCBA, the imaginary part of $\overline{G_r^n(\epsilon)}$ exists in the region of ϵ for which $\Gamma > |\epsilon_n+\epsilon-\mu|$. Therefore the integrals in Eq. (6.54) are non-zero only when $m = n$, *i.e.*, the contribution is entirely due to transitions within the band of an LL. We obtain

$$\sigma_{xx} = \frac{2e^2}{3\pi^2}\left(\frac{\omega_c}{\Gamma}\right)\beta\omega_c\sum_{n=0}^{\infty}(2n+1)f_n(1-f_n)+\mathcal{O}\left(\frac{\Gamma}{\omega_c}\right)\,. \tag{6.56}$$

Notice that at finite temperatures, there is a singular contribution in σ_{xx} as $\Gamma\to 0$. However, as we have seen above, σ_{xx} vanishes for $\Gamma = 0$ at all temperatures. Further at $T = 0$, there is no possibility of intra band transition within an LL and so σ_{xx} vanishes again. Therefore the expression (6.56) has a pertinent role only at finite temperatures, and in the presence of disorder. In short, $\sigma_{xx}(\Gamma, T=0) = 0$; $\sigma_{xx}(\Gamma=0, T) = 0$. In the high field and low broadening limit, $\Gamma/\omega_c \ll 1$, and so we neglect the higher order terms in Γ/ω_c. Note that $\sigma_{xx}(T)$ is evaluated for those specific value of B (or ρ) for which $\nu = p$ is an integer.

A low temperature expansion of Eq. (6.56) yields

$$\sigma_{xx}(T) = \frac{16e^2N}{3\pi^2}\left(\frac{\omega_c}{\Gamma}\right)y \equiv \frac{16e^2N}{3\pi^2}\left(\frac{\omega_c}{\Gamma}\right)\frac{T_0}{T}\exp\left[-\frac{T_0}{T}\right]\,. \tag{6.57}$$

It may be noted that there is now a competition between two energy scales — the temperature T and the broadening Γ in Eq. (6.57). For very low temperatures, y is exponentially small (see Eq. (6.50)) and the value of σ_{xx} need not be large although $\omega_c/\Gamma \gg 1$. In fact, at $T=0$, $y=0$ leading to a vanishing of σ_{xx}. Further, we see that $\sigma_{xx}(T)$ is thermally activated with a temperature dependent prefactor, in agreement with the experiment of Katayama *et al* [83]. This prefactor is clearly not universal any

more, since it depends on the integer filling p and the broadening of an LL, as given by Γ. The mismatch between the results of Ref.[93] which predicts universality and that of ours may be due to consideration of different types of the disorder potential; whereas they have taken a long range scatterer, we have considered δ-correlated short range disorder potential. Interestingly, Fogler *et al* [92] report that for long range scatterers, the prefactor is temperature dependent below a characteristic temperature. In concluding this section, we note that our results obey the phenomenological relation

$$\Delta\sigma_{xy} \equiv \sigma_{xy}(T) - \sigma_{xy}(0) \sim -\left(\frac{\Gamma}{\omega_c}\right)\sigma_{xx} \, , \tag{6.58}$$

which was proposed by Ando *et al* [95] based on general arguments.

6.4.2.1 σ_{xx} for Gaussian density of states

For the Gaussian density of states (6.32), the limits of integration in Eq. (6.54) runs from $-\infty$ to ∞. There is a possibility of inter Landau band transition at finite temperatures apart from the intra Landau band transition, since the Gaussian density of states has a long tail, unlike the SCBA density of states where there is a sharp cut-off. However, the contribution to σ_{xx} due to inter Landau band transition is exponentially weak, and behaves like $\exp[-\omega_c^2/2\Gamma^2]$. Note that $\Gamma/\omega_c \ll 1$. The major contribution therefore again comes from the intra Landau band transition. The vertex corrections are suppressed by the higher orders in Γ/ω_c. We thus obtain the diagonal conductivity for the Gaussian density of states

$$\sigma_{xx} \simeq \frac{e^2}{8\sqrt{2\pi}}\left(\frac{\omega_c}{\Gamma}\right)\beta\omega_c \sum_{n=0}^{\infty}(2n+1)f_n(1-f_n) \, , \tag{6.59}$$

which has the low temperature form

$$\sigma_{xx}(T) = \frac{e^2 N}{\sqrt{2\pi}}\left(\frac{\omega_c}{\Gamma}\right) y \, , \tag{6.60}$$

which qualitatively agrees with $\sigma_{xx}(T)$ obtained from the SCBA density of states as in Eq. (6.57). This exercise serves to demonstrate that the crucial features of σ_{xx} are of not artifacts of the SCBA.

6.5 Resistivities and comparison with experiment

We now take up the discussion of resistivities of quantum Hall states which is of primary interest to us. Cage *et al* [13] and Yoshihiro *et al* [12] have found that $\rho_{xy}(T)$ decreases with increase in temperature and the deviation from its zero temperature value, $\Delta\rho_{xy}(T) \equiv \rho_{xy}(T) - \rho_{xy}(0)$ obeys a linear relationship with $\rho_{xx}^{\min}$ as

$$\Delta\rho_{xy} = -S\rho_{xx}^{\min} . \tag{6.61}$$

Cage *et al* [13] have further reported that the linearity remains for the temperature range 1.2–4.2K for which the value of $\rho_{xx}^{\min}$ changes up to four decades. The value of S depends on the device and the cooling process and hence is not reproducible. However, the linear relationship (6.61) is universal. The sign of S is *not* always positive as Wel *et al* [80] have observed that $\rho_{xy}(T)$ increases with temperature. We shall see that both the signs of S along with the linearity (6.61) can be obtained in different physical regimes of temperature and broadening, (although in a narrow range of temperatures for positive S). Presumably, these physical regimes correspond to the above mentioned experiments. Both the regimes belong to low temperatures and low broadening, as we show below.

In the previous section, we have determined $\sigma_{xy}(T)$ and $\sigma_{xx}(T)$. Now by symmetry, $\sigma_{yx}(T) = -\sigma_{xy}(T)$ and $\sigma_{yy}(T) = \sigma_{xx}(T)$. We then invert the conductivity matrix to obtain the resistivity matrix with the components

$$\rho_{xy}(T) = -\frac{\sigma_{xy}(T)}{\sigma_{xx}^2(T) + \sigma_{xy}^2(T)} = -\rho_{yx}(T) ; \; \rho_{xx}(T) = \frac{\sigma_{xx}(T)}{\sigma_{xx}^2(T) + \sigma_{xy}^2(T)} = \rho_{yy}(T) . \tag{6.62}$$

Using the conductivities obtained from SCBA DOS (Eqs. 6.49 and 6.57), we get

$$\rho_{xy}(T) = \left(\frac{2\pi}{e^2N}\right) \frac{1-4y}{(32/3\pi)^2(\omega_c/\Gamma)^2y^2 + (1-4y)^2} ; \tag{6.63}$$

$$\rho_{xx}(T) = \left(\frac{2\pi}{e^2N}\right) \frac{(32/3\pi)(\omega_c/\Gamma)y}{(32/3\pi)^2(\omega_c/\Gamma)^2y^2 + (1-4y)^2} . \tag{6.64}$$

We shall study these resistivities for two different situations below.

(i) If Γ/ω_c is so small that $(\Gamma/\omega_c)^2 = \alpha y$ with $\alpha \sim 1$, then $(\omega_c/\Gamma)^2 y^2 \sim y$. We then obtain

$$\rho_{xy}(T) = \rho_{xy}(0)\left[1 - \left\{\alpha\left(\frac{32}{3\pi}\right)^2 - 4\right\} y\right] ; \tag{6.65}$$

$$\rho_{xx}(T) = \frac{2\pi}{e^2 N}\left(\frac{32}{3\pi}\right)\left[\frac{\omega_c}{\Gamma}\right] y , \tag{6.66}$$

where $\rho_{xy}(0) = 2\pi/e^2 N$ is the Hall resistivity at $T = 0$.

First of all, $\rho_{xx}(T)$ which is thermally activated with the activation gap $T_0 = \omega_c/2$ with a prefactor $\sim 1/T$, is in agreement with the best fit data of Weiss *et al* [81], who find that in the lowest order of y, $\rho_{xx}^{\min} \sim (1/T)\exp[-\omega_c/2T]$. Note that since we are at the centre of the plateau (ν is an integer), Eqs. (6.64) and (6.66) do indeed correspond to the $\rho_{xx}^{\min}$ which is measured. Secondly, the Hall resistivity *decreases* with increase in temperature, with $\Delta\rho_{xy}(T)$ also being thermally activated, again in agreement with experiments of Cage *et al* [13] and Yoshihiro *et al* [12]. Finally, the linear relation (6.61) for $S > 0$ holds in the rather narrow range of temperatures over which $(\Gamma/\omega_c)^2 \sim y$. In such a case S (which is effectively temperature independent) is given by

$$S = \frac{3\pi}{32}\left[\alpha\left(\frac{32}{3\pi}\right)^2 - 4\right]\left(\frac{\Gamma}{\omega_c}\right) . \tag{6.67}$$

The constancy of S remains over a decade in ρ_{xx}, which is smaller than that of Cage *et al* [13] who find S to be constant over four decades in ρ_{xx}.

(ii) Consider the case where Γ/ω_c is small ($\Gamma/\omega_c \ll 1$) but $(\Gamma/\omega_c)^2 \gg y$. Then we obtain from Eqs. (6.63–6.64),

$$\rho_{xy}(T) = \rho_{xy}(0)\,[1 + 4y] ; \tag{6.68}$$

$$\rho_{xx}(T) = \left(\frac{2\pi}{e^2 N}\right)\frac{32}{3\pi}\left(\frac{\omega_c}{\Gamma}\right) y . \tag{6.69}$$

Here $\rho_{xy}(T)$ *increases* with temperature and $\rho_{xx}(T)$ behaves the same way as in case(i). Interestingly, in this case the linear relation (6.61) between ρ_{xx} and $\Delta\rho_{xy}$ is more rigorous, with a positive slope given by

$$S = -\frac{3\pi}{8}\left(\frac{\Gamma}{\omega_c}\right) . \tag{6.70}$$

Such a behaviour is seen by Wel *et al* [80].

We shall now proceed to estimate the effective masses m^* from the reported measurements [12, 13] below. It is clear from the discussion above that we can hope only to get overall order of magnitude agreement. Given the accuracy of quantization

$$\mathcal{R} \equiv \left| \frac{\Delta\rho_{xy}}{\rho_{xy}(0)} \right| \tag{6.71}$$

at temperature T, the carrier density ρ and the filling factor N, one can estimate m^* from Eq. (6.65). We find, for the choice $\alpha = 1$ in Eq. (6.65), with the reported accuracy of 4.2 ppm at $T = 3\mathrm{K}$ for $N = 4$ IQHE state in a GaAs sample having $\rho = 5.61 \times 10^{11}$ cm.$^{-2}$, $m^* = 0.075$ m$_e$. Their further measurement at $T = 1.2\mathrm{K}$ with accuracy 0.017 ppm gives the value of $m^* = 0.14$ m$_e$. In the measurement of Yoshihiro *et al* [12] in Si MOSFET with $\rho = 1.0 \times 10^{12}$ cm.$^{-2}$, they find $\mathcal{R} = 0.2$ ppm at $T = 0.5\mathrm{K}$ for $N = 4$ IQHE state. We estimate $m^* = 0.67$ m$_e$ from this measurement for Si MOSFET sample. We know that the values of m^* in GaAs and Si MOSFET samples are 0.07m$_e$ and 0.2m$_e$ respectively. Note that it is possible to improve the agreement by further fine tuning the parameter α. In short, the estimated effective masses agree with the known ones for the respective samples in the order of magnitude.

6.6 Compressibility

The compressibility of the system can be obtained from the density-density correlation Π_{00} as

$$\kappa = \left(\frac{1}{e^2\rho^2}\right) \lim_{\mathbf{q}\to 0} Re\, \Pi_{00}(0, \mathbf{q}) \ . \tag{6.72}$$

We now evaluate $\Pi^E_{\tau\tau}(\omega_j, \mathbf{q})$ which reduces to $\Pi_{00}(\omega, \mathbf{q})$ with the analytical continuation.

Without the vertex corrections, we find

$$\begin{aligned} \Pi^{(0)E}_{\tau\tau} &= -\frac{e^2}{2\pi l^2} \sum_{n=0}^{\infty} \sum_{m=0}^{\infty} I_{nm}(\omega_j) \Big[\delta_{mn} \\ &\quad + \frac{\mathbf{q}^2 l^2}{2} \{(n+1)\delta_{m,n+1} + n\delta_{m,n-1} - (2n+1)\delta_{mn}\}\Big] + \mathcal{O}((\mathbf{q}^2)^2) \ . \end{aligned} \tag{6.73}$$

Using the Eq. (C.9), we evaluate κ by the Taylor expansion in powers of Γ/ω_c as before. The vertex contributions will not be considered as those are in higher order of Γ/ω_c. We, therefore, find

$$\kappa = \left(\frac{1}{e^2\rho^2}\right)\mathcal{K}\,, \tag{6.74}$$

where

$$\mathcal{K} = \frac{e^2 m^*}{2\pi}\beta\omega_c \sum_{n=0}^{\infty} f_n(1-f_n) + \mathcal{O}\left(\frac{\Gamma}{\omega_c}\right)^2 . \tag{6.75}$$

Again, the thermal contribution to κ is entirely due to intra Landau band transition.

A low temperature expansion of Eq. (6.75) yields

$$\kappa = \frac{2m^*}{\pi\rho^2}\frac{T_0}{T}\exp\left[-\frac{T_0}{T}\right] . \tag{6.76}$$

At T=0, $\kappa = 0$, *i.e.*, the Hall fluid is incompressible, as we know. At low temperatures, κ is non-zero but exponentially small and hence the fluid is effectively incompressible. Figure (6.3) shows how the value of κ increases with increase in temperature for a given values of ρ/m^* and $\mathcal{N}$. The smooth behaviour of κ with temperature upto a value 5K where QHE has practically vanished clearly shows that there is no phase transition involving the fluids. The same conclusion has been arrived at by Chang *et al* [107] by their measurement of $\rho_{xx}(T)$ for a wide range of temperatures.

6.7 Conclusion

We have considered a quantum Hall system in the presence of weak disorder and determined the diagonal conductivity σ_{xx} and off-diagonal conductivity σ_{xy} at finite temperatures, within the SCBA. We have considered only the integer value of filling factor ν which is in fact the central point of a given plateau in ρ_{xy} and the point of minimum in ρ_{xx}. We have shown that σ_{xy} acquires a temperature dependence due to the intra Landau level transitions. σ_{xx} vanishes in either of the zero temperature and zero impurity limits, *i.e.*, σ_{xx} is non-zero only when both temperature and impurity are non-zero. At low temperatures, $\sigma_{xx}(T)$ does activate with a temperature dependent prefactor. Inverting the conductivity matrix, we obtain $\rho_{xx}(T)$ and $\rho_{xy}(T)$. We have found that

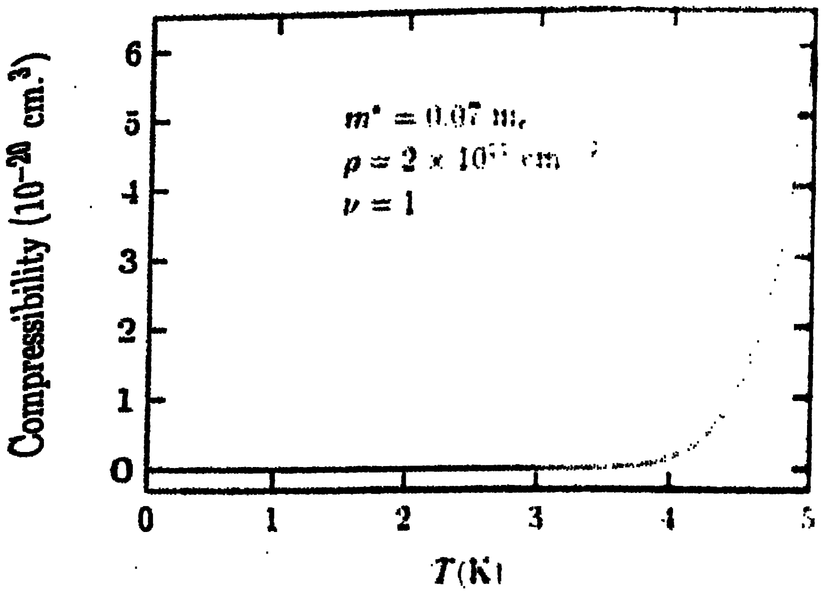

Figure 6.3: The compressibility as a function of temperature for the integer quantum Hall state $\nu = 1$. We have chosen $m^* = 0.07\, m_e$ and $\rho = 2 \times 10^{11}$ cm^{-2}.

depending on the physical regimes of T and Γ. $\rho_{xy}(T)$ either decreases or increases with increase in temperature. $\rho_{xx}(T)$ is thermally activated as $\rho_{xx} \sim (1/T)\exp[-\omega_c/2T]$. Further $\Delta\rho_{xy}$ is shown to obey a linear relationship with ρ_{xx} in agreement with the experiments. An estimation of effective mass from the measured value of $\rho_{xy}(T)$ turns out to be reasonable, and finally, our determination of compressibility shows that there is no phase transition involved, again in agreement with experiments.

Chapter 7

A brief survey of literature

The purpose of this chapter is to present some of the developments on QHE which are relevant to the thesis. This, however, do not exhaust all the aspects of QHE in the sense of a detailed review.

The discovery of IQHE by Klitzing *et al* [1] with high accuracy in quantization of Hall resistivity in two dimensional condensed matter systems brought a great surprise. Yet another surprise was in store when Tsui *et al* [2] discovered that the quantization occurs even in the fractional filling factors. We discuss some of the aspects of these surprising phenomena below.

7.1 The integer quantum Hall effect

In the presence of high magnetic field, LL are formed in the system of the 2DEG. If the density of the electrons is such that exactly *integer* number of LL are filled, the chemical potential (Fermi energy) lies in the gap of two LL. In the disorderless system, chemical potential has a discontinuity at these 'magic' filling factors. This leads to a 'charge gap' which makes the system incompressible. Due to this charge gap, the diagonal conductivity $\sigma_{xx} = 0$. The Hall conductivity $\sigma_H = ie^2/2\pi$ since the number of filled LL is an integer i. In the presence of disorder, the LL are broadened and the localized states appear. As long as the chemical potential lies in the region of localized states [8–10], the change in the electron density or magnetic field will not alter the

conductivities; then σ_{xx} remains zero and σ_H is pinned at the value $ie^2/2\pi$. When the chemical potential hits the extended states, a transition from one quantum Hall state to another occurs.

The quantization of σ_H with high precision and its universality, *i.e.*, independence of the sample geometry, electron density *etc.* indicates that it must be consequence of a general principle. Laughlin [9] showed that the quantization occurs due to the gauge invariance and the existence of the mobility gap. This argument was further extended by Halperin [10], who pointed out that the IQHE states contain gapless edge excitations. Although the electronic states in the bulk are localized, the electronic states at the edge of the sample are extended [11]. The nontrivial transport properties of the IQHE states come from the gapless edge excitations [10, 108]. The Hall conductance was also shown to be a topological quantity [11]. The value of quantization, however, changes with temperature and it approaches the value $ie^2/2\pi$ as $T \to 0$ [12, 13].

7.2 The fractional quantum Hall effect

The FQHE occurs in a partially filled Landau level. Therefore, the charge gap which is essential for QHE is not due to the single particle spectra; it is due to the electron-electron interactions. By an argument similar to that of Laughlin [9] for IQHE, Karlhede *et al* [7] have shown the exactness of quantization in the FQHE as well. The FQHE is observed both in the lowest and higher Lanadu levels [4]. The FQHE in higher Landau levels may be understood as simply the addition of inert filled Landau levels to the FQHE in the lowest LL. We are thus concerned with the filling factor $\nu < 1$.

Laughlin [14] made a variational guess to obtain a remarkably good ground state wave function for $\nu = 1/m$ states:

$$\Psi_{1/m} = \prod_{i<j}^{N} (z_i - z_j)^m e^{-\sum_k |z_k|^2/4l^2} . \tag{7.1}$$

Here $z_j = x_j + iy_j$ are the complex coordinates of the N particles and $l = (eB)^{-1/2}$ is the Magnetic length. Note that Ψ_1 is the ground state wave function of the filled

lowest Landau level. The wave function $\Psi_{1/m}$ is antisymmetric, analytic, and has a homogeneous polynomial in its Jastrow part which makes it an eigen state of angular momentum. The significant feature of $\Psi_{1/m}$ is that the ground state has 'deep nodes' as any two particles approach each other. Laughlin compared this wave function with that of exact diagonalization in few electron systems with different kinds of interaction potentials and found excellent overlap between them. Interestingly, the Laughlin states are found to be the exact ground state wave functions for a wide class of short range interactions [17, 58]. In their finite size calculations, Yoshioka *et al* [109] have found a discontinuity in the chemical potential at $\nu = 1/3$. The gap of charge excitations appears to be size dependent. Chakraborty *et al* [110] have found that the gap in the thermodynamic limit is in agreement with that of collective excitation result [71] in the single mode approximation. However, the experimental value for the gap is lower [111] than the theoretical values.

Laughlin [14] obtained the charge of the quasihole (quasiparticle) excitations of the Laughlin states to be fractional and is given by $e^* = +(-)e/m$. Halperin [15] argued that the quasiparticles possess fractional statistics [112], given by $\theta = \pi/m$. Subsequently Arovas *et al* [16] derived the statistics of the quasiparticles by calculating the Berry phase from the Lauglin wave function. These quasiparticles or quasiholes at their magic densities condense into a Laughlin like state to form a hierarchy of the FQHE states [15, 17]. Generically, the quasiparticle (quasihole) excitations of the FQHE states with $\nu = p/q$ (p, q are integers) have charge $e^* = -(+)ep/q$ and statistics $\theta = -(+)\pi/q$.

Jain [18] has proposed the composite fermion model (CFM), which provides an alternative hierarchy to the one above, for FQHE states. In this highly successful model, IQHE and FQHE states are treated in the same footing. The strong correlation between electrons in the FQHE states are modeled by attaching an even number ($2s$) of vortices to each electron and an weak residual interaction between the charge-flux composites. The statistics of the charge-flux composites remain fermionic and hence they are called composite fermions. The IQHE of composite fermions with $\nu^* = p$ leads

to FQHE state $\nu = p/(2sp+1)$ in original electron system. Jain's proposed ground state wave function for these states:

$$\Psi_\nu = \prod_{i<j}^{N} (z_i - z_j)^{2s} \Psi_p \,. \tag{7.2}$$

where Ψ_p is the IQHE wave function with p filled Landau level. Note that $p = 1$ corresponds to the Laughlin states. Numerical studies with a small number of particles show, like Laughlin state, a good overlap between Jain wave functions and exact ground state wave functions [113]. One may argue that the Jain wave functions are not good variational wave functions as they have admixtures of higher Landau level wave functions. However, Trivedi and Jain [114] found by calculating ground state energies for noninteracting electrons that the Jain states have, in fact, very small admixture of the higher Landau levels. Recently, Morf and d'Ambrumenil [115] have determined effective mass of composite fermions numerically in a finite size system.

A field theoretic version of the CFM was first developed by Lopez and Fradkin [19] for a system of spinless electrons. This is known as fermionic CS theory. They derived [72] also the linear response functions for $\nu = p/(2sp+1)$ states in the random phase approximation (RPA), employing this theory. They further derived [54] the modulus square of the many body wave functions for these states, employing the density-density correlation function which was derived in RPA

Using the above theory, Kalmayer and Zhang [116] argued that impurity driven fluctuation of the CS gauge fields causes metalic phase near $\nu = 1/2$ which is commonly known as the '$\nu = 1/2$ anomaly' [117, 25]. Recall that in the CFM, the excitation gap for a state $\nu = p/(2sp+1)$ is $\bar{\omega}_c = 2\pi\rho/m^*p$. the effective cyclotron energy of composite fermions. At $\nu = 1/2$ which correspond to $s = 1/2$ and $p = \infty$, the CS mean magnetic field exactly cancels the external magnetic field and hence the system behave as two dimensional gas of free fermions (in zero magnetic field). Halperin, Lee, and Read (HLR) [20] argued that the composite fermions form a Fermi sea at $\nu = 1/2$ and all even denominator states, in general. They further explained the anomaly in surface accoustic wave experiments [25, 26] at $\nu = 1/2$ in terms of free composite fermions. A good number of experiments [21–24, 27–33] also have been performed in finding

the evidence of the composite fermions. Most of the experiments are performed at or near $\nu = 1/2$. Rezayi and Read [68] have also shown from their numerical study in spherical geometry that the $\nu = 1/2$ state is Fermi-liquid like, in agreement with the above prediction. Taking into account the electron electron interactions, HLR further conclude that the effective mass of CF diverges at the Fermi surface, if the range of electrostatic interaction is shorter than, or equal to, that of Coulomb interaction. Due to the infra red gauge field fluctuations, this divergence is manifested in the energy gaps of states near $\nu = 1/2s$. However, the gauge field fluctuations do not affect the linear response at $\nu = 1/2s$, due to a mutual cancellation with another singular term [118, 119]. Consequently the states $\nu = 1/2s$ are characterized by a finite effective mass m^* [118]. In a recent paper, Lee *et al* [120] report that the suppression of Shubnikov-de Haas oscillations of CF near $\nu = 1/2$ in the experiments [22–24] is due to strong dephasing of CF and renormalization of effective mass. They have further estimated m^* following the method of HLR, and found close resemblance with the result of Mörf and d'Ambrumenil [115] who have calculated m^* numerically. All the above theoretical analyses are based on the fermionic CS theory in RPA.

In the above RPA approach, the low energy excitations are on a scale set by the cyclotron energy rather than by interaction energy. In an improved 'modified' RPA method, Simon *et al* [121] have defined an effective mass m^* that is set phenomenologically by the interaction scale [20]. It has been pointed out [122] that there is a further drawback in fermionic CS theory under above approximations. In the limit of large magnetic field, the static response of electrons to a spatially varying magnetic field, would largely be determined by kinetic energy considerations in this approximation, which is incorrect. Simon *et al* [122] have proposed a method to 'remedy' the problem by attaching an orbital magnetization to each composite fermion to separate current into magnetization and transport contributions.

There exists a parallel development in terms of bosonic CS theory. By a singular gauge transformation on Laughlin wave function $\Psi_{1/m}$, Girvin and MacDonald [123] transformed the fermionic wave function into a bosonic one where m (odd) statistical

flux quanta are attached to each particle. They showed that the transformed density matrix exhibits an algebraic off diagonal long range order (ODLRO) in the Laughlin state. The average statistical flux cancels the applied magnetic flux at $\nu = 1/m$. Therefore the singular gauge transformation makes the system into that of bosons in zero net magnetic field. The ODLRO indicates that such bosons are superconducting. Therefore the superconducting state of the bosons corresponds to the quantum Hall liquid of the electrons. A related but distinct ODLRO was found by Read [62] in the Laughlin state by considering a superfluid analogy microscopically. The order parameter possesses broken symmetry [62]. Rezayi and Haldane [124] numerically found that the related order parameter at $\nu = 1/3$. $2/5$ states is nonzero. Zhang. Hansson. and Kivelson [60] developed Chern-Simons-Landau-Ginzburg (CSLG) theory for the FQHE. Phenomenological aspects of FQHE can be obtained from the CSLG theory [59]. Zhang [59] derived Lauglin wave function and ODLRO of Girvin and MacDonald from the CSLG theory. Lee, Kivelson. and Zhang [125] studied the transitions between quantum Hall states within the CSLG theory. Kivelson. Lee. and Zhang [126] have constructed a global phase diagram for the QHE states in the magnetic field and impurity plane. They further derived the law of corresponding states from the CSLG theory.

7.3 Scaling theories

A comprehensive review of scaling theories in IQHE is provided recently by Huckestein [94]. We briefly review here of the relevant ones.

The scaling theory of localization [127] predicts the absence of extended states in two dimensional systems. However in the presence of a strong magnetic field, the delocalized states appear [128]. These states show their existence only at a single critical energy, *i.e.*, at the center of the Landau band, and therefore a continuous transition between quantum Hall liquids occurs. At zero temperature, the Hall conductivity is thus expected to exhibit very sharp transitions whenever the Fermi energy passes the critical energy [129]. This is indeed true, as it is observed that the plateaus of quan-

tization can be extremely broad and the transition between them are extremely sharp as the temperature is lowered [130, 131]. At the same time, the diagonal conductivity shows sharp spikes (maxima) at the position of plateau transitions (see Fig. 1.1).

In Si-MOSFET, Yamane *et al* [132] have observed that σ_{xx} and σ_{xy} are not independent and they depend on a single parameter. In contrast, Wei *et al* [98] have observed two parameter flow diagram in σ_{xx} and σ_{xy} in InGaAs-InP heterostructure, which was predicted by Levine *et al* [97] in renormalization group analysis. They have found a stable flow towards $(\sigma_{xx},\ \sigma_{xy}) = (0,\ n)\frac{e^2}{2\pi}$ which describes the widening of the plateaus, and an unstable fixed point corresponding to $\sigma_{xy}^c = (n+1/2)\frac{e^2}{2\pi}$, describing the critical transition. Due to the experimental difficulty to study the critical transitions in terms of σ_{xx} and σ_{xy}, Wei *et al* [84] have first studied the critical transitions in terms of resistivities. They have found the scaling law in critical transitions between the plateaus; $(d\rho_{xy}/dB)^{\max}$ and the inverse width in ρ_{xx}, $(\Delta B)^{-1}$ behave as T^{-k} with $k = 0.42$. This scaling law has been field theoretically derived by Pruisken [133], and obtained by Huo, Hetzel, and Bhatt [134] in numerical simulation. At finite temperatures, the system size is given by the phase coherence length L_ϕ [135] which diverges as $L_\phi \sim T^{-p/2}$ as $T \to 0$ where the exponents p and k are related *via* another exponent ν as $k = p/2\nu$. The localization length ξ diverges at the critical point *via* $\xi(E_F,\ B) \sim (B - B_c(E_F))^{-\nu}$. The effective system size behaves as $L_{\text{eff}}^{1/\nu} \propto T^{-1/k}$. Koch *et al* [89] have measured the exponent ν by studying samples of the different sizes. They have found $(d\rho_{xy}/dB)^{\max}$ and ΔB saturate at low temperatures, and the saturation temperature decreases with the increase of system size. The saturation value of ΔB is then related as $\Delta B \propto L^{-1/\nu}$. Koch *et al* [89] have found the value of the exponent ν to be 2.3, in good agreement with the numerical result [136], as well as analytical one [137] which incorporates the effect of quantum tunneling in the percolation picture.

There are further elegant method to study the finite size scalings. (i) The diagonal conductivity σ_{xx} relates the Thouless number. In their numerical study on IQHE, Ando *et al* [138] have obtained size dependence of the Thouless number which gives the information about the critical behaviour. The dependence of eigen energies of

a finite system with the change in the boundary conditions can distinguish between the extended and localized states [139]. The eigen energies of localized states do not change with the boundary condition for a large system compared to the localization length, while eigen energies of the extended states exhibit a shift with the change in the boundary condition [140]. (ii) To distinguish extended and localized states, the ability of an eigen state to contribute to Hall conductivity σ_{xy} also plays a major role. Thouless *et al* [141] and Niu *et al* [142] have found that σ_{xy} is proportional to the Chern number, which is topologically invariant. Arovas *et al* [143] have shown that the zeros of the eigen states with finite Chern number can be moved all over the space with the suitable choice of the boundary angle, and for the eigen states with zero Chern number, the zeros are confined in space. The former type of states are extended, while latter ones are localized which do not have any contribution to σ_{xy}. Huo and Bhatt [144] have used the density of states with non zero Chern number as a finite size scaling quantity and they have concluded that the extended states are only at a single energy E_c.

The scaling laws are not restricted only to IQHE. Indeed, Engel *et al* [145] have observed same universal value of exponent k in the quantum Hall transitions from 1/3 to 2/5 FQHE states. Jain *et al* [146] have proposed a new class of variational wave function in the presence of disorder as a generalization to the CFM wave function (7.2). As a consequence of these wave functions they have found the law of corresponding states which relates the behaviour of the transitions in the fractional Hall regime to that in the integer Hall regime. For example, the transition fron 1/3 to 2/5 plateau is characterized by the same critical exponents as the transition between integer plateaus. Apart from the transition from on QHS to another QHS, there are also transitions from quantum Hall to insulator state, driven by the magnetic field. Shahar *et al* [147] have recently observed that the diagonal resistivity at this transition is universal for integer and fractional states, and has a value close to one quantum unit of resistance. As we have mentioned earlier, Kivelson, Lee, and Zhang [126] proposed a global phase diagram in the disorder-magnetic field plane. They derived a set of correspondence

rules using CSLG theory, and relate the properties of all QHE states to those of the $\nu = 1$ state. The high disorder and high B field limit is the insulating phase which is bordered by the $\nu = 1$ IQHE and $\nu = 1/3$, $1/5$ FQHE quantum Hall phases.

7.4 The role of spin

Thus far our discussions have ignored the spin degree of freedom of the electrons. That would be justified in the strong magnetic field limit since the spins are then fully polarized in the direction of the magnetic field. However, as is pointed out by Halperin [34], the rather small value of g factor in GaAs leads to a smaller Zeeman energy compared to cyclotron energy, and the Zeeman energy even does not dominate over the Coulomb interaction energy. Therefore, the possibility of quantum Hall states that may not be fully polarized can not be ruled out. Halperin has further constructed the ground state wave function for unpolarized $\nu = 2/5$ state. Baskaran and Tosatti[148] have shown how the Halperin's unpolarized state becomes almost a spin singlet state, even though it is not an eigenstate of spin operator. The state $\nu = 8/5$, which is the particle-hole conjugate state of $\nu = 2/5$, has been seen experimentally [36] as unpolarized state in the small Zeeman energy limit. Similarly, the states $\nu = 2/3$ and $3/5$ are also seen experimentally [37, 38] as unpolarized and partially polarized respectively for small Zeeman energy. These states make a transition to their fully polarized phase with the increase of Zeeman energy in tilted magnetic field experiments. It turns out that the critical tilt angle of magnetic field the QHE disappears, but it reemerges at higher tilt angles.

Much of the early theoretical work based on finite size numerical calculation with the tunable g factor is reviewed in Ref.[6]. We discuss here the most important ones. The states $\nu = 2/(2n + 1)$ and $3/5$ appear to be unpolarized and partially polarized respectively. The Laughlin states $\nu = 1/(2n + 1)$ are fully polarized even in the zero Zeeman energy limit. Chakraborty *et al* [110] have found, for vanishing Zeeman energy, the spin-reversed quasiparticle and spin-polarized quasihole as the lowest energy excitation of fully polarized $\nu = 1/3$ state. This makes the daughter state $\nu = 2/5$ to

be unpolarized.

The even denominator $\nu = 5/2$ state which has been experimentally observed [4] is rather unexpected. This state is unpolarized and the direct evidence for it comes through the observation [53] that the unpolarized $\nu = 5/2$ state is quickly destroyed in tilted field studies. The theoretical understanding of this effect is not complete. Haldane and Rezayi [67] have constructed a trial wave function for the unpolarized $\nu = 1/2$ state which is a partner of unpolarized $\nu = 5/2$ state in the lowest Landau level. However, no even denominator state other than $\nu = 5/2$ state is seen experimentally in a single layer system.

Kallin and Halperin [69] have studied collective charge density and spin density excitations of IQHE states in the small Zeeman energy limit. They have also found the spin-wave excitations for odd IQHE states. Longo and Kallin [77] have studied spin flip excitations in the FQHE states.

It has been found from pseudo potential models [57], and finite size studies for the Coulomb interactions [39–41, 149] that the ground state at $\nu = 1/m$ (m odd) is fully polarized as it is independent of g as $g \to 0$. There is always a gap for current excitations even at $g = 0$ [7]. Though the ground state is the same, the quasiparticle excitations change substantially as g is lowered. While for larger values of g the quasiparticles have charge $\pm e$ and spin $S_z = 1/2$, near $g = 0$, the quasiparticles have infinite size and possess macroscopic spin due to the Coulombic interaction [150]. In this vanishing g limit, the gap for QHE in $\nu = 1$ state is not of single particle origin, (which would be expected in high Zeeman energy limit), it is a many body correlation effect. These new quasiparticles possess nontrivial spin order and topological quantum number — they are known as Skyrmions [151]. Three recent experiments [152–154] have proven the evidence of Skyrmions in $\nu = 1$ state. The partially polarized IQHE states such as $\nu = 3,\ 5$ may possess Skyrmion excitations in their ferromagnetic ground state; however they are not the lowest energy excitations [155]. Jain and Wu [156] also have found for the case of higher Landau levels that the addition of a single electron does not destroy the ferromagnetic ground state by the production of Skyrmions. Before

the work of Sondhi *et al* [150], Lee and Kane [65] have shown that $\nu = 2$ and $1/2$ states are unpolarized due to skyrmions. Recently, Nayak and Wilczek[157] have argued that spin singlet states can be understood as arising from primary polarized states by Skyrmion condensation. The energy of the Skyrmions is determined by the spin stiffness. Recently Nakajima and Aoki [78] have computed the spin stiffness using reduced Haldane pseudo potential within the CFM for $\nu = 1/3$ and $1/5$ states, and their results are in agreement with Sondhi *et al* [150], and Moon *et al* [64] who have calculated from first principle.

7.5 Bilayer systems

Technological progress has made it possible to produce bilayer 2DEG systems of extremely high mobility. In these systems, a pair of 2DEG are separated by a distance d, comparable to the inter-particle distance in the same layer. Stormer *el al* [158] were the first to observe QHE in bilayer systems. Such a spin polarized bilayer system can be mapped into a single layer spin-1/2 system. In this mapping, the layer degree of freedom acts as a 'pseudo-spin', in analogy with spin-1/2 system in a single layer. Although these two systems seems to be equivalent, they differ in a fundamental way: While the electron electron interaction is spin independent, it, in fact, depends on the layer in which the electrons reside. Due to this difference, there are certain wave functions that are acceptable for bilayer QHS, but are excluded in the single layer spin-1/2 systems. For example, Yoshioka, MacDonald, and Girvin [159] proposed the so called (3,3,1) state as a ground state for a bilayer $\nu = 1/2$ QHS which has no analogue in single layer systems.

In a single layer system, the gaps for IQHE are generally of single particle origin, while those in the FQHE states arise from many body effects. In contrast, by tuning sample parameters appropriately, both single particle and many body regimes can be achieved for a given QHS in a bilayer system. There are two energy scales associated with bilayer systems: (i) the single particle tunneling gap (Δ_{SAS}) separating the lowest symmetric and antisymmetric states and (ii) the many body Coulomb interaction

between electrons in different layers. Each can lead to a QHE: in association they can either enhance or destroy QHE.

For a pair of identical widely separated layers, the QHE spectrum is equivalent to that of each individual layer with the exception that the total filling factor associated with each Hall plateau is twice the corresponding single layer value. Thus, for example, no $\nu = 1$ QHE would be found since no $\nu = 1/2$ QHE has ever been observed in a single layer system. However, the smallest amount of inter layer tunneling can lead to odd integer QHE states since it opens up the gap Δ_{SAS}. In the absence of Coulomb interaction, the electrons of a double layer occupy the symmetric state and the pair of layers act as a single layer. The Coulomb interaction can drastically modify the properties of this bilayer states by mixing antisymmetric states into the many body wave functions. This leads the electrons within the same layer to be more strongly correlated than electrons in different layers. MacDonald *et al* [160] have drawn a phase diagram in the $\Delta_{\mathrm{SAS}}/(e^2/\epsilon l)$ and d/l plane, where $e^2/\epsilon l$ is the Coulomb energy, l is the magnetic length, and d is the inter layer distance. The larger values of d/l correspond to larger intra layer correlation compared to inter layer correlation. For sufficiently large d/l, QHE disappears [160, 161]. Therefore, the system undergoes a phase transition as the barrier between electron layers increases or magnetic field increases since $1/l \propto \sqrt{B}$. MacDonald *et al* [160] and Brey [161] have argued that this could be the reason for experimentally observed [162, 163] destruction of odd integer QHE.

Even in the absence of tunneling, bilayer QHE with no single layer analogue can occur if the inter layer Coulomb interactions are sufficiently strong [164, 165, 159, 166] when typically $d/l \sim 1$. The experimentally observed [167, 168] bilayer $\nu = 1/2$ state (*i.e.*, 1/4 filling in each layer) is a good evidence for such a regime. This new state has close resemblance with the Laughlin 1/3 state as far as the intralayer correlations are concerned, but it contains additional inter layer correlations as well. Yoshioka *et al* [159] have shown that (3,3,1) wave function is a good wave function for this state if $d/l \sim 1$. He *et al* [166] have examined the range of d/l over which $\nu = 1/2$ state is favourable in a finite size numerical study. They report also that both interlayer tunneling and finite

layer thickness are responsible for suppressing $\nu = 1/2$ state. In a recent paper, He *et al* [169] have argued from their numerical study using realistic sample parameters that the experimentally observed $\nu = 1/2$ state in both the experiments [167, 168] is stabilized by the competition between intralayer and interlayer electron electron interaction.

Similarly in the absence of tunneling, $\nu = 1$ QHE in bilayer system is predicted [165, 159, 166] to be the many body effect.[1] This collective state cannot exist for arbitrarily weak inter layer coupling, unlike the aforementioned tunneling $\nu = 1$ state. Instead, this state is expected [159, 166, 170] to undergo a phase transition to a compressible state at some critical interlayer spacing. In a recent experiment, Lay *et al* [171] have observed that the ground state at $\nu = 1$ evolves continuously form a single particle QHE stabilized by large Δ_{SAS} at low particle density ρ to a many body QHE state stabilized by strong inter layer interaction at an intermediate ρ. They further report that as ρ is further increased, an incompressible to compressible transition occurs. Interestingly, this state, unlike bilayer $\nu = 1/2$ state, is predicted [172, 173] to possess a broken symmetry which may lead to neutral gapless mode, Kosterlitz-Thouless phase transition, and Josephson and Meissner effects.

Two distinct physical mechanisms for generating $\nu = 1$ QHE in double layer systems lead to a rich phase diagram. In a recent experiment, Murphy *et al* [174] have shown a phase diagram. In the weak tunneling limit, they observe the above predicted phase transition from a Laughlin-like incompressible state to a compressible phase when the interlayer separation exceeds a critical value. In addition, they find additional phase transition between distinct incompressible $\nu = 1$ state, driven by the application of a magnetic field parallel to the layers. Subsequently Yang *et al* [175] have argued that the spontaneous symmetry breaking analogous to that of spin-1/2 easy plane ferromagnet, with the layer degree of freedom playing the role of spin, is responsible for this new phase transition. While Yang *et al* [175] have provided a phenomenological theory of the zero temperature phase diagram associated with spontaneous interlayer coherence, Moon *et al* [64] have derived the effective action, which is used in the phenomenological

[1]Recall that in a single layer spin-1/2 system, $\nu = 1$ state is due to the many body correlation effect in the vanishing g limit [150].

theory, microscopically.

Lopez and Fradkin [52] have studied bilayer system within the CFM using CS theory. A detailed discussion on it is provided in section (3.5). Nakajima and Aoki [176] have numerically analyzed the effect of interlayer tunneling in bilayer $\nu = 1/m$ (m odd integer) states in terms of composite fermion picture

There are various other aspects of QHE such as edge states and cooperative ring exchange theory which we do not survey in this thesis.

Appendix A

Form factors at zero temperature

In this appendix, we present the details of evaluation of Π^r_{00} component of the polarization tensor $\Pi^r_{\mu\nu}$ at zero temperature. The evaluation of other components follows a similar procedure.

The component Π^r_{00} is given by

$$\Pi^r_{00}(x,x') = ie^2 G^r(x,x')G^r(x',x) \;, \tag{A.1}$$

where the single particle Greens function

$$G^r(x,x') = -i\langle T[\psi^r(x)\psi^{r*}(x')]\rangle \tag{A.2}$$

can be obtained by solving differential equation

$$(i\partial_0 - H^r + \mu)G^r(x,x') = \delta^{(3)}(x,x') \tag{A.3}$$

with appropriate boundary condition. Here $H^r = -\frac{1}{2m^*}D_k^{r2} - (g/2)\mu_B\sigma$ is the Hamiltonian of the system within the MF ansatz, where $D_\mu = \partial_\mu - ie\mathcal{A}_\mu$. $\mathcal{A}_\mu$ is the sum of all the mean gauge fields. We solve H in the Landau gauge

$$\mathcal{A}_2(x) = \mathcal{A}_0(x) = 0 \;, \; \mathcal{A}_1(x) = -\bar{B}x_2 \;, \tag{A.4}$$

to obtain the eigen states

$$\psi_{nk\sigma}(x) = \frac{1}{\sqrt{l_0}} e^{ikx_1} v_n\left(\frac{x_2}{l_0} + K_1 l_0\right) v_\sigma \tag{A.5}$$

with the corresponding eigen values

$$\epsilon_{n\sigma} = (n + \frac{1}{2})\bar{\omega}_c - \frac{g}{2}\mu_B\sigma \; : \; n = 0, 1, 2, \cdots, \sigma = \pm 1 \; . \tag{A.6}$$

The Landau levels are infinitely degenerate with finite degeneracy per unit area, $\rho_L = 1/2\pi l_0^2$, where $l_0 = (e\bar{B})^{-1/2}$ is the magnetic length corresponding to the effective mean magnetic field $\bar{B}$. v_n in Eq. (A.5) is a shifted simple harmonic oscillator wave function of n-th level and v_σ is either $|\uparrow>$ or $|\downarrow>$, the spin dependent part of the eigen states.

The Greens function $G^r(x, x')$ can be expressed in the form of an integral over frequencies as follows:

$$G^r(x, x') = \int_C \frac{d\omega_1}{2\pi} e^{-i\omega_1(t-t')} \langle X|G^r(\omega_1 \pm i\eta)|X'\rangle \; . \tag{A.7}$$

where X represents the spatial coordinate and the operator

$$G^r(\omega_1 \pm i\eta) = \frac{1}{\omega_1 + \mu - H^r \pm i\eta} \; . \tag{A.8}$$

The choice of the contour C for the integration over frequencies is dictated by the boundary condition which defines the ground state. Let p be the number of fully filled LL. Then the contour must pass below the poles at $\omega_1 = -\mu + \epsilon_n$ for $0 \leq n \leq p - 1$ which corresponds to retarded Greens function $G^r(\omega_1 + i\eta)$ and C passes above for all the other poles for $n \geq p$, corresponding to advanced Greens function $G^r(\omega_1 - i\eta)$.

The Fourier transform of $\Pi^r_{00}(x, x')$ is given by

$$\begin{aligned}
\Pi^r_{00}(q, q') &= ie^2 \int d^3x d^3x' e^{-iqx} e^{iq'x'} G^r(x, x') G^r(x', x) \\
&= ie^2 2\pi\delta(\omega - \omega') \int d^2X d^2X' e^{i\mathbf{q}\cdot X} e^{-i\mathbf{q}'\cdot X'} \\
&\quad \int \frac{d\omega_1}{2\pi} \langle X|G^r(\omega_1 \pm i\eta)|X'\rangle \langle X'|G^r(\omega_1 + \omega \pm i\eta)|X\rangle \; .
\end{aligned} \tag{A.9}$$

Then introducing complete set of eigen states

$$\int \frac{dk}{2\pi} \sum_n |nk\rangle\langle nk| = 1 \tag{A.10}$$

in Eq. (A.9) and using Eq. (A.5) for the wave functions, we obtain

$$\Pi^r_{00}(q, q') = (2\pi)^3 \delta^{(3)}(q - q') \Pi^r_{00}(\omega, \; \mathbf{q}) \; , \tag{A.11}$$

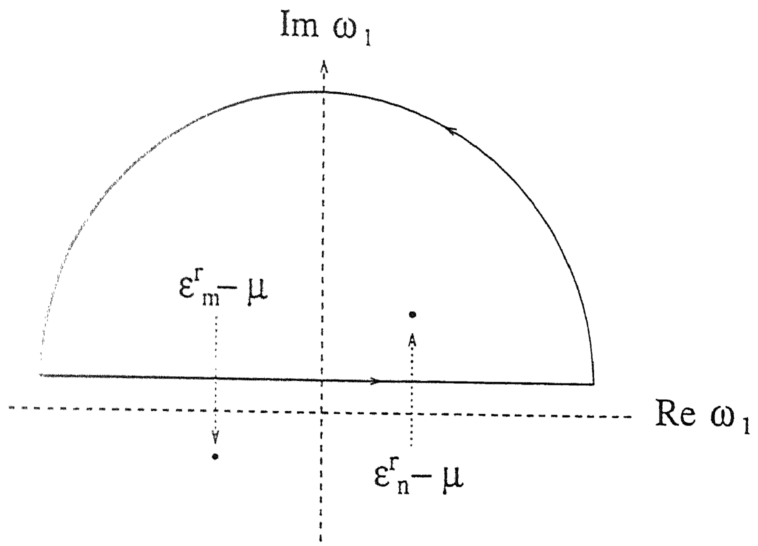

Figure A.1: The contour for the integration (A.14) in the complex ω_1 plane. While one pole is inside the contour, the other one is outside of it.

where

$$\Pi^r_{00}(\omega, q) = ie^2 \frac{1}{2\pi l_0^2} \int \frac{d\omega_1}{2\pi} \sum_n \sum_m \frac{1}{(\omega_1 + \mu - \epsilon^r_n \pm i\eta)(\omega_1 + \omega + \mu - \epsilon^r_m \pm i\eta)}$$
$$\int d\chi_1 v^*_m(\chi_1) v_n(\chi_1 + q_x l_0) e^{-iq_y l_0 \chi_1} \int d\chi_2 v^*_n(\chi_2 + q_x l_0) v_m(\chi_2) e^{iq_y l_0 \chi_2} , \tag{A.12}$$

with

$$\chi_1 = \frac{x_2}{l_0} + k_2 l_0 \, ; \; \chi_2 = \frac{x_2'}{l_0} + k_2 l_0 \, . \tag{A.13}$$

Note that the relation (A.11) as a consequence of translational invariance of the system.

We first evaluate the integral

$$\int \frac{d\omega_1}{2\pi i} \frac{1}{(\omega_1 + \mu - \epsilon^r_n \pm i\eta)(\omega_1 + \omega + \mu - \epsilon^r_m \pm i\eta)} . \tag{A.14}$$

Consider the contour (see Fig. A.1) in the complex ω_1 plane. The integral is nonvanishing only if the two poles are in opposite side of the real axis, *i.e.*, one pole inside the contour while the other outside of it. Using Cauchy's residue theorem, we obtain

$$\int \frac{d\omega_1}{2\pi i} \frac{1}{(\omega_1 + \mu - \epsilon^r_n \pm i\eta)(\omega_1 + \omega + \mu - \epsilon^r_m \pm i\eta)}$$

$$= \begin{cases} \frac{1}{\omega+\epsilon_n^r-\epsilon_m^r+i\eta} & : \; m < p_r,\; n \geq p_r \\ -\frac{1}{\omega+\epsilon_n^r-\epsilon_m^r-i\eta} & ; \; n < p_r,\; m \geq p_r \\ 0 & ; \; \text{otherwise} \end{cases} . \tag{A.15}$$

where p_r is the number of Landau levels filled by the particles of spin index r. Therefore,

$$\Pi_{00}^r(\omega,\ \mathbf{q}) = \frac{e^2}{2\pi l_0^2}\left[\sum_{n=0}^{p_r-1}\sum_{m=p_r}^{\infty}\frac{1}{\omega+\epsilon_n^r-\epsilon_m^r-i\eta} - \sum_{n=p_r}^{\infty}\sum_{m=0}^{p_r-1}\frac{1}{\omega+\epsilon_n^r-\epsilon_m^r+i\eta}\right]$$
$$\times \int d\chi_1 v_m^*(\chi_1)v_n(\chi_1+q_xl_0)e^{-iq_yl_0\chi_1}\int d\chi_2 v_n^*(\chi_2+q_xl_0)v_m(\chi_2)e^{iq_yl_0\chi_2} . \tag{A.16}$$

Similarly, one gets

$$\Pi_{01}^r(\omega,\ \mathbf{q}) = -\frac{ie^2}{4\pi m^* l_0^3}\left[\sum_{n=0}^{p_r-1}\sum_{m=p_r}^{\infty}\frac{1}{\omega+\epsilon_n^r-\epsilon_m^r-i\eta} - \sum_{n=p_r}^{\infty}\sum_{m=0}^{p_r-1}\frac{1}{\omega+\epsilon_n^r-\epsilon_m^r+i\eta}\right]$$
$$\times \left[\int d\chi_1 v_m^*(\chi_1)v_n(\chi_1+q_xl_0)e^{-iq_yl_0\chi_1}\int d\chi_2 v_n^*(\chi_2+q_xl_0)v_m(\chi_2)\chi_2 e^{iq_yl_0\chi_2}\right.$$
$$\left. + \int d\chi_1 v_m^*(\chi_1)v_n(\chi_1+q_xl_0)e^{-iq_yl_0\chi_1}\int d\chi_2(\chi_2+q_xl_0)v_n^*(\chi_2+q_xl_0)v_m(\chi_2)e^{iq_yl_0\chi_2}\right] . \tag{A.17}$$

and

$$\Pi_{11}^r(\omega,\ \mathbf{q}) = -\frac{e^2}{8\pi m^{*2} l_0^4}\left[\sum_{n=0}^{p_r-1}\sum_{m=p_r}^{\infty}\frac{1}{\omega+\epsilon_n^r-\epsilon_m^r-i\eta} - \sum_{n=p_r}^{\infty}\sum_{m=0}^{p_r-1}\frac{1}{\omega+\epsilon_n^r-\epsilon_m^r+i\eta}\right]$$
$$\times \left[\int d\chi_1(\chi_1+q_xl_0)v_m^*(\chi_1)v_n(\chi_1+q_xl_0)e^{-iq_yl_0\chi_1}\int d\chi_2 v_n^*(\chi_2+q_xl_0)v_m(\chi_2)\chi_2 e^{iq_yl_0\chi_2}\right.$$
$$+ \int d\chi_1\chi_1 v_m^*(\chi_1)v_n(\chi_1+q_xl_0)e^{-iq_yl_0\chi_1}\int d\chi_2(\chi_2+q_xl_0)v_n^*(\chi_2+q_xl_0)v_m(\chi_2)e^{iq_yl_0\chi_2}$$
$$+ \int d\chi_1\chi_1 v_m^*(\chi_1)v_n(\chi_1+q_xl_0)e^{-iq_yl_0\chi_1}\int d\chi_2 v_n^*(\chi_2+q_xl_0)\chi_2 v_m(\chi_2)e^{iq_yl_0\chi_2}$$
$$+ \int d\chi_1 v_m^*(\chi_1)(\chi_1+q_xl_0)v_n(\chi_1+q_xl_0)e^{-iq_yl_0\chi_1}$$
$$\left.\times \int d\chi_2(\chi_2+q_xl_0)v_n^*(\chi_2+q_xl_0)v_m(\chi_2)e^{iq_yl_0\chi_2}\right] . \tag{A.18}$$

The integrals over χ_1 and χ_2 in Eqs. (A.16)–(A.18) can be performed by the Taylor's expansion of the integrands in powers of q_xl_0 and q_yl_0. Then expressing the polarization tensor $\Pi_{\mu\nu}^r(\omega,\ \mathbf{q})$, by the requirement of gauge, translational, and rotational

invariances, in the form

$$\Pi^r_{\mu\nu}(\omega, \mathbf{q}) = \Pi^r_0(\omega, \mathbf{q}^2)(q^2 g_{\mu\nu} - q_\mu q_\nu) + \left(\Pi^r_2(\omega, \mathbf{q}^2) - \Pi^r_0(\omega, \mathbf{q}^2)\right)$$
$$\times \left(\mathbf{q}^2\delta_{ij} - q_i q_j\right)\delta_{\mu i}\delta_{\nu j} + i\Pi^r_1(\omega, \mathbf{q}^2)\epsilon_{\mu\nu\lambda}q^\lambda , \tag{A.19}$$

we obtain the form factors. In the lowest order of $\mathbf{q}^2$, these are given by

$$\Pi_0^{\uparrow,\downarrow} = -\frac{e^2 p_{\uparrow,\downarrow}}{2\pi}\frac{\bar{\omega}_c}{\omega^2 - \bar{\omega}_c^2} \ ; \ \Pi_1^{\uparrow,\downarrow} = \Pi_0^{\uparrow,\downarrow}\bar{\omega}_c \ ; \tag{A.20}$$

$$\Pi_2^{\uparrow,\downarrow} = -\frac{e^2}{4\pi m^*}\bar{\omega}_c^2\left[\frac{3}{\omega^2 - \bar{\omega}_c^2} - \frac{4}{\omega^2 - 4\bar{\omega}_c^2}\right] p_{\uparrow,\downarrow}\left(p_{\uparrow,\downarrow} - \sigma\frac{g}{2}\frac{m^*}{m_e}\right) . \tag{A.21}$$

Appendix B

Response function in TDHFA

In this appendix, we shall evaluate Π^r_{00} in TDHFA. We adopt the diagrammatic method that was developed by Kallin and Halperin [69].

The single particle Hartree-Fock Green's function is given by

$$G^r_n(\omega) = \frac{1}{\omega - \epsilon^r_n - \Sigma^r_n + i\delta(n,r)} . \tag{B.1}$$

where $\delta(n,r) = 0^+$ for $n < p_r$ and $\delta(n,r) = 0^-$ for $n \geq p_r$. G^r_n is diagrammatically shown in Fig. (B.1). In the strong field approximation (the effective field B here), the self energy, which is diagrammatically shown in Fig. (B.1), is given by

$$\Sigma^r_n = -\int \frac{d^2r}{2\pi l_0^2} V(r) e^{-r^2/2l_0^2} L^1_{p_r-1}\left(\frac{r^2}{2l_0^2}\right) L^0_n\left(\frac{r^2}{2l_0^2}\right) . \tag{B.2}$$

where $V(r) = e^2/\epsilon r$ is the Coulomb potential. Note that the same index r stands for both spin and spatial coordinates. The associated Laguerre polynomial is given by

$$L^m_n(x) = \frac{1}{n!} e^x x^{-m} \frac{d^n}{dx^n}\left(e^{-x} x^{n+m}\right) . \tag{B.3}$$

The response function Π^r_{00} may be expressed as (see Fig. B.2)

$$\Pi^r_{00}(\omega, \mathbf{q}) = \sum_{n_1,n_2} \sum_{r_1,r_2} M_{n_1n_2}(\mathbf{q}) D^{r_1r_2}_{n_1n_2}(\omega) \Gamma^{r_1r_2}_{n_1n_2}(\omega, \mathbf{q}) \delta_{r_1,r_2} \delta_{r_1,r} . \tag{B.4}$$

Here the matrix element (contribution of the left vertex of Fig. B.2) is obtained as,

$$M_{n_1n_2}(\mathbf{q}) = \left(\frac{2^{n_2} n_2!}{2^{n_1} n_1!}\right)^{1/2} e^{-\overline{\mathbf{q}}^2/2} \left[(q_x + iq_y) l_0\right]^{n_1-n_2} L^{n_1-n_2}_{n_2}(\overline{\mathbf{q}}^2) . \tag{B.5}$$

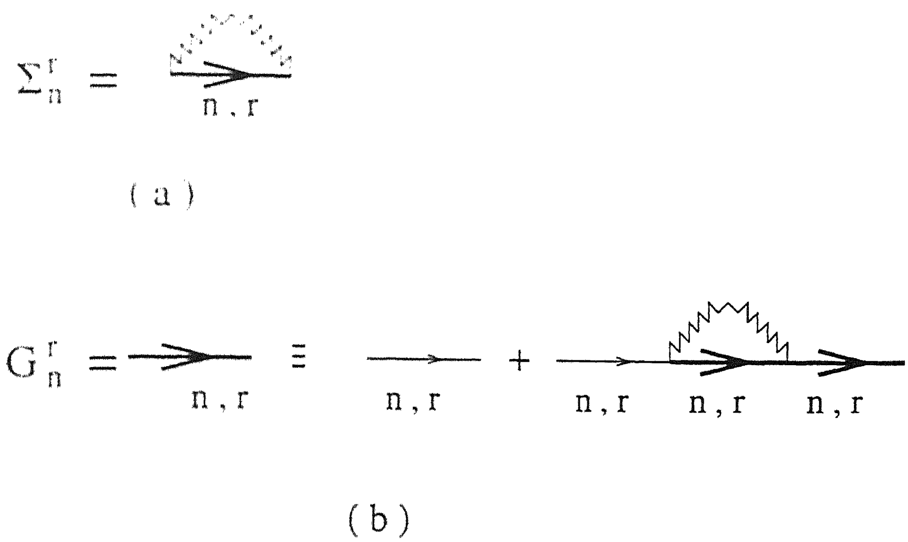

Figure B.1: Thick (thin) lines represent single particle Hartree-Fock (bare) Green's functions. The wiggly lines represent the Coulomb interaction. (a) The self energy Σ_n^r for the particles of spin index r in the n th Landau level. (b) The single particle Hartree-Fock Green's function G_n^r for n th landau level and spin index r.

The two-particle propagator (see Fig. B.2) is given by

$$D_{n_1n_2}^{r_1r_2}(\omega) = \int \frac{d\omega'}{2\pi i} G_{n_1}^{r_1}(\omega') G_{n_2}^{r_2}(\omega + \omega') \tag{B.6}$$

$$= \left[\frac{\theta(p_{r_1} - n_1)\theta(n_2 - p_{r_2} - 1)}{\omega - (\epsilon_{n_1}^{r_1} - \epsilon_{n_2}^{r_2}) - (\Sigma_{n_1}^{r_1} - \Sigma_{n_2}^{r_2}) + i\eta} - \frac{\theta(p_{r_2} - n_2)\theta(n_1 - p_{r_1} - 1)}{\omega - (\epsilon_{n_1}^{r_1} - \epsilon_{n_2}^{r_2}) - (\Sigma_{n_1}^{r_1} - \Sigma_{n_2}^{r_2}) - i\eta} \right], \tag{B.7}$$

where the function $\theta(x)$ is defined as

$$\theta(x) \equiv \begin{cases} 1 & \text{for} \quad x > 0 \\ 0 & \text{for} \quad x < 0 \end{cases} . \tag{B.8}$$

Finally, $\Gamma_{n_1n_2}^{r_1r_2}$ which is the corrected vertex (due to Coulomb interaction between the particle and hole pair) function is diagrammatically shown in Fig. (B.2). Here we have assumed that only single exciton present at a time. In other words, $e^2/\epsilon l_0 \ll \bar{\omega}_c$.

Now if we define

$$\Phi_{n_1n_2}^{r_1r_2}(\omega, \mathbf{q}) \equiv D_{n_1n_2}^{r_1r_2}(\omega)\Gamma_{n_1n_2}^{r_1r_2}(\omega, \mathbf{q}) , \tag{B.9}$$

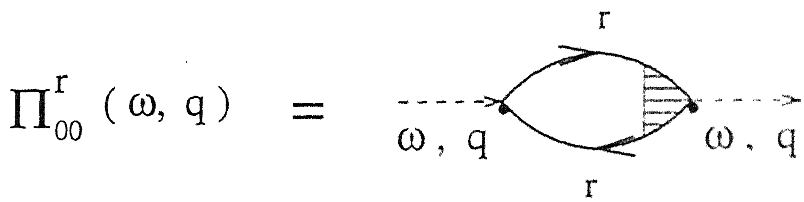

(a)

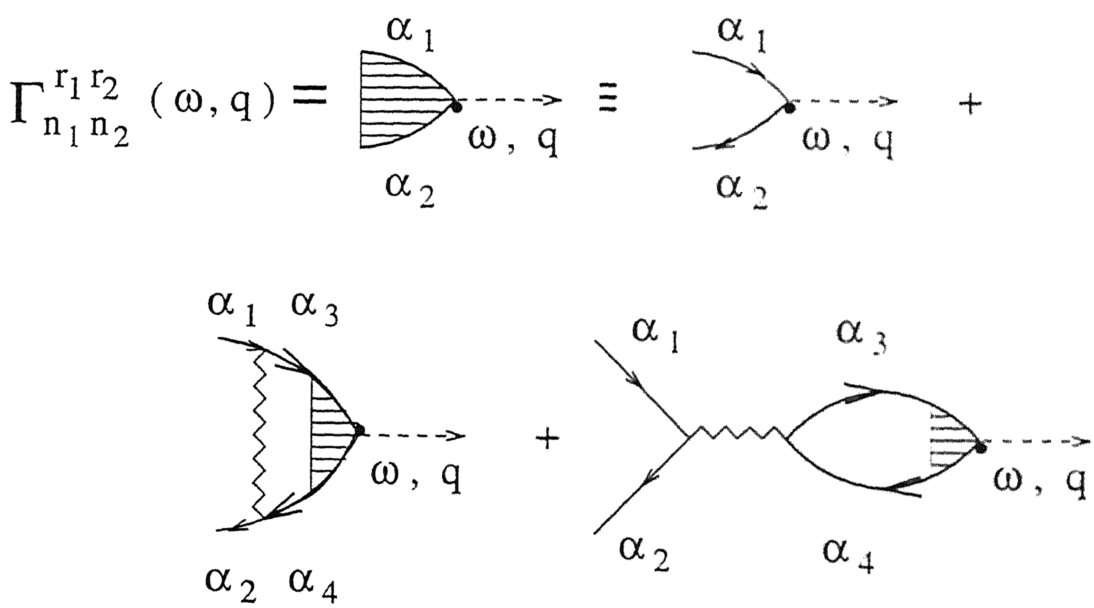

(b)

Figure B.2: $\alpha_i = (n_i, r_i)$ denotes collectively the Landau level index n_i and the spin index r_i. Thick (thin) lines represent single particle Hartree-Fock (bare) Green's functions. The dashed lines represent the probes. (a) Response function $\Pi^r_{00}(\omega, \mathbf{q})$ is diagrammatically shown. The shaded portion represents the vertex correction due to the Coulomb interaction. (b) The vertex function $\Gamma^{r_1 r_2}_{n_1 n_2}(\omega, \mathbf{q})$ is diagrammatically shown.

then the response function can be written as

$$\Pi^{r}_{00}(\omega,\,\mathbf{q}) = \sum_{r_1,r_2}\sum_{n_1,n_2} M_{n_1n_2}(\mathbf{q})\Phi^{r_1r_2}_{n_1n_2}(\omega,\,\mathbf{q})\delta_{r_1,r_2}\delta_{r,r_1}\ , \tag{B.10}$$

where $\Phi^{r_1r_2}_{n_1n_2}(\omega,\,\mathbf{q})$ satisfies the matrix equation,

$$\begin{aligned}\sum_{n_3,n_4}\sum_{r_3,r_4}\Big[&\delta_{n_1,n_3}\delta_{n_2,n_4}\delta_{r_1,r_3}\delta_{r_2,r_4}\left[\{D(\omega)\}^{-1}\right]^{r_3r_4}_{n_3n_4} - \delta_{r_1,r_3}\delta_{r_2,r_4}\tilde{V}^{(1)}_{n_1n_4n_2n_3}(\mathbf{q}) \\ &+ \delta_{r_1,r_2}\delta_{r_3,r_4}\tilde{V}^{(2)}_{n_1n_4n_3n_2}(\mathbf{q})\Big]\,\Phi^{r_3r_4}_{n_3n_4}(\omega,\,\mathbf{q}) = M^{*}_{n_1n_2}(\mathbf{q})\delta_{r_1,r_2}\ .\end{aligned} \tag{B.11}$$

Diagrammatically, $M^{*}_{n_1n_2}(\mathbf{q})$ is given by the first diagram of Fig. (B.2). The interaction between an excited electron and hole which is represented by the ladder diagrams in the second diagram of Fig. B.2. The corresponding matrix element due to to Coulomb interaction is given by

$$\begin{aligned}\tilde{V}^{(1)}_{n_1n_4n_2n_3}(\mathbf{q}) &= \left(\frac{2^{n_4}2^{n_2}n_4!n_2!}{2^{n_1}2^{n_3}n_1!n_3!}\right)^{1/2}\int\frac{d^2r}{2\pi l_0^2}V(\mathbf{r}-l_0^2\mathbf{q}\times\hat{z})e^{-r^2/2l_0^2} \\ &\times\left[\frac{x+iy}{l_0}\right]^{n_1-n_2}\left[\frac{x-iy}{l_0}\right]^{n_3-n_4}L^{n_1-n_2}_{n_2}\left(\frac{r^2}{2l_0^2}\right)L^{n_3-n_4}_{n_4}\left(\frac{r^2}{2l_0^2}\right)\ .\end{aligned} \tag{B.12}$$

The matrix element for the bubble diagrams (see the third diagram of Fig. B.2) is obtained as

$$\begin{aligned}\tilde{V}^{(2)}_{n_1n_4n_3n_2}(\mathbf{q}) &= \left(\frac{2^{n_4}2^{n_2}n_4!n_2!}{2^{n_1}2^{n_3}n_1!n_3!}\right)^{1/2}\frac{\tilde{V}(\mathbf{q})}{2\pi l_0^2}l_0^{n_1+n_3-n_2-n_4} \\ &\times (q_x+iq_y)^{n_1-n_2}(q_x-iq_y)^{n_3-n_4}L^{n_1-n_2}_{n_2}(\bar{\mathbf{q}}^2)L^{n_3-n_4}_{n_4}(\bar{\mathbf{q}}^2)\ ,\end{aligned} \tag{B.13}$$

where $\tilde{V}(\mathbf{q})$ is the Fourier transform of the Coulomb potential.

Solving $\Phi^{r_1r_2}_{n_1n_2}(\omega,\,\mathbf{q})$ from Eq. (B.11), we substitute it in Eq. (B.10) to obtain the response function,

$$\begin{aligned}&\Pi^{r}_{00}(\omega,\,\mathbf{q}) = \\ &e^2\left[\sum_{n_2<p_r}\sum_{n_1\geq p_r}\frac{|M_{n_1n_2}(\mathbf{q})|^2}{\omega-(\epsilon^r_{n_1}-\epsilon^r_{n_2})-(\Sigma^r_{n_1}-\Sigma^r_{n_2})+\tilde{V}^{(1)}_{n_1n_2n_2n_1}(\mathbf{q})-\gamma\tilde{V}^{(2)}_{n_1n_2n_1n_2}(\mathbf{q})+i\eta}\right. \\ &\left.-\sum_{n_1<p_r}\sum_{n_2\geq p_r}\frac{|M_{n_1n_2}(\mathbf{q})|^2}{\omega-(\epsilon^r_{n_1}-\epsilon^r_{n_2})-(\Sigma^r_{n_1}-\Sigma^r_{n_2})+\tilde{V}^{(1)}_{n_1n_2n_2n_1}(\mathbf{q})-\gamma\tilde{V}^{(2)}_{n_1n_2n_1n_2}(\mathbf{q})-i\eta}\right]\ .\end{aligned} \tag{B.14}$$

The factor $\gamma = 2$ when both the spin states in an LL from which the excitation occurs are fully occupied. Otherwise the value of the parameter $\gamma = 1$.

In a similar manner, the Fourier transform of the spin-flip response function

$$\chi^{ab}(x,\, x') = ie^2 \mathrm{Tr}\left[\sigma_a G(x,\, x')\sigma_b G(x',\, x)\right], \tag{B.15}$$

may be obtained as

$$\begin{aligned}
\chi^{ab}(\omega,\, \mathbf{q}) &= e^2 \mathrm{Tr}[\sigma_a \sigma_b] \\
\times &\left[\sum_{n_2 < p_{r_1}} \sum_{n_1 \geq p_{r_2}} \frac{|M_{n_1 n_2}(\mathbf{q})|^2}{\omega - (\epsilon_{n_1}^{r_2} - \epsilon_{n_2}^{r_1}) - (\Sigma_{n_1}^{r_2} - \Sigma_{n_2}^{r_1}) + \Gamma_{n_1 n_2 n_2 n_1}^{(1)}(\mathbf{q}) + i\eta} \right. \\
&\left. - \sum_{n_2 < p_{r_2}} \sum_{n_1 \geq p_{r_1}} \frac{|M_{n_1 n_2}(\mathbf{q})|^2}{\omega + (\epsilon_{n_1}^{r_1} - \epsilon_{n_2}^{r_2}) + (\Sigma_{n_1}^{r_1} - \Sigma_{n_2}^{r_2}) - \Gamma_{n_1 n_2 n_2 n_1}^{(1)}(\mathbf{q}) - i\eta} \right],
\end{aligned} \tag{B.16}$$

where σ_a (σ_b) creates spin state r_1 (r_2) destroying spin state r_2 (r_1). Therefore, $r_1 \neq r_2$. Note that the bubble diagrams (see the third diagram of Fig. B.2) do not contribute to the spin-flip response function. This is because in this response function, particle and hole possess different spins, and the Coulomb interaction can not flip the spin.

Appendix C

The evaluation of I_{nm}

In this Appendix, we shall evaluate

$$I_{nm}(\omega_j) = -\frac{1}{\beta} \sum_{s=-\infty}^{\infty} \overline{G^n(i\xi_s)}\, \overline{G^m(i\xi_s - i\omega_j)} \,, \tag{C.1}$$

where

$$\overline{G^n(i\xi_s)} = \frac{1}{i\xi_s + \mu - \epsilon_n - \Sigma_n(i\xi_s)} \tag{C.2}$$

with

$$\Sigma_n(i\xi_s) = \frac{1}{2}(i\xi_s + \mu - \epsilon_n) \pm \frac{i}{2}\sqrt{\Gamma^2 - (i\xi_s + \mu - \epsilon_n)^2} \,. \tag{C.3}$$

We evaluate I_{nm} by the contour integration method.

Let us consider the integral

$$S_{nm} = \int_C \frac{dZ}{2\pi i} n_F(Z) \overline{G^n(Z)}\, \overline{G^m(Z - i\omega_j)} \,, \tag{C.4}$$

where

$$n_F(Z) = \frac{1}{1 + e^{\beta Z}} \tag{C.5}$$

is the Fermi function. The contour is shown in Fig. (C.1). There are poles at $Z = i\frac{\pi}{\beta}(2s+1)$. The integrand also has branch cuts on the two lines $Z = \epsilon$ and $Z = \epsilon + i\omega_j$, where ϵ is real. To illustrate, for $\overline{G^n(Z)}$, the range of ϵ is $\epsilon_n - \mu - \Gamma$ to $\epsilon_n - \mu + \Gamma$. The evaluation of residues at the poles of S_{nm} reproduces I_{nm}. In other words, I_{nm} is equivalent to S_{nm} when S_{nm} is evaluated along the branch cuts, where the contributions

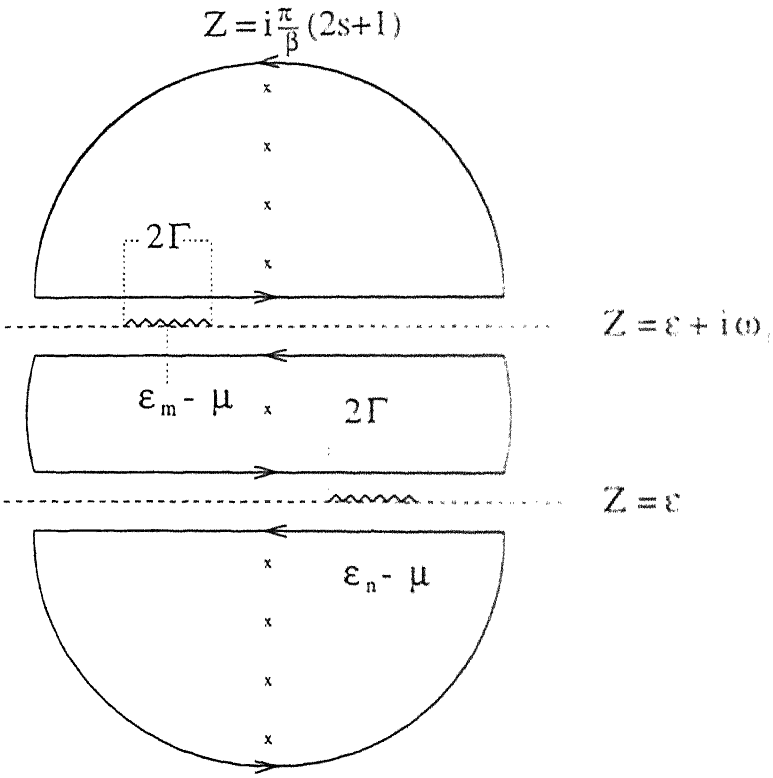

Figure C.1: The contour for S_{nm} in Eq. (C.4) is shown. The wiggly lines represent the branch cuts along the lines $z = \epsilon$ and $z = \epsilon + i\omega_j$. The cross points are the poles located at $z = i\frac{\pi}{\beta}(2s + 1)$.

above and below the cuts are subtracted:

$$
\begin{aligned}
I_{nm}(\omega_j) &= \int_{\epsilon_n-\mu-\Gamma}^{\epsilon_n-\mu+\Gamma} \frac{d\epsilon}{2\pi i} n_F(\epsilon)\overline{G^m(\epsilon - i\omega_j)} \left[\overline{G^n(\epsilon+i\delta)} - \overline{G^n(\epsilon-i\delta)}\right] \\
&+ \int_{\epsilon_m-\mu-\Gamma}^{\epsilon_m-\mu+\Gamma} \frac{d\epsilon}{2\pi i} n_F(\epsilon)\overline{G^n(\epsilon + i\omega_j)} \left[\overline{G^m(\epsilon+i\delta)} - \overline{G^m(\epsilon-i\delta)}\right] .
\end{aligned} \tag{C.6}
$$

Now the factor

$$
\begin{aligned}
\overline{G^n(\epsilon+i\delta)} - \overline{G^n(\epsilon-i\delta)} &= \overline{G^n_r(\epsilon)} - \overline{G^n_a(\epsilon)} \\
&= 2i \operatorname{Im} \overline{G^n_r(\epsilon)} .
\end{aligned} \tag{C.7}
$$

Therefore

$$
\begin{aligned}
I_{nm}(\omega_j) &= 2\int_{\epsilon_n-\mu-\Gamma}^{\epsilon_n-\mu+\Gamma} \frac{d\epsilon}{2\pi} n_F(\epsilon)\overline{G^m(\epsilon - i\omega_j)} \operatorname{Im} \overline{G^n_r(\epsilon)} \\
&+2\int_{\epsilon_m-\mu-\Gamma}^{\epsilon_m-\mu+\Gamma} \frac{d\epsilon}{2\pi} n_F(\epsilon)\overline{G^n(\epsilon + i\omega_j)} \operatorname{Im} \overline{G^m_r(\epsilon)} .
\end{aligned} \tag{C.8}
$$

We now analytically continue: $\omega_j \to \omega + i\delta$ to obtain

$$
\begin{aligned}
I_{nm}(\omega + i\delta) &= 2\int_{\epsilon_n-\mu-\Gamma}^{\epsilon_n-\mu+\Gamma} \frac{d\epsilon}{2\pi} n_F(\epsilon) \operatorname{Im} \left[\overline{G^n_r(\epsilon)}\right] \overline{G^m_a(\epsilon - \omega)} \\
&+2\int_{\epsilon_m-\mu-\Gamma}^{\epsilon_m-\mu+\Gamma} \frac{d\epsilon}{2\pi} n_F(\epsilon) \operatorname{Im} \left[\overline{G^m_r(\epsilon)}\right] \overline{G^n_r(\epsilon + \omega)} ,
\end{aligned} \tag{C.9}
$$

which is the required result.

Bibliography

[1] K. von Klitzing, G. Dorda, and M. Pepper. Phys. Rev. Lett. **45**, 494 (1980).

[2] D. C. Tsui, H. L. Stormer, and A. C. Gossard. Phys. Rev. Lett. **48**, 1559 (1982).

[3] D. C. Tsui, Physica **B 164**, 59 (1990).

[4] R. L. Willett, J. P. Eisenstein, H. L. Stormer, D. C. Tsui, A. C. Gossard, and J. H. English, Phys. Rev. Lett. **59**, 1776 (1987).

[5] R. E. Prange and S. M. girvin eds., *The Quantum Hall Effect*, Springer-Verlag, New York, 1987.

[6] T. Chakraborty and P. Pietilainen, *The Fractional Quantum Hall Effect*, Springer series in solid state sciences **85**, Springer-Verlag, 1988.

[7] A. Karlhede, S. A. Kivelson, and S. L. Sondhi, in *Correlated Electron Systems*, eds. V. J. Emery, World-Scientific, Singapore, 1993.

[8] R. E. Prange, Phys. Rev. **B 23**, 4802 (1981).

[9] R. B. Laughlin, Phys. Rev. **B 23**, 5632 (1981).

[10] B. I. Halperin, Phys. Rev. **B 23**, 2185 (1982).

[11] D. J. Thouless, in Ref.[5].

[12] K. Yoshihiro, J. Kinoshita, K. Inagaki, C. Yamanouchi, J. Moriyama, and S. Kawaji, Physica **B 117**, 706 (1984).

[13] M. E. Cage, B. F. Field, R. F. Dziuba, S. M. Girvin, A. C. Gossard, and D. C. Tsui, Phys. Rev. **B 30**, 2286 (1984).

[14] R. B. Laughlin, Phys. Rev. Lett. **50**, 1395 (1983).

[15] B. I. Halperin, Phys. Rev. Lett. **52**, 1583 (1984).

[16] D. P. Arovas, J. R. Schreiffer, and F. Wilczek, Phys. Rev. Lett. **53**, 722 (1984).

[17] F. D. M. Haldane, Phys. Rev. Lett. **51**, 605 (1983).

[18] J. K. Jain, Phys. Rev. Lett. **63**, 199 (1989).

[19] A. Lopez and E. Fradkin, Phys. Rev. **B 44**, 5246 (1991); see also E. Fradkin, *Field Theories of Condensed Matter Systems*, Addison-Wesley, Redwood City, 1991.

[20] B. I. Halperin, P. A. Lee, and N. Read, Phys. Rev. **B 47**, 7312 (1993).

[21] R. R. Du, H. L. Stormer, D. C. Tsui, L. N. Pfeiffer, and K. W. West, Phys. Rev. Lett. **70**, 29444 (1993).

[22] D. R. Leadley, H. L. Stormer, C. T. Foxon, and J. J. Harris, Phys. Rev. Lett. **72**, 1906 (1994); D. R. Leadley, M. v. d. Burgt, R. J. Nicholas, C. T. Foxon, and J. J. Harris, preprint cond-mat/9508059.

[23] R. R. Du, H. L. Stormer, D. C. Tsui, L. N. Pfeiffer, and K. W. West, Phys. Rev. Lett. **73**, 3274 (1994).

[24] H. C. Manoharan, M. Shayegan, and S. J. Klepper, Phys. Rev. Lett. **73**, 3270 (1994).

[25] R. L. Willett, M. A. Paalanen, K. W. West, L. N. Pfeiffer, and D. J. Bishop, Phys. Rev. Lett. **64**, 112 (1990).

[26] R. L. Willett, R. R. Ruel, M. A. Paalanen, K. W. West, and L. N. Pfeiffer, Phys. Rev. **B 47**, 7344 (1993).

[27] R. L. Willett, R. R. Ruel, M. A. Paalanen, K. W. West, and L. N. Pfeiffer, Phys. Rev. Lett. **71**, 3846 (1993).

[28] W. Kang, H. L. Stormer, L. N. Pfeiffer, K. W. Baldwin, and K. W. West, Phys. Rev. Lett. **71**, 3850 (1993).

[29] V. J. Goldman, B. Su, and J. K. Jain, Phys. Rev. Lett. **72**, 2065 (1994).

[30] X. Ying, V. Bayot, M. B. Santos, and M. Shayegan, Phys. Rev. **B 50**, 4969 (1994).

[31] V. Bayot, E. Grivei, H. C. Manoharan, X. Ying, and M. Shayegan, Phys. Rev. B **52**, R8621 (1995).

[32] I. V. Kukushkin, R. J. Haug, K. v. Klitzing, and K. Ploog, Phys. Rev. Lett. **72**, 736 (1994).

[33] I. V. Kukushkin, R. J. Haug, K. v. Klitzing, and K. Ploog, Phys. Rev. **B 51**, 18045 (1995).

[34] B. I. Halperin, Helv. Phys. Acta. **56**, 75 (1983).

[35] R. G. Clark, S. R. Haynes, A. M. Suckling, J. R. Mallett, P. W. Wright, J. J. Harris, and C. T. Foxon, Phys. Rev. Lett. **62**, 1536 (1989).

[36] J. P. Eisenstein, H. L. Stormer, L. N. Pfeiffer, and K. W. West, Phys. Rev. Lett. **62**, 1540 (1989).

[37] J. P. Eisenstein, H. L. Stormer, L. N. Pfeiffer, and K. W. West, Phys. Rev. **B 41**, 7910 (1990).

[38] L. W. Engel, S. W. Hwang, T. Sajoto, D. C. Tsui, and M. Shayegan, Phys. Rev. B **45**, 3418 (1992).

[39] T. Chakraborty and F. C. Zhang, Phys. Rev. **B 29**, 7032 (1984).

[40] F. C. Zhang and T. Chakraborty, Phys. Rev. **B 30**, 7320 (1984).

[41] E. H. Rezayi, Phys. Rev. **B 36**, 5454 (1987).

[42] S. S. Mandal and V. Ravishankar, (to appear in Phys. Rev. **B 54**, 1996).

[43] S. S. Mandal and V. Ravishankar, (to appear in Phys. Rev. **B 54**, 1996).

[44] S. S. Mandal, (unpublished).

[45] S. S. Mandal and V. Ravishankar, (to be published).

[46] D. Stein, K. v. Klitzing, and G. Weimann, Phys. Rev. Lett. **51**, 130 (1983).

[47] J. Maksym, J. Phys. Condens. Matter **1**, 6299 (1989); T. Chakraborty and P. Pietilainen, Phys. Rev. **B 41**, 10862 (1990).

[48] X. G. Wu, G. Dev, and J. K. Jain, Phys. Rev. Lett. **71**, 153 (1993).

[49] J. Frohlich, T. Kerler, and P. A. Marchetti, Nucl. Phys. **B 374**, 111 (1992).

[50] A. Balatsky and E. Fradkin, Phys. Rev. **B 43**, 10622 (1991).

[51] L. Belkhir and J. K. Jain, Phys. Rev. Lett. **70**, 643 (1992).

[52] A. Lopez and E. Fradkin, Phys. Rev. **B 51**, 4347 (1995).

[53] J. P. Eisenstein, R. L. Willett, H. L. Stormer, D. C. Tsui, A. C. Gossard, and J. H. English, Phys. Rev. Lett. **61**, 997 (1988).

[54] A. Lopez and E. Fradkin, Phys. Rev. Lett. **69**, 2126 (1992).

[55] W. Kohn, Phys. Rev. **123**, 1242 (1961).

[56] E. Fradkin, Nucl. Phys. **B 389**, 587 (1993).

[57] F. D. M. Haldane, in Ref.[5].

[58] S. A. Trugman and S. A. Kivelson, Phys. Rev. **B 31**, 5280 (1985).

[59] S. C. Zhang, Int. J. Mod. Phys. **B 6**, 25 (1992).

[60] S. C. Zhang, T. H. Hansson, and S. Kivelson, Phys. Rev. Lett. **62**, 82 (1989).

[61] R. Rajaraman and S. L. Sondhi, preprint cond-mat/9601125.

[62] N. Read, Phys. Rev. Lett. **62**, 86 (1989).

[63] Z. F. Ezawa and A. Iwazaki, Phys. Rev. **B 48**, 15189 (1993).

[64] K. Moon, H. Mori, K. Yang, S. M. Girvin, A. H. MacDonald, L. Zheng, D. Yoshioka, and S. C. Zhang, Phys. Rev. **B 51**, 5138 (1995).

[65] D. H. Lee and C. L. Kane, Phys. Rev. Lett. **64**, 1313 (1990).

[66] J. K. Jain. Phys. Rev. **B 41**, 7653 (1990).

[67] F. D. M. Haldane and E. H. Rezayi, Phys. Rev. Lett. **60**, 956 (1988).

[68] E. Rezayi and N. Read, Phys. Rev. Lett. **72**, 900 (1994).

[69] C. Kallin and B.I. Halperin, Phys. Rev. **B 30**, 5655 (1984).

[70] A. H. MacDonald, J. Phys. **C 18**, 1003 (1985).

[71] S. M. Girvin, A. H. MacDonald, and P. M. Platzmann, Phys. Rev. Lett. **54**, 581 (1985); Phys. Rev. **B 33**, 2481 (1986).

[72] A. Lopez and E. Fradkin, Phys. Rev. **47**, 7080 (1993).

[73] G. D. Mahan, in *Many-Particle Physics*, 2nd. Edition, Plenum, New York, 1990.

[74] A. Pinczuk, J. P. Valladares, D. Heiman, A. C. Gossard, J. H. English, C. W. Tu, L. Pfeiffer, and K. West, Phys. Rev. Lett. **61**, 2701 (1988).

[75] A. Pinczuk, B. S. Dennis, L. N. Pfeiffer, and K. W. West, Phys. Rev. Lett. **70**, 3983 (1993).

[76] M. V. Klein, in *Light Scattering in Solids I*, ed. by M. Cardona, Springer-Verlag, New York, 1983.

[77] J. P. Longo and C. Kallin, Phys. Rev. **B 47**, 4429 (1993).

[78] T. Nakajima and H. Aoki, Phys. Rev. Lett. **73**, 3568 (1994).

[79] A. Hartland, K. Jones, J. M. Williams, B. L. Gallagher, and T. Galloway, Phys. Rev. Lett. **66**, 969 (1991).

[80] W. V. D. Wel, C. J. P. M. Harmans and J. E. Mooij, Surf. Sci. **170**, 226 (1986).

[81] D. Weiss, S. Stahl, G. Weimann, K. Ploog and K. von Klitzing, Surf. Sci. **170**, 285 (1986).

[82] R. G. Clark, J. M. Mallett, S. R. Haynes, J. J. Harris, and C. T. Foxon, Phys. Rev. Lett. **60**, 1747 (1988).

[83] Y. Katayama, D. C. Tsui, and M. Shayegan, Phys. Rev. **B 49**, 7400 (1994).

[84] H. P. Wei, D. C. Tsui, A. M. M. Paalanen, and A. M. M. Pruisken, Phys. Rev. Lett. **61**, 1294 (1988).

[85] H. P. Wei, S. W. Hwang, D. C. Tsui, and A. M. M. Pruisken, Surf. Sci. **229**, 34 (1990).

[86] B. Huckestein, B. Kramer, R. Meisels, K. Y. Lim, F. Kuchar, G. Weimann, and W. Schlapp, in *Proceedings of the 20th International Conference "The Physics of Semiconductors"*, edited by E. M. Anastassakis and J. D. Joannopoulos (World Scientific, Singapore) 1991.

[87] S. W. Hwang, H. P. Wei, L. W. Engel, D. C. Tsui, and A. M. M. Pruisken, Phys. Rev. **B 48**, 11416 (1993).

[88] J. Wakabayashi, M. Yamane, and S. Kawaji, J. Phys. Soc. Jpn. **58**, 1903 (1989).

[89] S. Koch, R. J. Haug, K. von Klitzing, and K. Ploog, Phys. Rev. **B 43**, 6828 (1991).

[90] M. E. Cage in *The Quantum Hall Effect*, ed. by R. E. Prange and S. M. Girvin (Springer-Verlag, 1990).

[91] R. W. Rendell and S. M. Girvin, Phys. Rev. **B 23**, 6610 (1981).

[92] M. M. Fogler and B. I. Shklovskii, preprint cond-mat/9409083

[93] D. G. Polyakov and B. I. Shklovskii, Phys. Rev. Lett. **74**, 150 (1995).

[94] B. Huckestein, Rev. Mod. Phys. **67**, 357 (1995).

[95] T. Ando, Y. Matsumoto, and Y. Uemura, J. Phys. Soc. Jpn. **39**, 279 (1975).

[96] A. M. M. Pruisken in Ref.[5].

[97] H. Levine, S. B. Libby, and A. M. M. Pruisken, Phys. Rev. Lett. **51**, 1915 (1983).

[98] H. P. Wei, D. C. Tsui, M. A. Paalanen, and A. M. M. Pruisken in *High Magnetic Fields in Semiconductor Physics*, Springer series in Solid-State Sciences No. 71, edited by G. Landwehr (Springer, Berlin) 1987.

[99] S. Randjbar-Daemi, A. Salam, and J. Strathdee, Nucl. Phys. **B 340**, 403 (1990).

[100] J. E. Hetric, Y. Hosotani, and B.-H. Lee, Ann. Phys. (N. Y.), **209**, 151 (1991).

[101] J.I. Kapusta, M. E. Carrington, B. Bayman, D. Seibert, and C. S. Song, Phys Rev. **B 46**, 7519 (1992).

[102] A. L. Fetter and C. B. Hanna, Phys. Rev. **B 45**, 2335 (1992).

[103] J. E. Hetric and Y. Hosotani, Phys. Rev. **B 45**, 2981 (1992).

[104] S. S. Mandal, S. Ramaswamy, and V. Ravishankar, Mod. Phys. Lett. **B 8**, 561 (1994); Int. J. Mod. Phys. **B 8**, 3095 (1994).

[105] W. Zawadzki and R. Lassnig, Solid State Commun. **50**, 537 (1984).

[106] E. Gornik, R. Lassnig, G. Strasser, H. L. Stormer, A. C. Gossard, and W. Wiegmann, Phys. Rev. Lett. **54**, 1820 (1985).

[107] See, A. M. Chang, in Ref.[5].

[108] M. Buttiker, Phys. Rev. **B 38**, 9375 (1988).

[109] D. Yoshioka, B. I. Halperin, and P. A. Lee, Phys. Rev. Lett. **50**, 1219 (1983).

[110] T. Chakraborty, P. Pietilainen, and F. C. Zhang, Phys. Rev. Lett. **57**, 130 (1986).

[111] S. Kawaji, J. Wakabayashi, J. Yoshino, and H. Sakaki, J. Phys. Soc. Jpn. **53**, 1915 (1984).

[112] J. M. Leinaas and J. Myrheim, Nuovo Cimento **37 B**, 1 (1977); F. Wilczek, Phys. Rev. Lett. **49**, 957 (1982).

[113] G. Dev and J. K. Jain, Phys. Rev. **B 45** , 1223 (1992).

[114] N. Trivedi and J. K. Jain, Mod. Phys. Lett. **B 5**, 503 (1991).

[115] R. Morf and N. d'Abrumenil, Phys. Rev. Lett. **74**, 5116 (1995).

[116] V. Kalmeyer and S. C. Zhang, Phys. Rev. **B 46**, 9889 (1992).

[117] H. W. Jiang, H. L. Stormer, D. C. Tsui, L. N. Pfeiffer, and K. W. West, Phys. Rev. **B40**, 12013 (1989).

[118] A. Stern and B. I. Halperin, Phys. Rev. **B 52**, 5890 (1995).

[119] Y. B. Kim, P. A. Lee, and X. G. Wen, Phys. Rev. **B 52**, 17275 (1995).

[120] P. A. Lee, E. R. Mucciolo, and H. Smith, preprint cond-mat/9604146.

[121] S. H. Simon and B. I. Halperin, Phys. Rev. **B 48**, 17386 (1993); *ibid.* **50**, 1807 (1994); S. He, S. H. Simon, and B. I. Halperin, *ibid.* **50**, 1823 (1994).

[122] S. H. Simon, A. Stern, and B. I. Halperin, preprint cond-mat/9604103.

[123] S. M. Girvin and A. H. Macdonald, Phys. Rev. Lett. **58**, 1252 (1987).

[124] E. Rezayi and F. D. M. Haldane, Phys. Rev. Lett. **61**, 1985 (1988).

[125] D. H. Lee, S. L. Kivelson, and S. C. Zhang, Phys. Rev. Lett. **67**, 3302 (1991).

[126] S. L. Kivelson, D. H. Lee, and S. C. Zhang, Phys. Rev. **B 46**, 2223 (1992).

[127] E. Abrahamas, P. W. anderson, D. C. Licciardello, and T. V. Ramakrishnan, Phys. Rev. Lett. **42**. 673 (1979).

[128] H. Aoki and T. Ando, Solid State Commun **38**. 1079 (1981).

[129] J. T. Chalker, J. Phys. **C 20**, L493 (1987).

[130] S. Kawaji and J. Wakabayashi, in *Proceedings of the Oji International Seminar, Hakone, 1980, Physics in High magnetic fields*, ed. by S. Chikazumi and N. Miura (Springer-Verlag), 1981.

[131] M. A. Paalanen, D. C. Tsui, and A. C. Gossard, Phys. Rev. **B 25**, 5566 (1982).

[132] M. Yamane, J. Wakabayashi, and S. Kwaji, J. Phys. Soc. Jpn. **58**, 1899 (1989).

[133] A. M. M. Pruisken. Phys. Rev. Lett. **61**, 1298 (1988).

[134] Y. Huo, R. E. Hetzel, and R. N. Bhatt, Phys. Rev. Lett. **70**, 481 (1993).

[135] D. J. Thouless, Phys. Rev. Lett. **39**, 1167 (1977).

[136] B. Huckestein and B. Kramer, Phys. Rev. Lett. **64**, 1437 (1990).

[137] G. V. Milnikov and I. M. sokolov, JETP Lett. **48**, 536 (1988).

[138] T. Ando, J. Phys. Soc. Jpn. **52**, 1740 (1983).

[139] J. T. Edwards and D. J. Thouless, J. Phys. **C 5**, 807 (1972).

[140] D. J. Thouless, Phys. Rep. **13**, 93 (1974).

[141] D. J. Thouless, M. Kohmoto, M. P. Nightingale, and M. d. Nijs, Phys. Rev. Lett. **49**, 405 (1982).

[142] Q. Niu, D. Thouless, and Y. S. Wu, Phys. Rev. **B 31**, 3372 (1985).

[143] D. P. Arovas, R. N. Bhatt, F. D. M. Haldane, P. B. Littlewood, and R. Rammal, Phys. Rev. Lett. **60**, 619 (1988).

[144] Y. Huo and R. N. Bhatt, Phys. Rev. Lett. **68**, 1375 (1992).

[145] L. W. Engel, H. P. Wei, D. C. Tsui, and M. Shayegan, Surf. Sci. **229**, 13 (1990).

[146] J. K. Jain, S. A. Kivelson, and N. Trivedi, Phys. Rev. Lett. **64**, 1297 (1990).

[147] D. Shahr, D. C. Tsui, M. Shayegan, R. N. Bhatt, and J. E. Cnningham, Phys. Rev. Lett. **74**, 4511 (1995).

[148] G. Baskaran and E. Tosatti, Euro. Phys. Lett. **25**, 369 (1994).

[149] E. H. Rezayi, Phys. Rev. **B 43**, 5944 (1991).

[150] S. L. Sondhi, A. Karlhede, S. A. Kivelson, and E. H. Rezayi, Phys. Rev. **B 47**, 16419 (1993).

[151] See, *e.g.*, R. Rajaraman, *Solitons and Instantons*, Noth-Holand, Amsterdam, 1982.

[152] S. E. Barrett, G. Dabbagh, L. N. Pfeiffer, K. W. West, and R. Tyco, Phys. Rev. Lett. **74**, 5112 (1995).

[153] A. Schmeller, J. P. Eisenstein, L. N. Pfeiffer, and K. W. West, Phys. Rev. Lett. **75**, 4290 (1995).

[154] E. H. Aifer, B. B. Goldberg, and D. A. Broido, Phys. Rev. Lett. **76**, 680 (1996).

[155] X. G. Wu and S. L. Sondhi, Phys. Rev. **B 51**, 14725 (1995).

[156] J. K. Jain and X. G. Wu, Phys. Rev. **B 49**, 5085 (1994).

[157] C. Nayak anf F. Wilczek, preprint cond-mat/9505081.

[158] H. L. Stormer, J. P. Eisenstein, A. C. Gossard, W. Wiegmann, and K. Baldwin, Phys. Rev. Lett. **56**, 85 (1986).

[159] D. Yoshioka, A. H. MacDonald, and S. M. Girvin, Phys. Rev. **B 39**, 1932 (1989).

[160] A. H. MacDonald, P. M. Platzman, and G. S. Boebinger, Phys. Rev. Lett. **65**, 775 (1990).

[161] L. Brey, Phys. Rev. Lett. **65**, 903 (1990).

[162] G. S. Boebinger, H. W. Jiang,L. N. Pfeiffer, and K. W. West, Phys. Rev. Lett. **64**, 1793 (1990).

[163] Y. W. Suen, J. Jo, M. B. Santos, L. W. Engel, S. W. Hwang, and M. Shayegan, Phys. Rev. **B 44**, 5947 (1991).

[164] E. H. Rezayi and F. D. M. Haldane, Bull. Am. Phys. Soc. **32**, 892 (1987).

[165] T. Chakraborty and P. Pietilainen, Phys. Rev. Lett. **59**, 2784 (1987).

[166] S. He, X. C. Xie, S. D. Sarma, and F. C. Zhang, Phys. Rev. **B 43**, 9339 (1991).

[167] Y. W. Suen, L. W. Engel, M. B. Santos, M. Shayegan, and D. C. Tsui, Phys. Rev. Lett. **68**, 1379 (192).

[168] J. P. Eisenstein, G. S. Boebinger, L. N. Pfeiffer, K. W. West, and S. He, Phys. Rev. Lett. **68**, 1383 (1992).

[169] S. He, S. D. sarma, and X. C. Xie, Phys. Rev. **B 47**, 4394 (1993).

[170] H. A. Fertig, Phys. Rev. **B 40**, 1087 (1989).

[171] T. S. Lay, Y. W. Suen, H. C. Manoharan, X. Ying, M. B. Santos, and M. Shayegan, Phys. Rev. **B 50**, 17725 (1994).

[172] X. G. Wen and A. Zee, Phys. Rev. Lett. **69**, 1811 (1992); Phys. Rev. **B 47**, 2265 (1993).

[173] Z. F. Ezawa and A. Iwazaki, Phys. Rev. **B 47**, 7295 (1993); Phys. Rev. Lett. **70**, 3119 (1993); Phys. Rev. **B48**, 15189 (1993).

[174] S. Q. Murphy, J. P. Eisenstein, G. S. Boebinger, L. N. Pfeiffer, and K. W. West, Phys. Rev. Lett. **72**, 728 (1994).

[175] K. Yang, K. Moon, L. Zheng, A. H. MacDonald, S. M. Girvin, D. Yoshioka, and S. C. Zhang, Phys. Rev. Lett. **72**, 732 (1994).

[176] T. Nakajima and H. Aoki, Phys. Rev. **B 52**, 13780 (1995).

List of Publications

1. * *Effective P, T restoration in Chern-Simons Superconductivity*, Mod. Phys. Lett. **B 8**, 561 (1994), with S. Ramaswamy and V. Ravishankar.

2. * *Bulk properties of Chern-Simons superconductivity at finite temperatures*, Int. J. Mod. Phys. **B 8**, 3095 (1994), with S. Ramaswamy and V. Ravishankar.

3. * *Chern-Simons superconductivity at finite magnetic field*. Phys. Rev. **B 52**, 15537 (1995), with S. Ramaswamy and V. Ravishankar.

4. *Theory of arbitrarily polarized quantum Hall states: Filling fractions and wave functions*, to appear in Phys. Rev. **B 54**, 1996, with V. Ravishankar.

5. *Direct test of composite fermion model in quantum Hall systems*, to appear in Phys. Rev. **B 54**, 1996, with V. Ravishankar.

6. *Activated resistivities in the integer quantum Hall effect*, with V. Ravishankar, (submitted for publication).

---

* The papers not discussed in the thesis.

...ith $B^{\uparrow,\downarrow}$, in

Addendum and notes to the thesis

(1). The choice of the parameter $\theta_- = 0$ in section (2.2.1) corresponds to the constraint $\Delta\rho(x) = 0$, *i.e.*, at every point, the fermion densities with spin-up and spin-down must be the same. This leads to unpolarized states, and a_μ^- gauge field has no dynamical role. As a consequence of this strong constraint, the fluctuations cannot change the spin density. We have employed the condition in a rather weak sense, *i.e.*, only at the mean field level $\langle\Delta\rho\rangle = 0$, and obtained the observed sequence of unpolarized states [see Eq. (2.11)]. We have subsequently evaluated spin density fluctuations as well. It, therefore, appears that the choice $\theta_- = 0$ is not very appropriate to unpolarized states.

On the other hand, the choice $\theta_- = \infty$ again leads to unpolarized ground state having sequence of states identical to the sequence of states that we have obtained for $\theta_- = 0$. Here one imposes the weaker constraint $\langle\Delta\rho\rangle = 0$. Note that the sequence emerges as the natural limit of the partially polarized sequence (2.19), when $p_\uparrow = p_\downarrow$. Unlike the former case, the present choice does not give any strong constraint. Therefore $\theta_- = \infty$ is the appropriate choice of all the observed fractional quantum Hall states irrespective of spin polarization in the lowest Landau level.

It must be stressed that the latter choice of the parameter θ_- does not alter any of the results for unpolarized states that we have presented for the former case.

(2). It is not trivial to find out the value of the g factor as a coefficient of the Zeeman term in Eq. (2.2). The g factor may be renormalized due to the inclusion of the Chern-Simons magnetic field. In this thesis, we are not concerned with the renormalized value of the g factor since none of the conclusions that we arrive at is sensitive to the value of g , as long as Zeeman energy is small compared to $\bar{\omega}_c$.

(3). The effective cyclotron frequencies $\bar{\omega}_c^{\uparrow,\downarrow}$ do depend on the effective masses of spin-up

Erratum to the Thesis

1. (a) The sentence before Eq. (4.11) [The factor $\gamma = 2$ when $\cdots$] should be replaced by the following: The value of the factor γ depends on the quantity which we evaluate. (i) For density-density correlations, $\gamma = 2$ when the Landau level n_1 for both up and down spins is occupied and $\gamma = 1$ otherwise. (ii) For spin density correlations, $\gamma = 0$ for unpolarized states, $\gamma = 1$ for fully polarized states, and γ is fractional taking a value between 0 and 1 for partially polarized states.

   (b) Equation (4.34) should read as

$$\omega_n = n\bar{\omega}_c + E^{\uparrow}_{n0} - \tilde{V}^{(1)}_{n000n}(\mathbf{q}),$$

   since $\gamma = 0$ in this case.

   (c) Equations (4.35) – (4.37) should read respectively as

$$\begin{aligned}
\omega_1 &= \bar{\omega}_c - \frac{e^2}{\epsilon l_0}\frac{1}{4}\bar{\mathbf{q}}^2 , \\
\omega_2 &= 2\bar{\omega}_c + \frac{e^2}{\epsilon l_0}\left[\frac{1}{4}\sqrt{\frac{\pi}{2}} - \frac{1}{16}\sqrt{\frac{\pi}{2}}\bar{\mathbf{q}}^2\right] , \\
\omega_3 &= \omega_c + \frac{e^2}{\epsilon l_0}\left[\frac{3}{8}\sqrt{\frac{\pi}{2}} - \frac{1}{32}\sqrt{\frac{\pi}{2}}\bar{\mathbf{q}}^2\right] .
\end{aligned}$$

   (d) Equation (4.38) should be changed to

$$\mathrm{Res}\,(\Sigma_{\mathrm{unp}})\big|_{\omega_1} = -e^2\mathbf{q}^2\omega_c\frac{\nu}{2\pi}$$

.

   (e) Figures (4.1) – (4.3) in the thesis should be replaced by the following figures respectively.

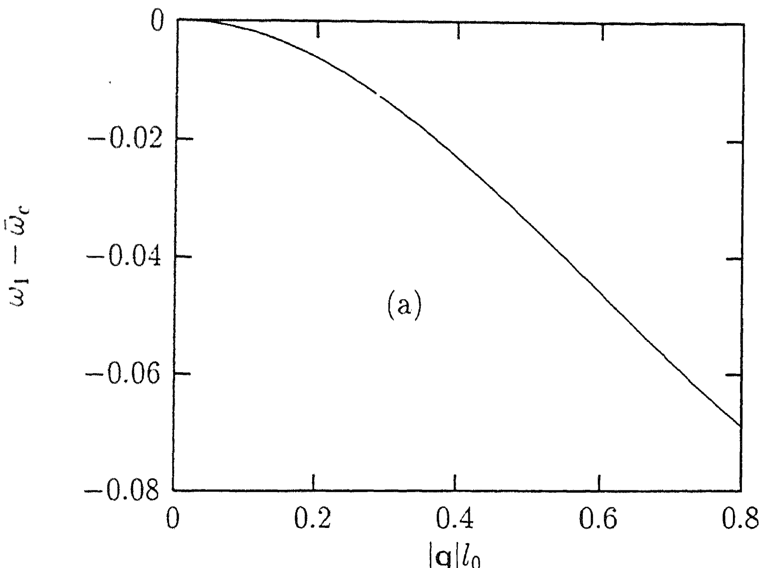

FIG. 1. The spin density excitation mode $\omega_1 - \bar{\omega}_c$ in the units of $e^2/\epsilon l_0$ for unpolarized $\nu = 2/3$ state.

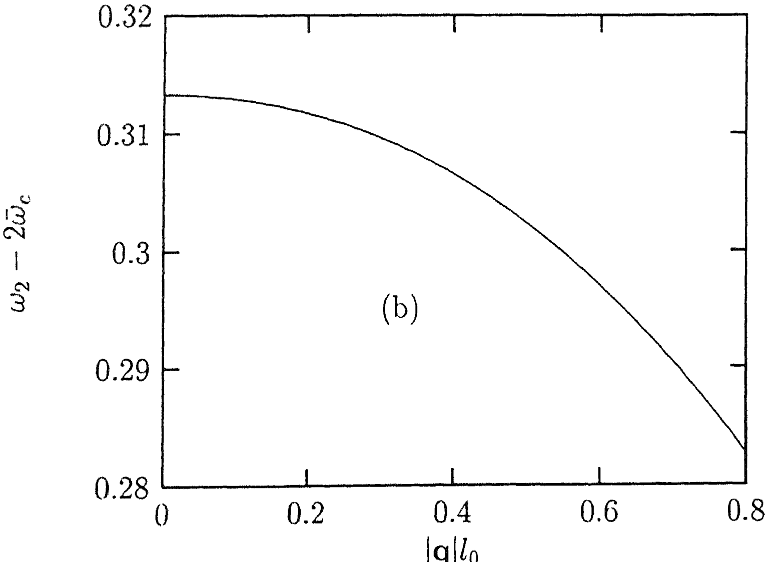

FIG. 2. The spin density excitation mode $\omega_2 - 2\bar{\omega}_c$ in the units of $e^2/\epsilon l_0$ for unpolarized $\nu = 2/3$ state.

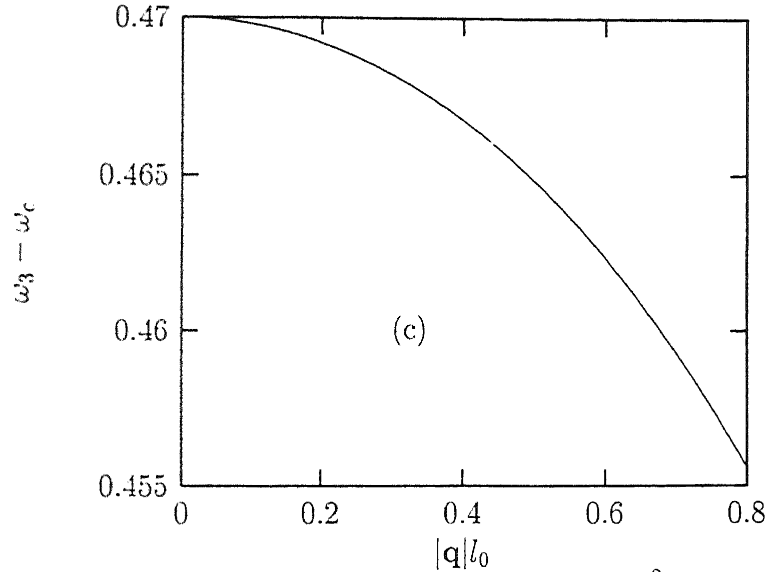

FIG. 3. The spin density excitation mode $\omega_3 - \omega_c$ in the units of $e^2/\epsilon l_0$ for unpolarized $\nu = 2/3$ state.

2. We have corrected the following misprints in chapter 6 below.

   (a) Equation (6.51) should be replaced with

$$\sigma_{xx} = -\lim_{\omega\to 0} \frac{1}{\omega} \operatorname{Im} \Pi^r_{11}(\omega, 0) .$$

   (b) Equation (6.54) should read as

$$\begin{aligned}\operatorname{Im} I_{nm}(\omega) = 2 &\int_{\epsilon_n-\mu-\Gamma}^{\epsilon_n-\mu+\Gamma} \frac{d\epsilon}{2\pi} n_F(\epsilon) \operatorname{Im} \overline{G^n_r(\epsilon)} \operatorname{Im} \overline{G^m_a(\epsilon-\omega)} \\ &+2 \int_{\epsilon_m-\mu-\Gamma}^{\epsilon_m-\mu+\Gamma} \frac{d\epsilon}{2\pi} n_F(\epsilon) \operatorname{Im} \overline{G^m_r(\epsilon)} \operatorname{Im} \overline{G^n_r(\epsilon+\omega)} .\end{aligned}$$

   (c) Equation (6.55) should be changed to

$$\sigma_{xx} = -\lim_{\omega\to 0} \frac{e^2}{4m^{*2}\omega} \frac{1}{2\pi l^4} \sum_{n=0}^{\infty} \sum_{m=0}^{\infty} \operatorname{Im} I_{nm}(\omega) \left[(n+1)\delta_{m,n+1} + n\delta_{m,n-1} - (2n+1)\delta_{mn}\right] .$$

3. $\chi^{+-}(\omega, \mathbf{q})$ in Eq. (5.16) should be replaced by $\chi^{-+}(\omega, \mathbf{q})$.

Date Slip

This book is to be returned on the date last stamped.
